NASA CR-135062
R76-912098-11



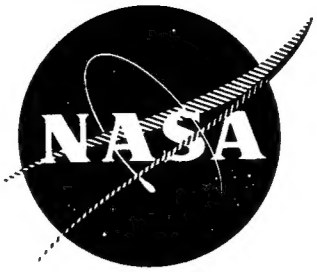


# MULTI-FIBER COMPOSITES

by

R.C. Novak

United Technologies Research Center

East Hartford, Ct. 06108

prepared for

National Aeronautics and Space Administration

NASA Lewis Research Center

Contract NAS3-18941

Ray F. Lark, Project Manager

NASA CR-135062
R76-912098-11


# MULTI-FIBER COMPOSITES

by

R.C. Novak

United Technologies Research Center

East Hartford, Ct. 06108

prepared for

National Aeronautics and Space Administration

NASA Lewis Research Center

Contract NAS3-18941

Ray F. Lark, Project Manager

# DISCLAIMER NOTICE


**THIS DOCUMENT IS BEST QUALITY AVAILABLE. THE COPY FURNISHED TO DTIC CONTAINED A SIGNIFICANT NUMBER OF PAGES WHICH DO NOT REPRODUCE LEGIBLY.**

| 1. Report No. | 2. Government Accession No. | 3. Recipient's Catalog No. |
|---|---|---|
| NASA CR-135062 | | |

| 4. Title and Subtitle | 5. Report Date |
|---|---|
| MULTI-FIBER COMPOSITES | April 1976 |
| | 6. Performing Organization Code |

| 7. Author(s) | 8. Performing Organization Report No. |
|---|---|
| R. C. Novak | R76-912098-11 |
| | 10. Work Unit No. |

| 9. Performing Organization Name and Address | 11. Contract or Grant No. |
|---|---|
| United Technologies Research Center<br>East Hartford, CT 06108 | NAS3-18941 |
| | 13. Type of Report and Period Covered |

| 12. Sponsoring Agency Name and Address | Contractor Report - Final |
|---|---|
| National Aeronautics & Space Administration<br>Washington, DC 20546 | 14. Sponsoring Agency Code |

15. Supplementary Notes

Project Manager, R. F. Lark, Materials & Structures Division, NASA Lewis Research Center, 21000 Brookpark Road, Cleveland, OH 44135

16. Abstract

The objective of this program is to develop resin matrix composites having improved resistance to foreign object damage in gas turbine engine fan blade applications. Materials evaluated include epoxy matrix graphite/glass and boron/glass hybrids, thermoplastic matrix boron/glass hybrids, and superhybrids consisting of graphite/epoxy, boron/aluminum, and titanium alloy sheets. Static, pendulum impact, and ballistic impact test results are reported for all materials. Superhybrid blade-like specimens are shown to be capable of withstanding relatively severe ballistic impacts from gelatin spheres without fracture. The effects of ply configuration and projectile angle of incidence on impact behavior are described. NASTRAN predictions of surface strains during ballistic impact are presented and shown to be in reasonable agreement with experimental measurements.

| 17. Key Words (Suggested by Author(s)) | | 18. Distribution Statement |
|---|---|---|
| composite materials | epoxy | Unclassified - unlimited |
| impact resistance | polysulfone | |
| graphite | hybrids | |
| boron | superhybrids | |

| 19. Security Classif. (of this report) | 20. Security Classif. (of this page) | 21. No. of Pages | 22. Price* |
|---|---|---|---|
| Unclassified | Unclassified | 114 | |

* For sale by the National Technical Information Service, Springfield, Virginia 22151

TABLE OF CONTENTS

LIST OF TABLES

LIST OF ILLUSTRATIONS

LIST OF ILLUSTRATIONS (Cont'd)

# I. INTRODUCTION

The low impact resistance of resin matrix composites remains a primary concern in their application as gas turbine engine fan blade materials in spite of a substantial effort in recent years to improve the tolerance to foreign object damage (FOD). The approach to improved impact resistance which has received the most attention is hybridization, in which a high strain energy reinforcement such as glass is combined with the primary reinforcing graphite or boron fibers in an epoxy matrix (Refs. 1-6). All these studies have indicated that hybridization results in an increase in resistance to catastrophic fracture over that of the unhybridized primary fiber composite. However, Pike and Novak (Ref. 6) concluded that under pendulum impact testing, the loads required to initiate damage in hybrids were generally lower than those for their unhybridized counterparts. As a result of this finding, modifications of hybrid materials were made as described in Ref. 4 in an attempt to increase the damage threshold. These modifications included the utilization of a thermoplastic (polysulfone) matrix rather than the conventional epoxy in order to invoke plasticity damage rather than fracture, through-thickness reinforcement to overcome delamination, and the inclusion of a metallic sheath (screen) for the purpose of distributing local loads. Each of these techniques showed promise in improving the FOD tolerance of the hybrids.

The incorporation of metallic sheaths was generalized by Chamis, Lark, and Sullivan (Ref. 7) to form a family of composites, termed superhybrids, which consist of resin matrix composite, metallic foil, and preconsolidated boron/aluminum layers. The presence of three structural elements within the composite permits a high degree of flexibility in designing to meet specific requirements. In particular, concentrating a metallic foil, such as titanium, in the leading edge region of a fan blade would be a logical step to improve composite FOD resistance.

The general objective of this program was to develop resin matrix composites having improved resistance to foreign object damage. The approach involved further exploration and optimization of the concepts which have shown the most promise to date including hybridization of the fibrous reinforcement, utilization of a thermoplastic matrix, and the superhybrid materials combining fibrous and homogeneous metallic elements. In addition the effects of ply configuration and leading edge protection schemes were to be evaluated.

The program was divided into three technical tasks which followed the approaches outlined above. During Task I hybrid combinations of graphite/glass, boron/glass, and graphite/boron/glass were investigated having both epoxy and thermoplastic matrices. In addition, superhybrid materials involving combinations of isotropic metals, metal matrix composites, and graphite/resin were studied. Static properties were measured on all materials, and ballistic damage tolerance was determined by impacting blade-like specimens with gelatin projectiles.

The effects of ply configuration on impact resistance were studied in Task II. Three hybrid materials were selected from Task I results and each was fabricated into blade-like ballistic specimens having four different ply configurations. These specimens and one superhybrid material were ballistically tested at two angles of incidence. Three of the specimens were instrumented with strain gages.

In Task III leading edge protection schemes were evaluated on ballistic specimens made from the most impact resistant material/ply configuration found in Task II.

## II. TASK I - MATERIALS STUDY

The objective of the initial task was to screen several materials, primarily in terms of ballistic impact resistance, for the purpose of selecting the best four systems for further evaluation under Task II. In addition to ballistic impact testing, pendulum impact and static property tests were conducted on each material. The details of this work are given below.

### 2.1 Experimental

#### 2.1.1 Materials

The materials systems studied in the program included the following:

1. T-300 graphite/S-glass/epoxy
2. AS graphite/S-glass/epoxy
3. AU graphite/S-glass/epoxy
4. AS graphite/S-glass/boron/epoxy
5. boron/S-glass/epoxy
6. boron/S-glass/polysulfone
7. boron/S-glass/polysulfone: AS graphite/S-glass/epoxy
8. $[Ti\text{-}6\text{-}4/B\text{-}Al/AS\ graphite\text{-}epoxy/Ti\text{-}6\text{-}4]_S$ (S.H. #1)
9. $[Ti\text{-}6\text{-}4/AS\ graphite\text{-}epoxy/Ti\text{-}6\text{-}4]_S$ (S.H. #2)
10. $[Ti\text{-}6\text{-}4/B\text{-}Al/AS\ graphite\text{-}epoxy]_S$ (S.H. #3)

All the graphite/glass/resin and boron/glass/resin materials were intraply hybrids, i.e., both reinforcing fiber types were present in each layer. The ratios of the fibers were nominally 80/20 for graphite/glass and 50/50 for boron/glass. Two variations of T-300 graphite/glass/epoxy were investigated. The first was a prepreg purchased from 3M Co., and had a spacing between glass bundles in each layer of approximately 1.9 cm. The second material was made by United Technologies Research Center (UTRC), and had a glass bundle spacing of 0.5 cm. The AU graphite/glass/epoxy was also purchased in prepreg form from 3M and had the same construction as the T-300/glass/epoxy from that source. All other materials were prepared by UTRC with the exception of the AS graphite-epoxy used in the superhybrids which was obtained from 3M. The boron/S-glass/polysulfone: AS graphite/S-glass/epoxy was a laminated material having an outer shell of the boron/glass/polysulfone and an inner core of graphite/glass/epoxy. As a result of the widely different hot pressing conditions for the two matrix materials (270°C, 6.9 $MN/m^2$, 5 min for the polysulfone and 150°C, 2.1 $MN/m^2$, 2 hrs for PR-288 epoxy), this material was prepared in a two step operation. The polysulfone matrix shells were fabricated and one side was sandblasted. These shells were stacked as the top and bottom layers in the laminate with a film of FM-1000 adhesive immediately adjacent to each, and the graphite/glass/epoxy prepreg in the center. The adhesive and the PR-288 matrix resin were then co-cured at 175°C, 4.2 $MN/m^2$ for 2 hrs.

The final three materials in the listing have been termed superhybrids. The exact constructions utilized for flat laminates with a nominal thickness of 0.3 cm are given in Tables I, II, and III. For laminates in which a smaller thickness was desired, such as those utilized for longitudinal tension, the same ratios of materials were maintained insofar as possible. For the sake of brevity, these materials will be designated as S.H. #1, S.H. #2, and S.H. #3 hereafter. All three materials were fabricated by the same general procedure. The titanium alloy foil was etched in a solution consisting of 40g sodium fluoride, 20g chromic oxide ($CrO_3$), 200 cc concentrated sulfuric acid, and 1 liter distilled water. The boron/aluminum was in the form of fully consolidated monolayer tape. Surface preparation of the tape consisted of vapor degrease, grit blast, and solvent rinse. The composite layers were stacked in molds in the sequences indicated in Tables I, II, and III and hot pressed at 175°C, 4.2 $MN/m^2$ for 2 hrs.

### 2.1.2 Testing

Specimens of each material were prepared for two general types of testing: static, including pendulum impact, for which flat panels were fabricated, and ballistic impact which utilized blade-like specimens having a tapered cross section.

The mechanical tests which were conducted on flat panels are briefly described below:

Flexure - 3 point loading at a span-to-depth ratio of 32:1.

Short beam shear - 3 point loading at a span-to-depth ratio of 4:1.

Pendulum impact - "Charpy" loading conditions; unnotched specimens having nominal dimensions of .25 cm thick x 1 cm wide x 5.5 cm long (thin specimens); striker was instrumented to provide load-time trace.

Longitudinal tension - straight-sided specimens, 15.2 cm long, with fiberglass doublers, 6.3 cm long, adhesively bonded at each end; strain measured with strain gages.

Transverse tension - straight-sided specimens, 10 cm long, with fiberglass doublers, 3.8 cm long, adhesively bonded at each end; strain measured with strain gages.

Longitudinal and transverse compression - "Celanese" method utilizing straight-sided specimen, 11.3 cm long, with 5 cm fiberglass doublers bonded at each end; end loading introduced by shear; strain measured with strain gages.

Table I

Superhybrid Laminate Composition

S.H. #1

Ti-6-4, 3 mil
FM 1000 adhesive
Titanium, 3 mil
FM 1000
B/Al, 5.6 mil/6061
FM 1000
B/Al, 5.6 mil/6061
FM 1000
AS/Epoxy
AS/Epoxy
AS/Epoxy
AS/Epoxy
AS/Epoxy
AS/Epoxy
FM 1000
Titanium, 3 mil
FM 1000
AS/Epoxy
AS/Epoxy
AS/Epoxy
AS/Epoxy
AS/Epoxy
AS/Epoxy
FM 1000
B/Al
FM 1000
B/Al
FM 1000
Titanium, 3 mil
FM 1000
Titanium, 3 mil

Table II

Superhybrid Laminate Composition

S.H. #2

Ti-6-4, 3 mil
FM 1000
Titanium, 3 mil
FM 1000
AS/Epoxy
AS/Epoxy
AS/Epoxy
AS/Epoxy
AS/Epoxy
AS/Epoxy
AS/Epoxy
AS/Epoxy
AS/Epoxy
AS/Epoxy
FM 1000
Titanium, 3 mil
FM 1000
AS/Epoxy
AS/Epoxy
AS/Epoxy
AS/Epoxy
AS/Epoxy
AS/Epoxy
AS/Epoxy
AS/Epoxy
AS/Epoxy
AS/Epoxy
FM 1000
Titanium, 3 mil
FM 1000
Titanium, 3 mil

Table III

Superhybrid Laminate Composition

S.H. #3

Ti-6-4, 3 mil
FM 1000
Titanium, 3 mil
FM 1000
B/Al, 5.6 mil/6061
FM 1000
B/Al, 5.6 mil/6061
FM 1000
AS/Epoxy
AS/Epoxy
AS/Epoxy
AS/Epoxy
AS/Epoxy
AS/Epoxy
AS/Epoxy
AS/Epoxy
AS/Epoxy
AS/Epoxy
AS/Epoxy
AS/Epoxy
AS/Epoxy
AS/Epoxy
AS/Epoxy
AS/Epoxy
FM 1000
B/Al
FM 1000
B/Al
FM 1000
Titanium, 3 mil
FM 1000
Titanium, 3 mil

Shear modulus - straight-sided specimens, 15.2 cm long x 2.5 cm wide, subjected to dead weight torsional loading.

Ballistic testing was conducted using the blade-like specimen and test procedure first described by Friedrich (Ref. 3). Briefly, the test apparatus consisted of a high pressure air cannon which was used for firing gelatin projectiles at cantilevered specimens. The gelatin projectiles were spheres, 2.5 cm in diameter having a density of approximately 1 g/cc. Projectile velocity just prior to impact was determined by using two photocell timers to measure the time for the projectile to travel a fixed distance. Figure 1 is a schematic diagram of the photocell system. This velocity was subsequently checked by examination of high speed movies (~8500 frames/sec) which were made of each test. The approximate projectile velocities were selected by varying tank pressure to the gun according to a predetermined calibration curve.

The specimen used in the ballistic testing had overall dimensions of 20.4 cm long x 7.6 cm wide. The cross-section was uniformly tapered in thickness from the center (mid chord) to both edges (leading edge and trailing edge) resulting in a "blade-like" geometry. However, unlike a blade, the cross-section was constant over the entire length and the specimen had neither camber nor twist. In addition the specimen was held between fiberglass doublers in a vise rather than having any designed root attachment.

## 2.2 Results and Discussion

### 2.2.1 Static and Pendulum Impact

Static and pendulum impact data for all materials are summarized in Tables IV and IVa. Several of the flexural moduli of the specimens were quite low, but in most cases the tensile moduli of the same materials were substantially higher. It is known that the shear deformation present in the three point flexural test can produce an error in the calculated bending modulus, however at the large span to depth ratio used in the tests (32/1), such effects are thought to be small. The fact that the flexural moduli of all the materials were approximately 15% less than the tensile moduli implies that there was a real difference in the two tests which was not accounted for. The low flexural moduli of the superhybrids were not considered to be surprising because the superhybrids were designed to have a balance of bending and torsional stiffness in an all 0° ply configuration. This is believed to be a feature of primary importance with superhybrids since utililization of angle plies inevitably involves greater material waste in cutting. The ability of the superhybrids to carry multi-directional loads means that the more valid property comparison is between superhybrids and angle ply composites of a conventional nature. This comparison is made in Task II of the program.

## WIRING SCHEMATIC OF BALLISTIC IMPACT TEST TIMING SYSTEM

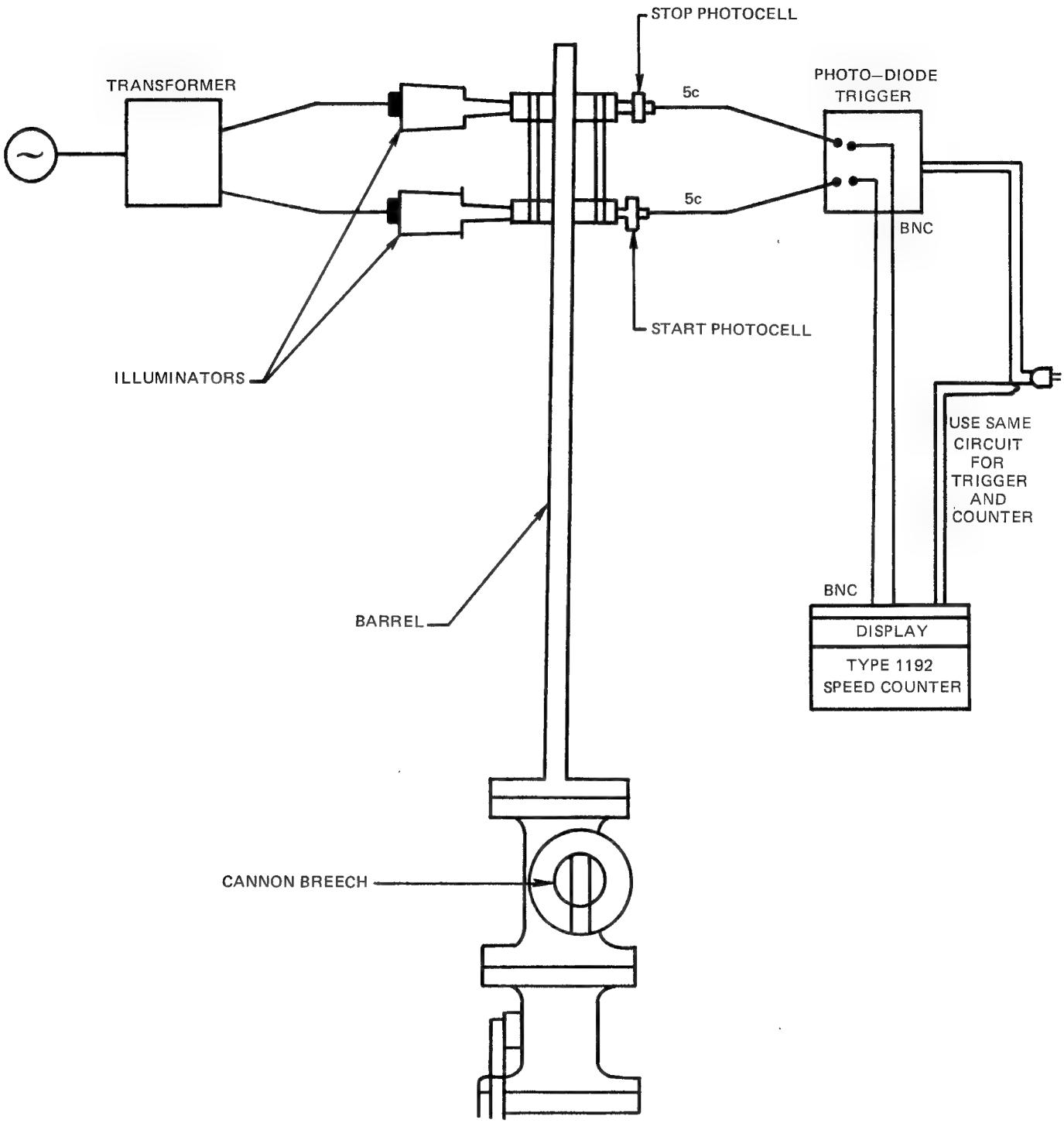


76–03–193–1

Table IV

Task I - Mechanical Test Results
0° Ply Configuration
S.I. Units

| | Flexural | | Shear | Thin Pendulum Impact | | Long. Tension | | Trans. Tension | | Long. Compression | | Trans. Compression | | Density | Shear Mod. |
|---|---|---|---|---|---|---|---|---|---|---|---|---|---|---|---|
| | σ | E | τ | Load | Energy | σ | E | σ | E | σ | E | σ | E | ρ | G |
| | ($MN/m^2$) | ($GN/m^2$) | ($MN/m^2$) | (N) | (joules) | ($MN/m^2$) | ($GN/m^2$) | ($MN/m^2$) | ($GN/m^2$) | ($MN/m^2$) | ($GN/m^2$) | ($MN/m^2$) | ($GN/m^2$) | (g/cc) | ($GN/m^2$) |
| T300/Glass/Epoxy (3M) | 1270 | 75.8 | 105 | 1550 | 3.5 | 1150 | 112 | 63 | 10.8 | 951 | 114 | 148 | 15.2 | 1.63 | 4.72 |
| | 1370 | 90.3 | 109 | 1420 | 4.5 | 1370 | 123 | 45 | 10.6 | 876 | 130 | 158 | - | | 5.19 |
| | 1500 | 82.7 | 109 | 1380 | 3.8 | 1200 | 108 | 57 | 10.6 | 1050 | 130 | 159 | 14.1 | | 5.14 |
| T300/Glass/Epoxy (UTRC) | 1740 | 130 | 67 | >1290 | 4.7 | 1440 | 152 | 36 | 12.8 | 1130 | 143 | - | - | 1.70 | 5.10 |
| | 1830 | 131 | 68 | 1590 | 5.3 | 1360 | 148 | 48 | 14.6 | 1180 | 159 | 109 | 11.7 | | 5.27 |
| | 1720 | 127 | 67 | 1520 | 4.1 | 1300 | 142 | 52 | 14.3 | 1130 | 128 | 124 | 12.8 | | 4.96 |
| AS/Glass/Epoxy | 1300 | 95.8 | 114 | 950 | 3.7 | 1090 | 106 | 73 | 13.5 | 1620 | 127 | 132 | 12.6 | 1.70 | 5.10 |
| | 1530 | 91.7 | 111 | 950 | 3.8 | 1230 | 108 | 70 | 13.7 | 1450 | 120 | 132 | 14.1 | | 4.96 |
| | 1450 | 95.1 | 113 | 950 | 4.2 | 965 | 106 | 46 | 12.3 | 1250 | 124 | 135 | 15.5 | | 5.03 |
| AS/Glass/B/Epoxy | 1580 | 120 | 60 | 1120 | 4.2 | 848 | 139 | 59 | 18.8 | 1300 | 141 | 129 | 16.4 | 1.80 | 9.31 |
| | 1520 | 127 | 106 | 1290 | 4.1 | 951 | 140 | 70 | 17.0 | 986 | 143 | 114 | 17.3 | | 10.0 |
| | 1290 | 134 | 98 | 1290 | 4.2 | 1000 | 141 | 70 | 16.2 | 1030 | 145 | 105 | 18.8 | | 8.76 |
| B/Glass/Epoxy | >1870 | 105 | 104 | >2170 | 13.7 | 1340 | 132 | 48 | 22.9 | 1820 | 178 | 241 | 22.1 | 2.02 | 7.45 |
| | >1920 | 108 | 102 | 2720 | 12.0 | 1310 | 134 | 44 | 23.9 | 1540 | 176 | 235 | 24.1 | | 6.89 |
| | >1960 | 111 | 107 | 2540 | 12.0 | 1250 | 143 | 61 | 18.8 | 1670 | 171 | 241 | 22.4 | | 7.31 |
| B/Glass/P1700 polysulfone | 1340 | 128 | 63 | 1090 | 10.0 | 1070 | 127 | - | - | 979 | 156 | 79 | 26.1 | 2.10 | 10.3 |
| | 1300 | 128 | 69 | 1090 | 9.9 | 1010 | 162 | 4 | 27.3 | 1080 | 155 | 112 | 23.9 | | 10.0 |
| | 1200 | 129 | 66 | 1020 | 10.0 | 1060 | 134 | 10 | 25.1 | 876 | 157 | 108 | 26.3 | | 10.7 |
| B/Glass/P1700/AS/Glass/Epoxy | 1300 | 100 | 79 | 1550 | 4.9 | 931 | 109 | 43 | 14.3 | 540 | 114 | 129 | 16.9 | 1.75 | 5.07 |
| | 1310 | 104 | 73 | 1660 | 5.8 | 848 | 111 | 41 | 13.0 | 610 | 111 | 142 | 16.6 | | 5.86 |
| | 1400 | 102 | 76 | 1600 | 6.6 | 1050 | 125 | 43 | 13.6 | 696 | 112 | 133 | 16.1 | | 5.48 |
| S.H. #1$(Ti/BAl/AS/Ti)_s$ | 1290 | 99.3 | 65 | 2540 | 2.6 | 786 | 117 | 146 | 42.1 | 896 | 115 | 122 | - | 1.98 | 13.1 |
| | 1250 | 94.5 | 74 | 2030 | 2.2 | 855 | 118 | 162 | 40.8 | 945 | 120 | 170 | 44.1 | | 12.1 |
| | 1110 | 98.6 | 74 | 2110 | 2.6 | 779 | 116 | 150 | 35.7 | 1020 | 126 | 176 | 44.8 | | 11.9 |
| S.H. #2$(Ti/AS/Ti)_s$ | 1110 | 66.0 | 88 | 2160 | 2.2 | 938 | 98 | 132 | 19.5 | 883 | 108 | 219 | 18.1 | 1.81 | 6.89 |
| | 1020 | 72.4 | 84 | 2240 | 3.0 | 951 | 92 | 148 | 20.3 | 807 | 96 | 272 | 22.3 | | 6.09 |
| | 1120 | 71.7 | 84 | 1900 | 1.6 | 724 | 94 | 131 | 20.6 | 924 | 101 | 241 | 20.1 | | 7.51 |
| S.H. #3$(Ti/BAl/AS)_s$ | 1320 | 90.3 | 74 | 2540 | 2.4 | 855 | 130 | 114 | 39.3 | 924 | 143 | 123 | - | 1.95 | 10.2 |
| | 965 | 93.8 | 74 | 2590 | 2.3 | 855 | 130 | 150 | 44.1 | 1080 | 149 | 156 | 35.7 | | 10.96 |
| | 1240 | 93.8 | 72 | 2670 | 2.4 | 855 | 124 | 131 | 43.8 | 1100 | 151 | 175 | 41.7 | | 9.10 |

Table IVa

Task I - Mechanical Test Results
0° Ply Configuration
English Units

| | Flexural | | Shear | Thin Pendulum Impact | | Long. Tension | | Trans. Tension | | Long. Compression | | Trans. Compression | | Density | Shear Mod. |
|---|---|---|---|---|---|---|---|---|---|---|---|---|---|---|---|
| | σ (ksi) | E (msi) | τ (ksi) | Load (lbs) | Energy (ft-lbs) | σ (ksi) | E (msi) | σ (ksi) | E (msi) | σ (ksi) | E (msi) | σ (ksi) | E (msi) | ρ (g/cc) | G (msi) |
| T300/Glass/Epoxy (3M) | 184 | 11.0 | 15.3 | 349 | 2.6 | 167 | 16.3 | 9.2 | 1.57 | 138 | 16.5 | 21.5 | 2.21 | 1.63 | .685 |
| | 199 | 13.1 | 15.8 | 320 | 3.3 | 198 | 17.8 | 6.6 | 1.54 | 127 | 18.9 | 22.9 | - | | .753 |
| | 217 | 12.0 | 15.8 | 310 | 2.8 | 174 | 15.7 | 8.3 | 1.54 | 152 | 18.9 | 23.1 | 2.05 | | .746 |
| T300/Glass/Epoxy(UTRC) | 253 | 18.8 | 9.8 | >291 | 3.5 | 209 | 22.0 | 5.2 | 1.85 | 164 | 20.7 | - | - | 1.70 | .739 |
| | 266 | 19.0 | 9.9 | 357 | 3.9 | 197 | 21.4 | 6.9 | 2.11 | 171 | 23.1 | 15.8 | 1.69 | | .765 |
| | 250 | 18.4 | 9.8 | 342 | 3.0 | 188 | 20.6 | 7.6 | 2.07 | 164 | 18.5 | 18.0 | 1.85 | | .719 |
| AS/Glass/Epoxy | 189 | 13.9 | 16.5 | 213 | 2.7 | 158 | 15.4 | 10.6 | 1.96 | 235 | 18.4 | 19.1 | 1.83 | 1.70 | .739 |
| | 222 | 13.3 | 16.1 | 213 | 2.8 | 179 | 15.7 | 10.2 | 1.99 | 211 | 17.4 | 19.2 | 2.04 | | .719 |
| | 211 | 13.8 | 16.4 | 213 | 3.1 | 140 | 15.4 | 6.7 | 1.79 | 181 | 18.0 | 19.6 | 2.25 | | .729 |
| AS/Glass/B/Epoxy | 229 | 17.4 | 8.7 | 252 | 3.1 | 123 | 20.2 | 8.5 | 2.73 | 189 | 20.5 | 18.7 | 2.38 | 1.80 | 1.35 |
| | 220 | 18.4 | 15.3 | 291 | 3.0 | 138 | 20.3 | 10.2 | 2.46 | 143 | 20.8 | 16.5 | 2.51 | | 1.45 |
| | 187 | 19.5 | 14.2 | 291 | 3.1 | 145 | 20.5 | 10.1 | 2.35 | 149 | 21.0 | 15.2 | 2.72 | | 1.27 |
| B/Glass/Epoxy | >271 | 15.3 | 15.1 | >487 | 10.1 | 194 | 19.1 | 7.0 | 3.32 | 264 | 25.8 | 34.9 | 3.20 | 2.02 | 1.08 |
| | >278 | 15.7 | 14.8 | 612 | 8.8 | 190 | 19.5 | 6.4 | 3.47 | 224 | 25.5 | 34.1 | 3.50 | | .999 |
| | >284 | 16.1 | 14.8 | 571 | 8.6 | 182 | 20.7 | 8.8 | 2.72 | 242 | 24.8 | 34.9 | 3.25 | | 1.06 |
| B/Glass/P1700 polysulfone | 195 | 18.5 | 9.2 | 244 | 7.5 | 155 | 18.4 | - | - | 142 | 22.6 | 11.5 | 3.78 | 2.10 | 1.49 |
| | 188 | 18.5 | 10.0 | 244 | 7.3 | 146 | 23.5 | 0.6 | 3.96 | 157 | 22.5 | 16.3 | 3.47 | | 1.45 |
| | 174 | 18.7 | 9.5 | 230 | 7.6 | 154 | 19.4 | 1.5 | 3.64 | 127 | 22.7 | 15.6 | 3.81 | | 1.55 |
| B/Glass/P1700/AS/Glass/Epoxy | 188 | 14.5 | 11.4 | 349 | 3.6 | 135 | 15.8 | 6.2 | 2.08 | 78 | 16.5 | 18.7 | 2.45 | 1.75 | .736 |
| | 190 | 15.1 | 10.6 | 373 | 4.3 | 123 | 16.1 | 6.0 | 1.88 | 89 | 16.1 | 20.6 | 2.41 | | .850 |
| | 203 | 14.8 | 11.0 | 359 | 4.9 | 152 | 18.1 | 6.2 | 1.97 | 101 | 16.2 | 19.3 | 2.33 | | .795 |
| S.H. #1$(Ti/BAl/AS/Ti)_s$ | 187 | 14.4 | 9.4 | 572 | 1.9 | 114 | 17.0 | 21.1 | 6.10 | 130 | 16.7 | 17.7 | - | 1.98 | 1.90 |
| | 181 | 13.7 | 10.7 | 456 | 1.6 | 124 | 17.1 | 23.5 | 5.91 | 137 | 17.4 | 24.6 | 6.40 | | 1.76 |
| | 161 | 14.3 | 10.7 | 475 | 1.9 | 113 | 16.8 | 21.7 | 5.17 | 148 | 18.3 | 25.5 | 6.50 | | 1.73 |
| S.H. #2$(Ti/AS/Ti)_s$ | 161 | 9.6 | 12.7 | 485 | 1.6 | 136 | 14.2 | 19.2 | 2.83 | 128 | 15.6 | 31.7 | 2.63 | 1.81 | 1.00 |
| | 148 | 10.5 | 12.2 | 504 | 2.2 | 138 | 13.4 | 21.4 | 2.95 | 117 | 13.9 | 39.4 | 3.23 | | .884 |
| | 162 | 10.4 | 12.2 | 426 | 1.2 | 105 | 13.6 | 19.0 | 2.99 | 134 | 14.7 | 34.9 | 2.92 | | 1.09 |
| S.H. #3$(Ti/BAl/AS)_s$ | 192 | 13.1 | 10.7 | 572 | 1.8 | 124 | 18.8 | 16.5 | 5.70 | 134 | 20.7 | 17.8 | - | 1.95 | 1.48 |
| | 140 | 13.6 | 10.7 | 582 | 1.7 | 128 | 18.9 | 21.7 | 6.40 | 156 | 21.6 | 22.6 | 5.18 | | 1.59 |
| | 180 | 13.6 | 10.4 | 601 | 1.8 | 128 | 18.0 | 19.0 | 6.35 | 159 | 21.9 | 25.4 | 6.04 | | 1.32 |

Other points of interest regarding the static data are as follows:

- good flexural strength in all materials with the expected exception of the superhybrids which are more isotropic in nature; boron/glass/epoxy specimens bottomed out in the test fixture and the strengths are therefore listed as minimum values

- good shear strength of superhybrids indicating good composite to metal adhesion; relatively low shear strength of T-300/glass/epoxy (UTRC)

- poor tensile strength of AS/boron/glass/epoxy possibly indicating that failure of the low volume fraction of high modulus boron initiated total composite failure

- poor transverse tensile strength of boron/glass/polysulfone

- good transverse tensile strength of AS/glass/epoxy and AS/glass/boron/epoxy

- excellent transverse tensile properties of the superhybrids and the effect of boron/aluminum on transverse tensile modulus (S.H. #1 and #3 vs S.H. #2)

- rather low transverse compressive strength of the superhybrids relative to the other composites without metallic components

- overall superhybrid densities about the same as boron or glass/epoxy composites

Regarding the low transverse compressive strength of the superhybrids, examination of the tested specimens indicated that the AS graphite/epoxy portion fractured but the metallic components, Ti-6-4 and/or boron/aluminum, buckled apparently after the graphite/epoxy fractured. Thus the low strength was due to the two step failure mode in which the graphite/epoxy fractured, then the thin metallic strips failed due to instability. The superhybrid with the highest transverse compressive strength was actually the one with the lowest volume fraction of metallic reinforcement (S.H. #2).

The pendulum impact data were further analyzed in order to gain more insight into the response of the materials under ballistic impact conditions. The thin specimen geometry was selected rather than the standard thickness of 1 cm as a result of the finding in Ref. 6 that the thin specimen produced better correlation with gelatin impact tests on thin flat panels. This was primarily

due to the fact that the fracture of the thick pendulum specimens was controlled by interlaminar shear failure whereas the thin pendulum specimens and the ballistic specimens failed in a combined shear and bending mode.

As mentioned previously the pendulum machine was instrumented in order to produce curves of load vs time during the test. Typical curves for each material are given in Figs. 2-7. The maximum load ($P_{max}$) and the energy absorbed per unit area are indicated in each instance.

The boron/glass/epoxy and boron/glass polysulfone materials exhibited behavior substantially different from that of the graphite/glass/epoxy hybrids. The epoxy matrix boron hybrids sustained much higher loads and therefore higher energies than the other materials. The thermoplastic matrix composites also absorbed large amounts of energy due to the ability of the specimens to continue to carry high loads after an initial failure, apparently delamination, occurred.

The superhybrids exhibited behavior very similar to that of homogeneous AS graphite/epoxy composites as reported in Ref. 6. The load-time curves were linear to fracture, and the load dropped to zero very quickly after the initiation of failure. This resulted in rather low energy absorption relative to the other materials.

Using the data obtained from the curves, the maximum bending and shear stresses which were reached in the specimens during the impacts were calculated from standard beam equations. These data and the other pertinent data obtained from the tests are presented in Tables V and Va. In addition the average static shear and flexural strengths are given for each material for comparison with the stresses calculated from the impact tests. Comparison of the observed failure modes with the calculated stresses and static strengths indicates that, in general, the specimens should have failed primarily in a bending mode since the flexural stresses in the impact specimens were close to the statically measured strengths. The observed failure modes bear this out. Superhybrids #1 and #3 exhibited combined bending and delamination failure and the calculated flexural and shear stresses were both near the static strengths. Thus these materials could be considered to be efficiently designed since large fractions of both allowables were reached in the test.

The material which showed the least consistency between stresses in the impact test and strengths measured statically was boron/glass/polysulfone. Both the shear and flexural stresses determined from the pendulum test were substantially lower than the static strengths. The specimens failed by delamination at shear stresses less than half of the measured strength. This discrepancy could have been due to variation in quality between the static and impact specimens, but both types of samples were cut from the same laminate so such an occurrence was unlikely. Somewhat related behavior was also observed

## THIN PENDULUM IMPACT LOAD – TIME CURVES FOR CONVENTIONAL HYBRIDS

T 300/GLASS/EPOXY INTRAPLY (3M Co)

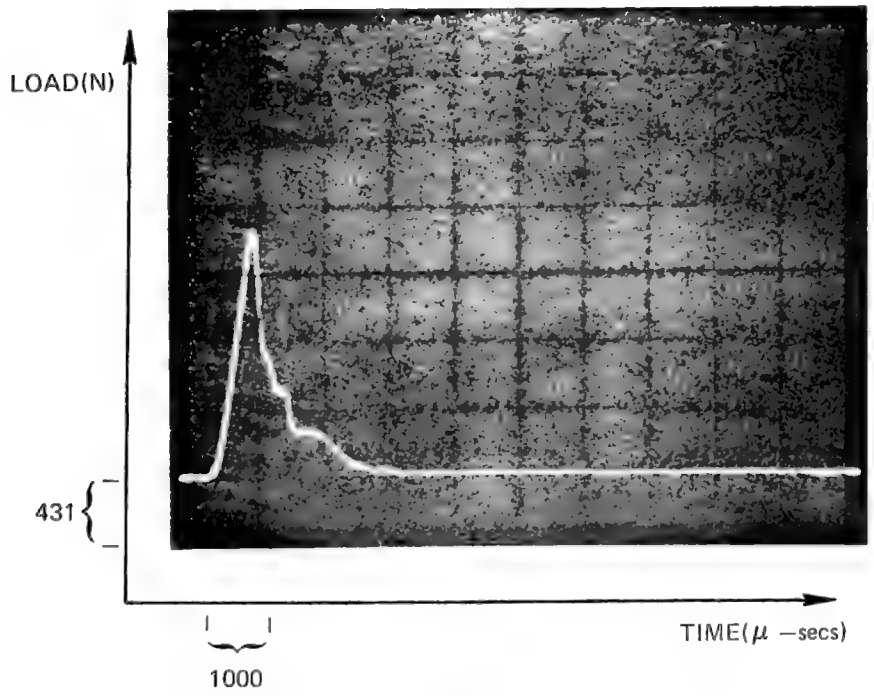


$P_{max}$ = 1420N (320 lbs)

ENERGY = $163 \times 10^3$ j/$m^2$

(78 ft–lbs/$in^2$)

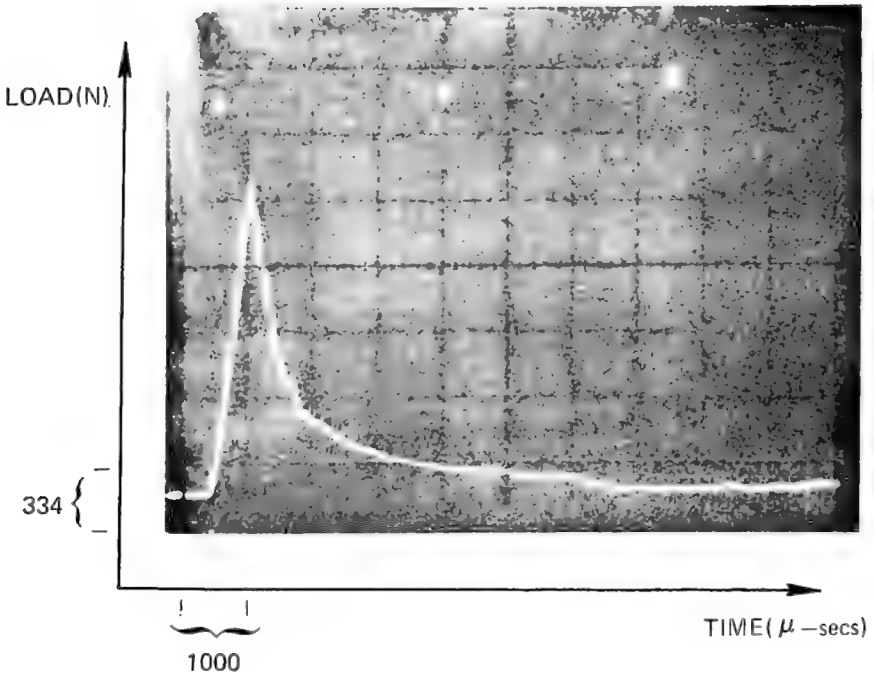


$P_{max}$ = 1590N (357 lbs)

ENERGY = $220 \times 10^3$ j/$m^2$

(105 ft–lbs/$in^2$)

76–02–208–2

## THIN PENDULUM IMPACT LOAD – TIME CURVES FOR CONVENTIONAL HYBRIDS

AS/GLASS/EPOXY/INTRAPLY

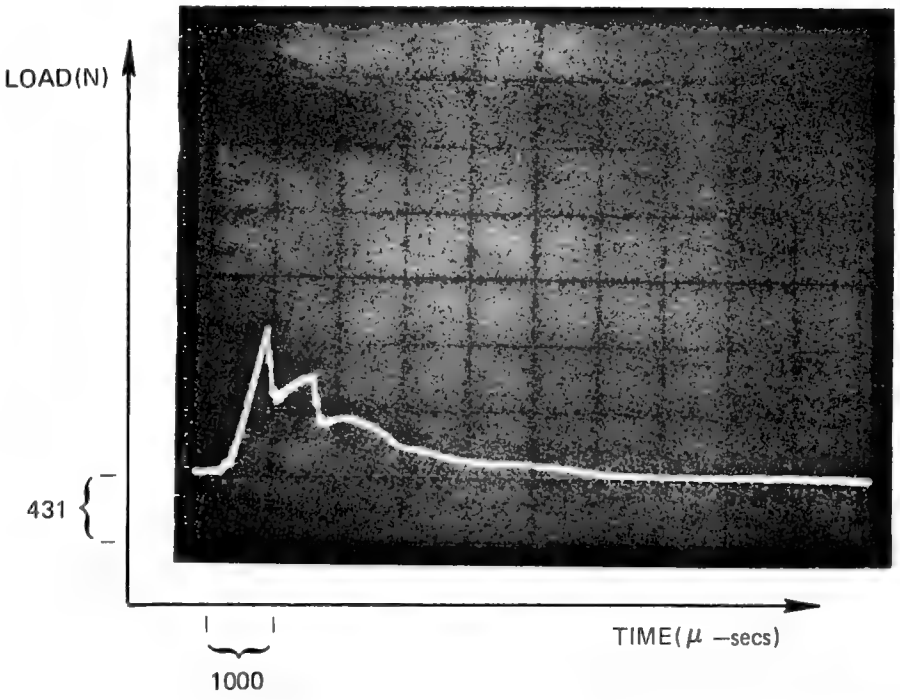


$P_{max}$ = 947N (213 lbs)

ENERGY = $193 \times 10^3$ j/$m^2$

(92 ft–lbs/$in^2$)

AS/BORON/GLASS/EPOXY INTRAPLY

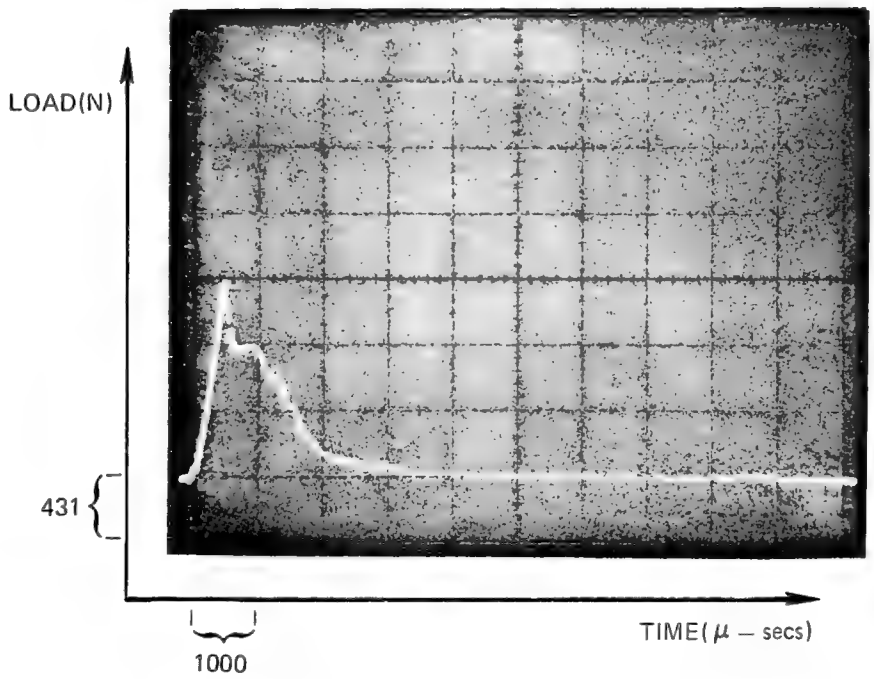


$P_{max}$ = 1290N (291 lbs)

ENERGY = $166 \times 10^3$ j/$m^2$

(79 ft – lbs/$in^2$)

76–02–208–6

## THIN PENDULUM IMPACT LOAD – TIME CURVES FOR ADVANCED HYBRIDS

BORON/GLASS/EPOXY INTRAPLY

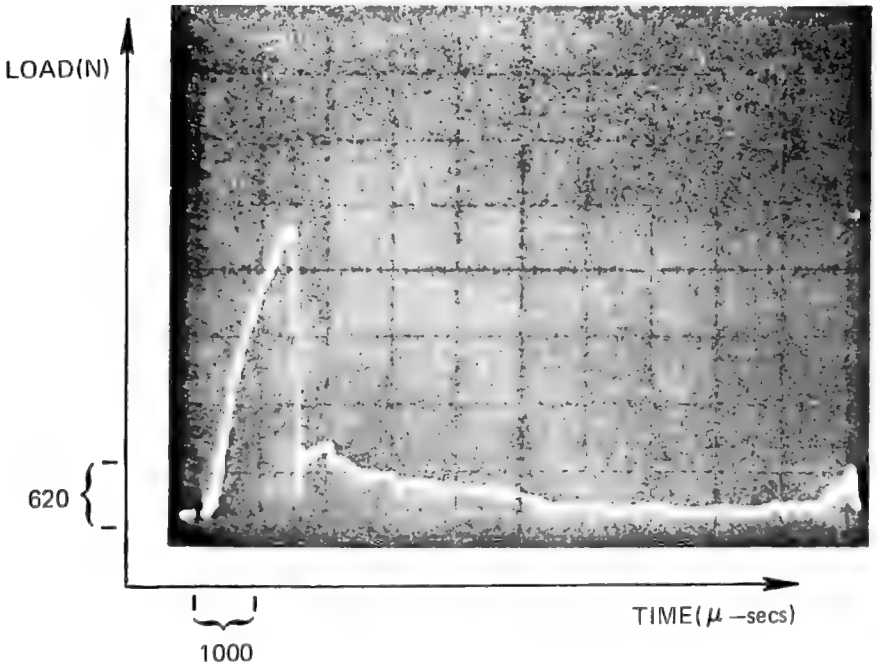


$P_{max}$ = 2540N (571 lbs)

ENERGY = $404 \times 10^3$ j/$m^2$

(193 ft–lbs/$in^2$)

BORON/GLASS/POLYSULFONE INTRAPLY

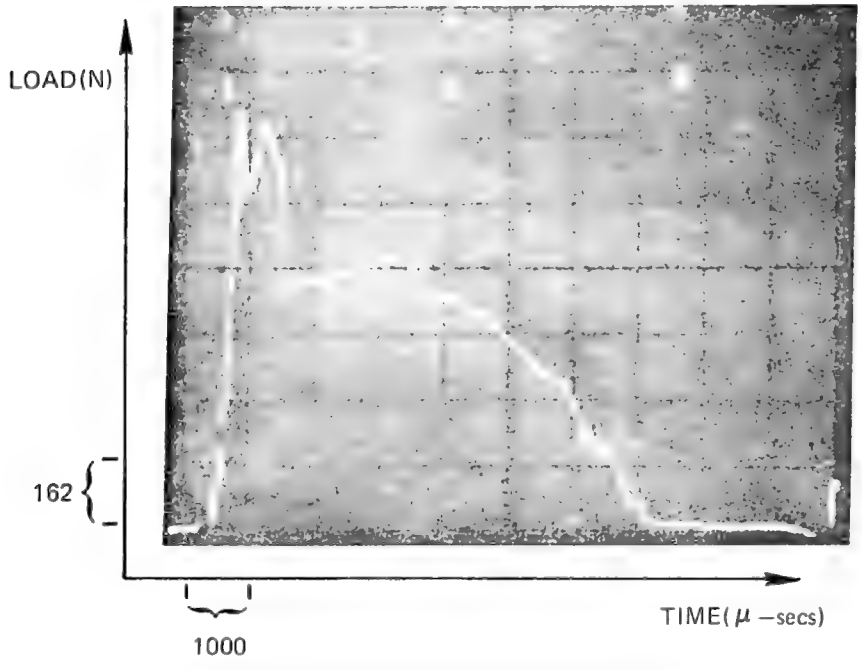


$P_{max}$ = 1020N (230 lbs)

ENERGY = $381 \times 10^3$ j/$m^2$

(182 ft–lbs/$in^2$)

76–02–208–1

## THIN PENDULUM IMPACT LOAD – TIME CURVE FOR ADVANCED HYBRID

BORON/GLASS/POLYSULFONE – AS/GLASS/EPOXY

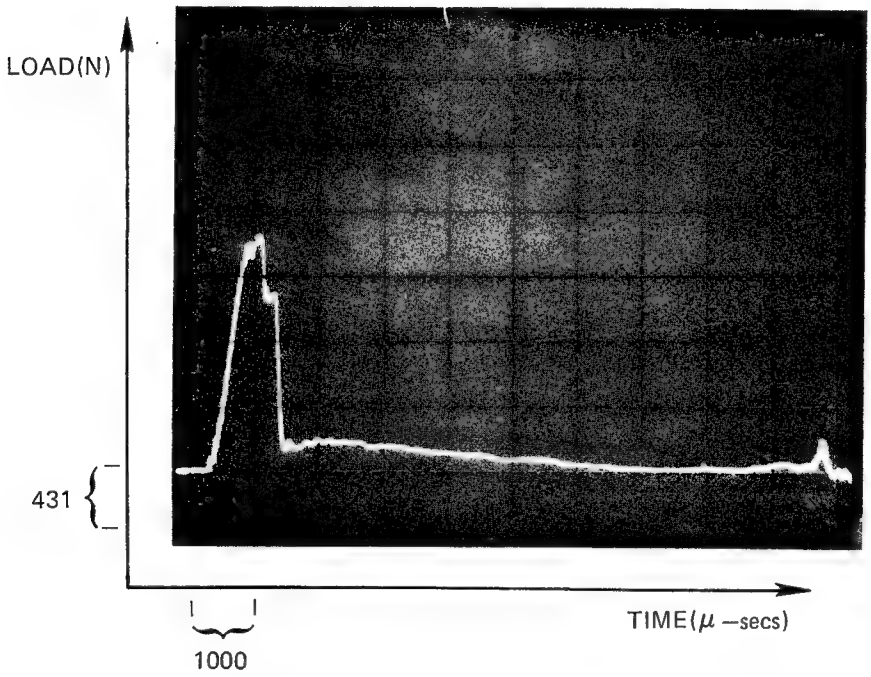


$P_{max}$ = 1552N (350 lbs)

ENERGY = $178 \times 10^3$ j/$m^2$

(85 ft – lbs/$in^2$)

76–02–208–4

## THIN PENDULUM IMPACT LOAD – TIME CURVES FOR SUPERHYBRIDS

SUPERHYBRID # 1

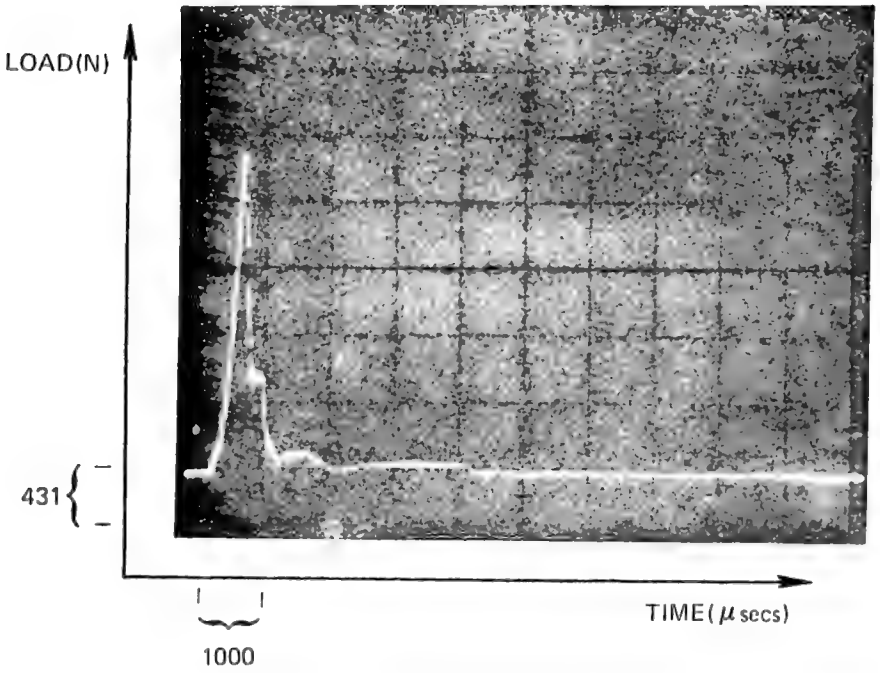


$P_{max}$ = 2110N (475 lbs)

ENERGY = $75 \times 10^3$ j/$m^2$

(36 ft – lbs/$in^2$)

SUPERHYBRID # 2

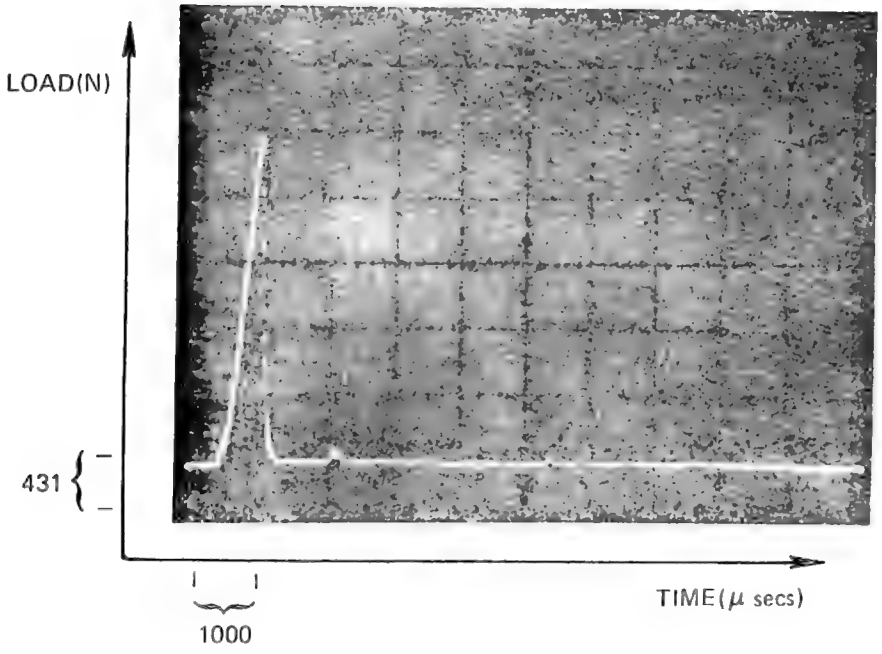


$P_{max}$ = 2160N (485 lbs)

ENERGY = $62 \times 10^3$ j/$m^2$

(30 ft – lbs/$in^2$)

76–02–208 3

## THIN PENDULUM IMPACT LOAD – TIME CURVE FOR SUPERHYBRID

SUPERHYBRID #3

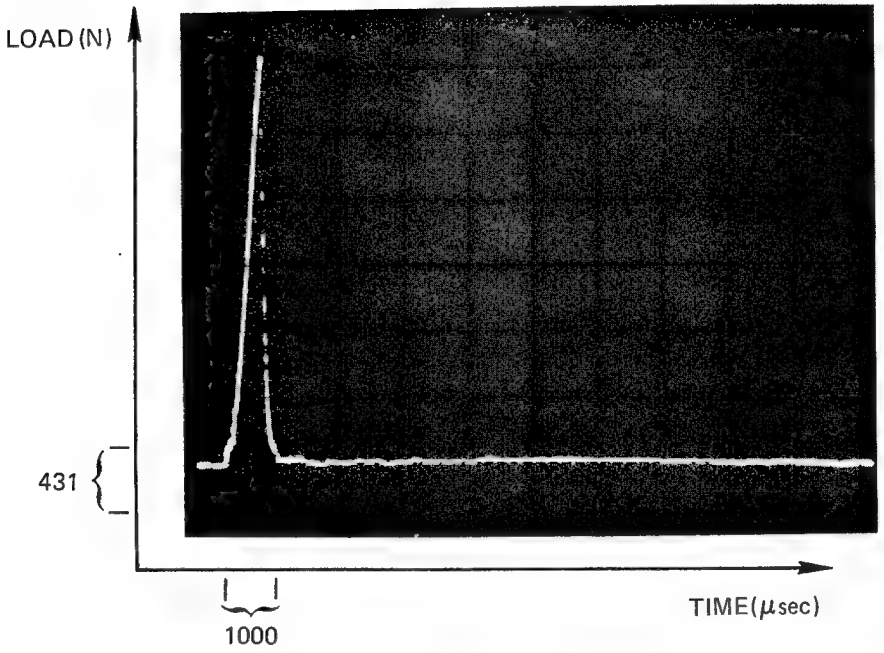


$P_{max}$ = 2670N (601 lbs)

ENERGY = $69 \times 10^3$ j/$m^2$

(33 ft–lbs/$in^2$)

76–02–208–5

Table V

Task I - Thin Pendulum Impact Results
S.I. Units

| | Width (cm) | Thickness (cm) | Load (N) | Energy (joules) | Max Shear Stress ($MN/m^2$) | Max Flexural Stress ($MN/m^2$) | Energy/Area ($10^3$ Joules/$m^2$) | Failure Mode | Static Results Ave Shear Strength ($MN/m^2$) | Static Results Ave Flex Strength ($MN/m^2$) |
|---|---|---|---|---|---|---|---|---|---|---|
| T300/G/Epoxy (3M) | 1.00 | .279 | 1550 | 3.48 | 41.6 | 1190 | 125 | Bend | 108 | 1380 |
| | 1.00 | .274 | 1420 | 4.49 | 38.8 | 1130 | 163 | Bend & backface shear | | |
| | .998 | .272 | 1380 | 3.77 | 38.1 | 1120 | 139 | Bend & splitting | | |
| T300/G/Epoxy (UTRC) | 1.00 | .236 | >1290 | 4.78 | - | - | 202 | Bend & splitting | 68 | 1770 |
| | 1.01 | .239 | 1590 | 5.29 | 49.6 | 1660 | 220 | Bend & splitting | | |
| | 1.00 | .239 | 1520 | 4.13 | 47.6 | 1590 | 172 | Bend & splitting | | |
| AS/G/Epoxy | 1.00 | .218 | 950 | 3.67 | 32.4 | 1190 | 168 | Bend & splitting | 112 | 1430 |
| | 0.998 | .216 | 950 | 3.73 | 33.0 | 1220 | 173 | Bend & splitting | | |
| | 1.00 | .216 | 950 | 4.17 | 32.8 | 1210 | 193 | Bend & splitting | | |
| AS/G/B/Epoxy | 1.01 | .254 | 1120 | 4.17 | 32.9 | 1030 | 163 | Bend | 90 | 1460 |
| | 1.01 | .254 | 1290 | 4.08 | 38.4 | 1190 | 160 | Bend | | |
| | 1.01 | .249 | 1290 | 4.15 | 38.8 | 1240 | 166 | Bend | | |
| B/G/Epoxy | 0.988 | .292 | >2170 | 13.65 | - | - | 472 | Bend | 103 | >1920 |
| | 0.991 | .292 | 2720 | 11.90 | 70.5 | 1920 | 411 | Bend & splitting | | |
| | 0.983 | .292 | 2540 | 11.60 | 66.3 | 1810 | 404 | Bend & splitting & delam | | |
| B/G/Polysulfone | 1.01 | .274 | 1090 | 10.10 | 29.5 | 855 | 366 | Delam & some bend | 66 | 1280 |
| | 1.01 | .269 | 1090 | 9.94 | 29.9 | 883 | 364 | Delam | | |
| | 1.00 | .269 | 1020 | 10.30 | 28.3 | 841 | 381 | Delam | | |
| B/G/P.S.-AS/G/Epoxy | 1.00 | .277 | 1550 | 4.95 | 41.9 | 1210 | 178 | Delam & bend | 76 | 1340 |
| | 1.01 | .279 | 1660 | 5.87 | 44.3 | 1260 | 209 | Delam & bend | | |
| | 1.00 | .279 | 1600 | 6.70 | 42.8 | 1220 | 239 | Delam & bend | | |
| S.H. #1 | 1.02 | .330 | 2540 | 2.62 | 56.5 | 1370 | 77 | Bend & delam of B/Al & delam @ center | 71 | 1210 |
| | 1.00 | .330 | 2030 | 2.22 | 46.1 | 1110 | 67 | Bend & delam of B/Al & delam @ center | | |
| | 0.996 | .348 | 2110 | 2.62 | 45.7 | 1010 | 75 | Bend & delam of B/Al & delam @ center | | |
| S.H. #2 | 1.01 | .345 | 2160 | 2.18 | 46.2 | 1070 | 62 | Bend | 86 | 1080 |
| | 1.01 | .338 | 2240 | 3.01 | 49.1 | 1160 | 88 | Bend & delam | | |
| | 1.01 | .335 | 1900 | 1.68 | 41.9 | 1000 | 49 | Bend | | |
| S.H. #3 | 1.01 | .345 | 2540 | 2.41 | 55.0 | 1270 | 70 | Bend & delam of B/Al & delam of AS | 73 | 1180 |
| | 0.993 | .348 | 2590 | 2.36 | 56.2 | 1290 | 68 | Bend & delam of B/Al & delam of AS | | |
| | 1.001 | .346 | 2670 | 2.39 | 58.2 | 1330 | 69 | Bend & delam of AS | | |

Table Va

Task I - Thin Pendulum Impact Results
English Units

| Material | Width (in) | Thickness (in) | Load (lbs) | Energy (ft-lbs) | Max Shear Stress (ksi) | Max Flexural Stress (ksi) | Energy/ Area (ft-lbs/in$^2$) | Failure Mode | Static Results: Ave Shear Strength (ksi) | Static Results: Ave Flex Strength (ksi) |
|---|---|---|---|---|---|---|---|---|---|---|
| T300/G/Epoxy(3M) | .394 | .110 | 349 | 2.57 | 6.03 | 172 | 59.3 | Bend | 15.6 | 200 |
| | .395 | .108 | 320 | 3.31 | 5.63 | 164 | 77.6 | Bend & backface shear | | |
| | .393 | .107 | 310 | 2.78 | 5.52 | 162 | 66.1 | Bend & splitting | | |
| T300/G/Epoxy(UTRC) | .395 | .093 | >291 | 3.53 | - | - | 96.1 | Bend & splitting | 9.8 | 256 |
| | .396 | .094 | 357 | 3.90 | 7.19 | 240 | 104.8 | Bend & splitting | | |
| | .395 | .094 | 342 | 3.05 | 6.91 | 231 | 82.1 | Bend & splitting | | |
| AS/G/Epoxy | .395 | .086 | 213 | 2.71 | 4.70 | 172 | 79.8 | Bend & splitting | 16.3 | 207 |
| | .393 | .085 | 213 | 2.75 | 4.78 | 177 | 82.3 | Bend & splitting | | |
| | .395 | .085 | 213 | 3.08 | 4.76 | 176 | 91.7 | Bend & splitting | | |
| AS/G/B/Epoxy | .396 | .100 | 252 | 3.07 | 4.77 | 150 | 77.5 | Bend | 13.1 | 212 |
| | .396 | .100 | 291 | 3.01 | 5.57 | 173 | 76.0 | Bend | | |
| | .396 | .098 | 291 | 3.06 | 5.62 | 180 | 78.8 | Bend | | |
| B/G/Epoxy | .389 | .115 | >487 | 10.07 | - | - | 225.0 | Bend | 14.9 | >278 |
| | .390 | .115 | 612 | 8.78 | 10.23 | 279 | 195.8 | Bend & splitting | | |
| | .387 | .115 | 571 | 8.57 | 9.62 | 263 | 192.6 | Bend & splitting & delam | | |
| B/G/Polysulfone | .396 | .108 | 244 | 7.46 | 4.28 | 124 | 174.4 | Delam & some bend | 9.6 | 186 |
| | .399 | .106 | 244 | 7.33 | 4.33 | 128 | 173.3 | Delam | | |
| | .394 | .106 | 229 | 7.58 | 4.11 | 122 | 181.5 | Delam | | |
| B/G/P.S.-AS/G/Epoxy | .395 | .109 | 349 | 3.65 | 6.08 | 175 | 84.8 | Delam & bend | 11.0 | 194 |
| | .396 | .110 | 373 | 4.33 | 6.42 | 183 | 99.4 | Delam & bend | | |
| | .395 | .110 | 359 | 4.94 | 6.20 | 177 | 113.7 | Delam & bend | | |
| S.H. #1 | .403 | .130 | 572 | 1.93 | 8.19 | 198 | 36.8 | Bend & delam of B/Al & delam @ center | 10.3 | 176 |
| | .394 | .130 | 456 | 1.64 | 6.68 | 161 | 32.0 | Bend & delam of B/Al & delam @ center | | |
| | .392 | .137 | 475 | 1.93 | 6.63 | 146 | 35.9 | Bend & delam of B/Al & delam @ center | | |
| S.H. #2 | .399 | .136 | 485 | 1.61 | 6.70 | 155 | 29.7 | Bend | 12.4 | 157 |
| | .399 | .133 | 504 | 2.22 | 7.12 | 168 | 41.8 | Bend & delam | | |
| | .399 | .132 | 427 | 1.24 | 6.08 | 145 | 23.5 | Bend | | |
| S.H. #3 | .396 | .136 | 572 | 1.78 | 7.97 | 184 | 33.1 | Bend & delam of B/Al & delam of AS | 10.6 | 171 |
| | .391 | .137 | 582 | 1.74 | 8.15 | 187 | 32.5 | Bend & delam of B/Al & delam of AS | | |
| | .390 | .137 | 601 | 1.76 | 8.44 | 193 | 32.9 | Bend & delam of AS | | |

in the ballistic impact testing of this material as will be discussed in a subsequent section. Both bits of evidence point to the possibility of a high strain rate effect which causes the material to fail in some manner at lower loads than anticipated. This is an area which warrants further study.

The thin pendulum testing of unidirectional specimens resulted in the conclusion that the best material in terms of both stress carrying ability and energy absorbing capacity was the boron/glass/epoxy hybrid. However, care must be taken in interpretation of the data and in extending any conclusions to the performance of the materials in the simulated blade testing. With the exception of the superhybrids, all materials were ballistically impacted in a multidirectional ply configuration giving rise to the possibility of different allowable stresses and failure modes than experienced in the pendulum testing of unidirectional composites. The issue was also complicated with the superhybrids because the pendulum specimens had a constant cross-section and a fixed ratio of the metallic and resin matrix materials. The ballistic impact blade-like specimen had a varying thickness cross section which was accomplished by varying the width of the graphite/epoxy plies. This resulted in a continuing change in the ratios of materials across the chord. The leading edge region, where the specimen was impacted, had a much higher ratio of metallic layers to resin matrix layers than did the pendulum impact specimen.

### 2.2.2 Ballistic Impact

Blade-like specimens were fabricated to evaluate response of the materials to impact by a "bird-like" projectile. At least two specimens having substantially different thicknesses were tested for each material. All specimens were impacted with a 2.54 cm diameter gelatin sphere at an angle of incidence of 30° and a nominal velocity of 274 m/sec (900 ft/sec). The ply configuration for all but the superhybrids was $\pm 45°/0°$ interspersed. All plies in the superhybrids were at 0° to the span direction.

The pertinent thickness dimensions, the measured projectile velocity and a brief description of the damage observed after test for each specimen are presented in Table VI. Photographs of the thinner specimen of each material are given in Figs. 8-13. Each photograph was taken looking at the leading edge from the impact side. Only the thin specimens were included in this series because the thick specimens generally suffered little or no damage.

Figures 8 and 9 show the four specimens made from the graphite/glass/epoxy intraply hybrid materials. As is evident in Fig. 8, there was not a substantial difference in the T-300/glass composites with the different glass spacing although the damage was somewhat more extensive with the narrow-spaced material. The AU primary fiber hybrid shown in Fig. 9 suffered the largest amount of delamination losing nearly all of the backface ply, while the AS reinforced

Table VI

Task I - Ballistic Impact Results

| No. | Material | L.E. Thickness (cm) | Mid Chord Thickness (cm) | Velocity (mps) | Visual Observations |
|---|---|---|---|---|---|
| 1 | AU/glass/epoxy | .084 | .390 | 283 | L.E. breakout, much delamination |
| 3A | AU/glass/eopxy | .185 | .485 | 279 | L.E. delamination |
| 2 | AU/glass/epoxy | .314 | .628 | 279 | No damage |
| 6 | T300/glass/epoxy (UTRC) | .071 | .374 | 284 | L.E. breakout, delamination |
| 7 | T300/glass/epoxy (UTRC) | .152 | .455 | 270 | L.E. delamination |
| 14 | B/glass/polysulfone | .165 | .475 | 288 | No damage |
| 14A | B/glass/polysulfone | .086 | .406 | 273 | Minor L.E. delamination |
| 24A | B/glass/epoxy | .165 | .472 | 254 | One ply delaminated @ L.E. |
| 58 | B/glass/epoxy | .076 | .414 | 257 | L.E. delamination |
| 38B | AS/glass/epoxy | .084 | .389 | 271 | L.E. breakout |
| 45 | AS/glass/epoxy | .160 | .460 | 274 | Some L.E. delamination |
| 39B | T300/glass/epoxy (3M) | .084 | .391 | 264 | L.E. breakout, delamination |
| 40 | T300/glass/epoxy (3M) | .168 | .450 | 268 | No damage |
| 47 | S.H. #2 | .112 | .401 | 275 | Very slight dent |
| 48 | S.H. #2 | .170 | .493 | 253 | No damage |
| 49 | S.H. #1 | .114 | .419 | 283 | Slight dent |
| 50 | S.H. #1 | .190 | .493 | 276 | No damage |
| 51 | S.H. #3 | .066 | .396 | 281 | Deep dent |
| 52 | S.H. #3 | .196 | .515 | 279 | No damage |
| 54 | AS/G/B/epoxy | .079 | .414 | 290 | L.E. breakout |
| 55 | AS/G/B/epoxy | .175 | .510 | 284 | Very minor L.E. damage |
| 56A | B/G/polysulfone-AS/glass/epoxy | .074 | .409 | 285 | L.E. Breakout, some tip delamination |
| 57 | B/G/polysulfone-AS/glass/epoxy | .119 | .452 | 291 | Very minor L.E. damage |

## T–300 GRAPHITE/GLASS/EPOXY IMPACTED SPECIMENS

WIDE BUNDLE SPACING (NAS–39B)

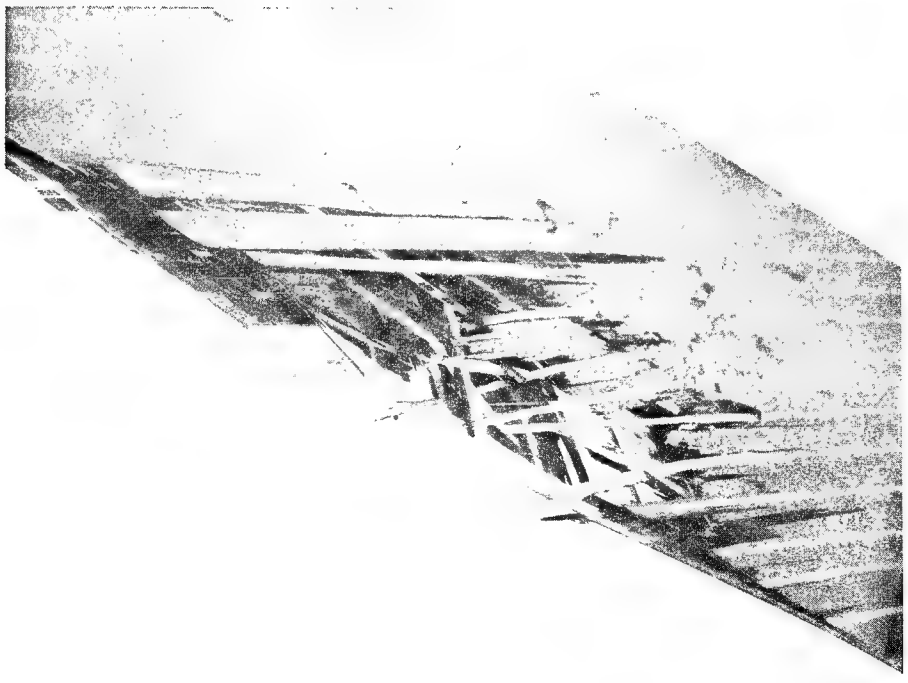

NARROW BUNDLE SPACING (NAS -6)

76–03–102 9

## TYPE A GRAPHITE/GLASS/EPOXY IMPACTED SPECIMENS

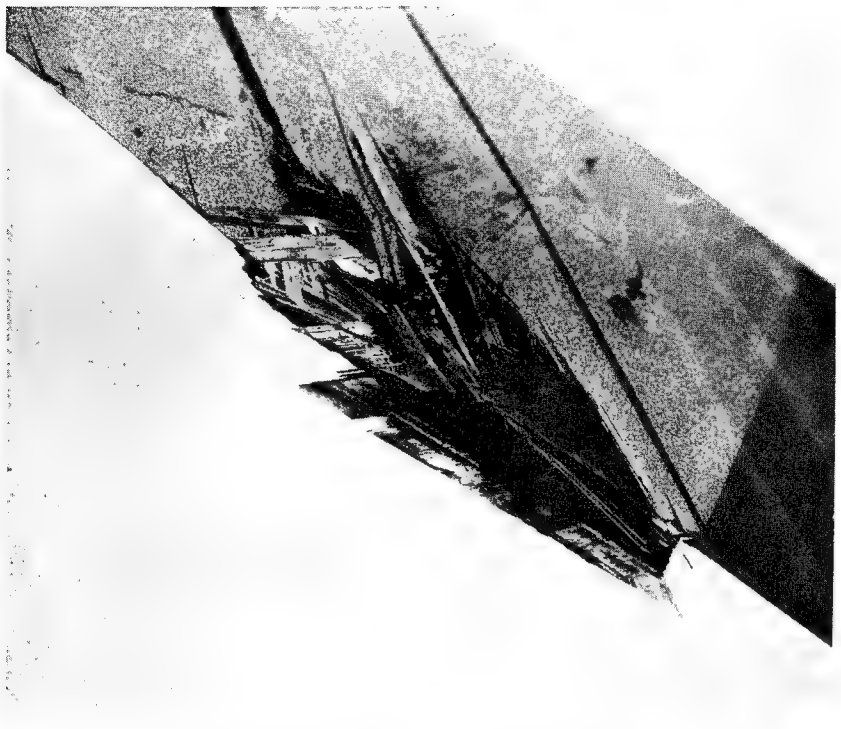

AU FIBER (NAS–1)

AS FIBER (NAS–38B)

76–03–102–8

specimen underwent very little delamination but did incur a substantial breakout at the point of impact. Specimens NAS-1 and NAS-6 were subjected to ultrasonic C-scan before and after impact to measure the extent of delamination. The tests confirmed the visual observations in that NAS-1 was delaminated over nearly 100% of its exposed area, while NAS-6 was about 75% delaminated. Based on the tests of the four graphite/glass hybrids it appears that the failure mode in these materials can be varied from primarily delamination to primarily local breakout by increasing the fiber matrix bond strength, but it does not seem possible to avoid a fairly large amount of damage under the given impact conditions.

Figure 10 shows the two boron/glass hybrids, NAS-58 having an epoxy matrix and NAS-14A having a polysulfone matrix. Both materials obviously suffered less damage than the graphite/glass hybrids. The boron/glass/polysulfone specimen underwent only a small amount of delamination at the leading edge directly under the point of impact. The damage in the epoxy matrix specimen was of a similar nature but more extensive.

The specimens having three or more reinforcing fibers are pictured in Fig. 11. Both materials failed in a local breakout mode, although in neither case was the extent of damage as great as was observed in the AS graphite/glass/epoxy specimen shown in Fig. 9. The boron/glass/polysulfone shell on NAS-56A apparently was quite effective in reducing damage since the specimen was very similar to the AS graphite/glass/epoxy specimen in other respects.

The three superhybrid specimens are shown in Figs. 12 and 13. None of the specimens showed any evidence of fracture as a result of impact. Specimen NAS-51, which was the S.H. #3 configuration sustained a dent in the leading edge at the point of impact. This result was similar to that reported in Ref. 3 for a solid Ti-6Al-4V specimen tested under similar conditions. Specimens NAS-47 and NAS-49 (S.H. #2 and #1, respectively) apparently performed even better, but as shown in Table VI, both were thicker than NAS-51.

As a result of the previous testing of each material in specimens of two thicknesses it was clear that the thickness of the specimen played an important role in the amount of damage incurred in the test. In addition, there were other variables such as projectile velocity and weight, which were not perfectly controlled from test to test, and it was felt that these too might have an influence on the results. In order to account for these variables, the procedure described in Ref. 4 was used to calculate a parameter related to the severity of each impact test. This involved first calculating the projectile energy deposited normal to the specimen surface as follows:

FIG. 10

## BORON/GLASS/RESIN IMPACTED SPECIMENS

EPOXY MATRIX (NAS–58)

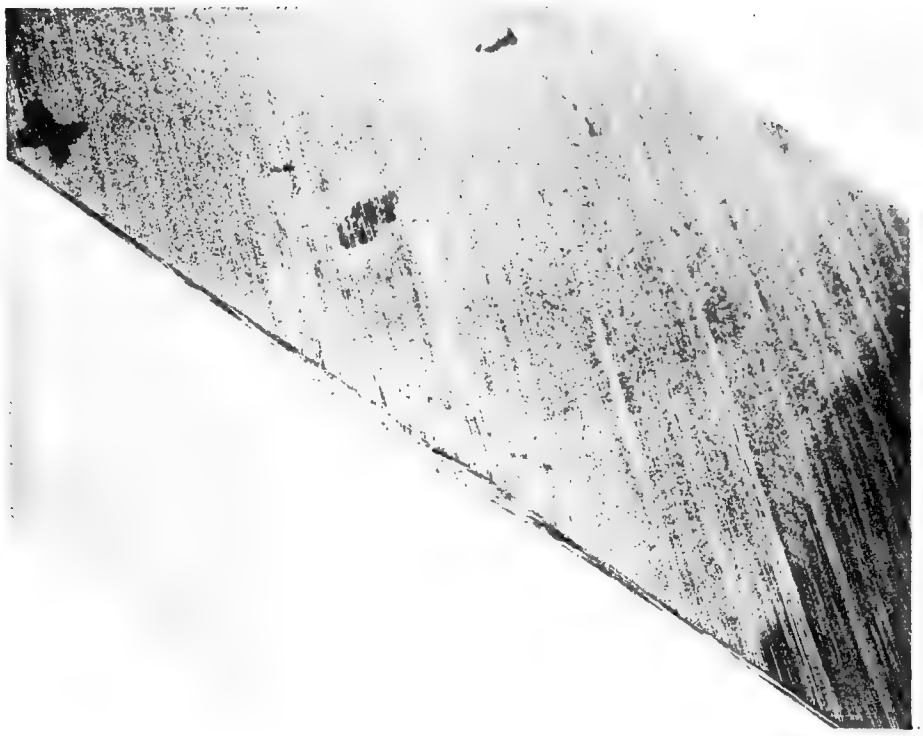

POLYSULFONE MATRIX (NAS–14A)

76–03–102–6

## MULTI–FIBER HYBRID IMPACTED SPECIMENS

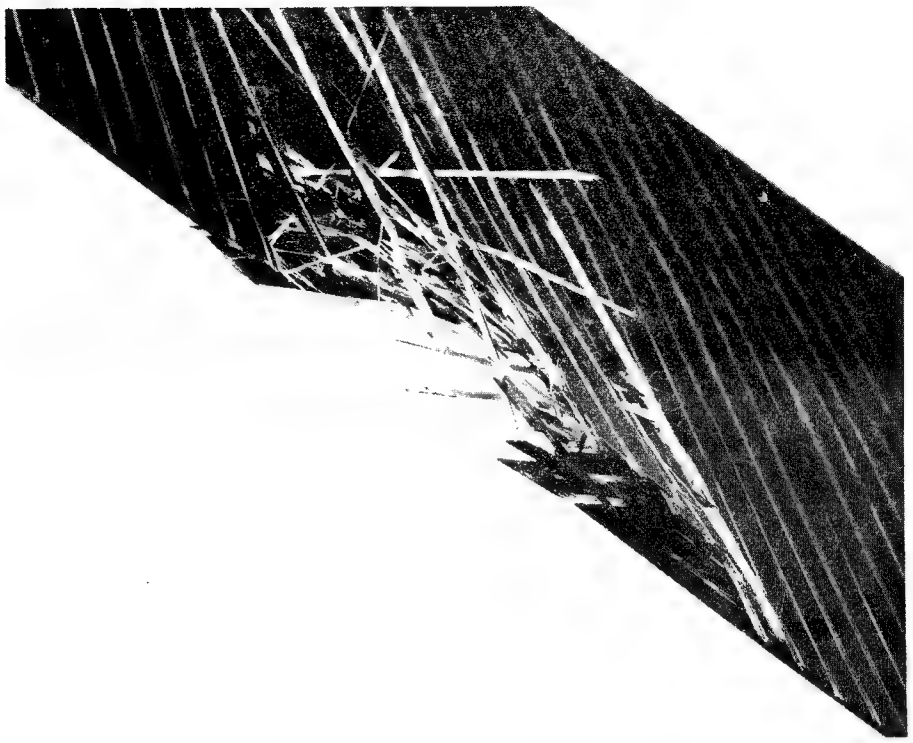

AS GRAPHITE/BORON/GLASS/EPOXY (NAS–54)

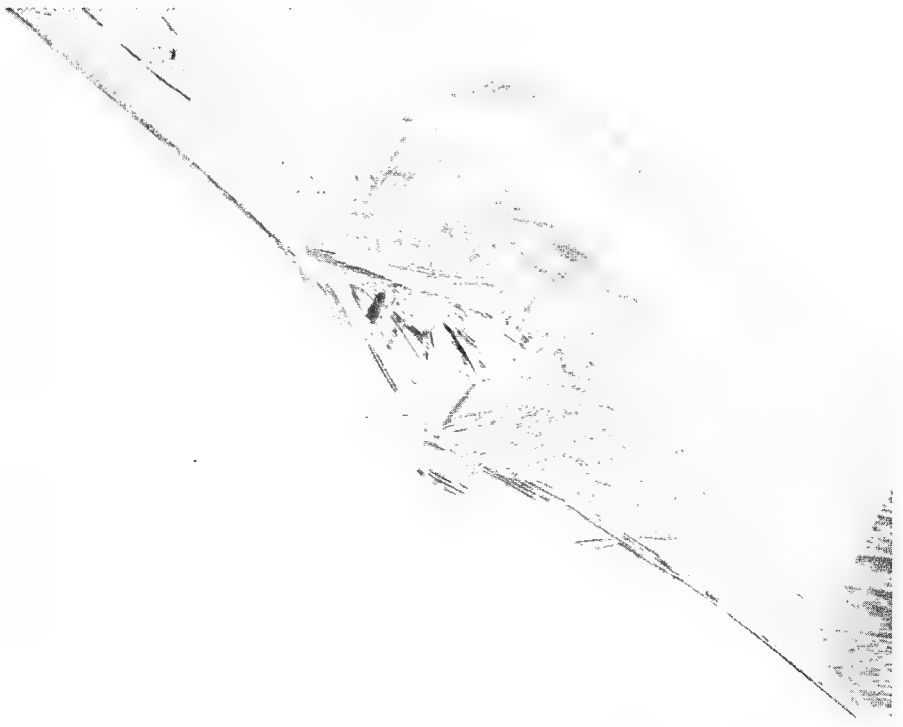

BORON/GLASS/POLYSULFONE: AS GRAPHITE/GLASS/EPOXY (NAS–56A)

76-03 102

FIG. 12

## SUPERHYBRID IMPACTED SPECIMENS

NAS–49

NAS–47

76–03–102–5

FIG. 13

## SUPERHYBRID IMPACTED SPECIMEN

NAS–51

76-03-102-4

$$\text{normal projectile energy} = 1/2\ m\ (v \sin \theta)^2$$

where $m$ = projectile mass x slice fraction
$v$ = projectile velocity
$\theta$ = angle of incidence.

The normal energy was then divided by the specimen leading edge thickness, t, to obtain the parameter K.E./t which was used to rank the severity of the impact.

The results of these calculations are presented in Table VII along with the percent of the original torsional rigidity retained after the impact, and a ranking of the visual appearance of the thin and thick specimens, exclusive of the superhybrids. The information summarized in this table served as the basis for the selection of materials for Task II.

Considering first the group of four graphite/glass/epoxy hybrids, the T-300 reinforced material supplied by 3M Co. and having the wide glass bundle spacing was selected for Task II on the basis of the excellent performance of the thicker specimen and the good modulus retention exhibited by the thin specimen coupled with the best visual appearance of this group. A review of specimen 39B in Fig. 8 indicates that a specimen can undergo a fairly large amount of damage yet retain a large fraction of its initial stiffness. Thus the use of stiffness retention alone as a measure of damage can be somewhat misleading, especially since such results are heavily dependent on failure mode.

The boron/glass hybrids performed well in terms of modulus retention in both the thin and thick configurations. However, the polysulfone matrix composites were subjected to more severe impact in both cases and had the best visual appearance ranking of all the materials. Consequently, boron/glass/polysulfone was selected for further study in Task II.

The hybrids with the multiple reinforcement, AS/boron/glass/epoxy and boron/glass/polysulfone: AS/glass/epoxy, both performed fairly well in terms of visual ranking and modulus retention. The thin specimen of the AS/boron/glass/epoxy, NAS-54, received the most severe impact of any of the specimens tested, while its counterpart in the other multifiber material, NAS-56A, received the least severe impact yet had a similar visual ranking and only an 87% retention of torsional rigidity. The behavior of the thick specimens of the two materials was also quite similar although in that case the core-shell material received the more severe impact (NAS-57). The AS/boron/glass/epoxy hybrid was selected for Task II because it appeared to be at least as good as the other material in impact resistance, and was much more straightforward to fabricate.

Table VII

Task I - Ballistic Test Data

| Material | Thin Specimens No. | KE/t Joules/cm | KE/t (ft-lbs/in.) | Visual Rank | Torsion Rigidity Retention (%) | Thick Specimens No. | KE/t Joules/cm | KE/t (ft-lbs/in.) | Visual Rank | Torsion Rigidity Retention (%) |
|---|---|---|---|---|---|---|---|---|---|---|
| T300/G/Epoxy (3M)* | 39B | 487 | 911 | 5 | 97 | 40 | 230 | 430 | 1+2 | 100 |
| T300/G/Epoxy (UTRC) | 6 | 561 | 1048 | 8 | 70 | 7 | 299 | 559 | 8 | 55 |
| AU/G/Epoxy (3M) | 1 | 570 | 1064 | 7 | 53 | 3A | 209 | 392 | 7 | 100 |
| | | | | | | 2 | 126 | 235 | - | 100 |
| AS/G/Epoxy | 38B | 460 | 861 | 6 | 83 | 45 | 254 | 475 | 6 | 100 |
| AS/G/B/Epoxy* | 54 | 639 | 1197 | 4 | 100 | 55 | 192 | 360 | 3 | 100 |
| B/G/Epoxy | 58 | 371 | 694 | 2 | 100 | 24A | 217 | 407 | 5 | 100 |
| B/G/Polysulfone* | 14A | 517 | 967 | 1 | 100 | 14 | 322 | 602 | 1+2 | 100 |
| B/G/P.S.:AS/G/Epoxy | 56A | 428 | 801 | 3 | 87 | 57 | 391 | 731 | 4 | 100 |
| S.H. #1* | 49 | 349 | 653 | | 100 | 50 | 207 | 387 | | 100 |
| S.H. #2 | 47 | 360 | 674 | | 100 | 48 | 187 | 350 | | 100 |
| S.H. #3 | 51 | 460 | 860 | | 100 | 52 | 164 | 307 | | 100 |

*Recommended for Task II

All three superhybrid materials had excellent visual appearance after the impact. However, the K.E./t parameters for all but NAS-51 were rather low due to the relatively thick leading edges. NAS-51 suffered the most damage but did not show any evidence of fracture as mentioned previously. Since all the materials performed well the decision on the selection for Task II testing was based on other factors. S.H. #2 had no boron/aluminum which reduced flexibility in design compared with the other two. S.H. #1 and S.H. #3 were identical except for the titanium foil in the center of S.H. #1 which resulted in slightly higher transverse properties for that material. The transverse properties were felt to be important in preventing or reducing the size of any local breakout which might occur due to impact, and as a result, S.H. #1 was chosen for further study.

Comparison of the ballistic and pendulum impact data indicates that many of the materials performed differently in the two tests, perhaps due to differences in ply angle or layer ratios as mentioned previously. All of the superhybrids appeared to perform much better in the ballistic test, although the comparison was somewhat complicated by the fact that most of the superhybrids were tested under less severe conditions than the other materials. Other contradictions between the two tests occurred with the boron/glass/epoxy and the T-300/glass/epoxy made by UTRC, both of which performed much better in the pendulum test. These findings support the conclusion of Ref. 8 that the pendulum test specimen geometry and ply configuration must duplicate that of the structure of interest as closely as possible if a meaningful assessment of material performance is to be made from the pendulum test.

## III. TASK II - PLY CONFIGURATION STUDY

The primary objectives of the second task of the program were to study the effect of ply configuration variation on the impact response of those materials other than the superhybrid, and to examine the effect of variation of projectile angle of incidence on the behavior of all the selected materials. Three of the specimens which were impacted were to be instrumented with strain gages to provide data for correlation with a finite element analysis of specimen response. In addition, static and pendulum impact properties were measured on angle-ply composites.

### 3.1 Experimental

#### 3.1.1 Materials

Each of the three conventional hybrids selected for Task II was evaluated under ballistic conditions in four ply configurations and two angles of incidence. The ply configurations were interspersed layups of $\pm 45°/0°$, $\pm 35°/0°$, $\pm 40°/\pm 10°/0°$, and $\pm 80°/\pm 15°/0°$. Typical ballistic specimen laminate designs are given below for boron/glass/polysulfone:

| Layer | Angle | | | | Width |
|---|---|---|---|---|---|
| 1 | +45 | +35 | +40 | +80 | 3.00 in. |
| 2 | 0 | 0 | -10 | -15 | 2.65 |
| 3 | -45 | -35 | -40 | -80 | 3.00 |
| 4 | 0 | 0 | +10 | +15 | 2.30 |
| 5 | +45 | +35 | +40 | +80 | 1.95 |
| 6 | 0 | 0 | -10 | -15 | 1.60 |
| 7 | -45 | -35 | -40 | -80 | 1.20 |
| 8 | 0 | 0 | -10 | -15 | 0.85 |
| 9 | 0 | 0 | 0 | 0 | 0.50 |
| 10 | 0 | 0 | 0 | 0 | 0.25 |
| ~~11~~ | ~~0~~ | 0 | ~~0~~ | 0 | ~~3.00~~ ℄ |

In addition to the ballistic testing of the conventional hybrids, three tests were performed on superhybrid #1. Since ply angle was not a variable of interest in the superhybrid concept, only the effects of projectile angle of incidence were studied. Static and pendulum impact tests were conducted on the conventional hybrids in the interspersed $\pm 45°/0°$ configuration. All material fabrication procedures were identical to those used in Task I.

### 3.1.2 Testing

Static and pendulum impact testing was conducted in the same manner as in Task I, as was the ballistic testing with the exception of the three instrumented specimens. Twelve strain gages were bonded to the backface of each specimen according to the arrangement shown in Fig. 14. The small arrows within each gage indicate the direction of strain measurement. Figure 15 is a schematic diagram of the system used to record the output of the gages during test. This system used strain gage ballast circuits to measure transient strain. The instantaneous voltage output of the gages was converted to strain by substituting known and measured valves of resistance and voltage into the equation

$$de_o = \frac{e_i R_b R_g}{(R_b+R_g)^2} F \varepsilon$$

where $e_i$ = exciting translator voltage
$e_o$ = voltage output
$R_b$ = translator ballast resistance
$R_g$ = strain gage resistance
$F$ = gage factor
$\varepsilon$ = strain

Twelve strain gage translators supplied voltage to the specimen gages. Upon specimen impact, resistance change of the gases caused output voltage oscillations. The voltage output signals were amplified and sent through a network to a wide band Group II tape recorder and dual beam oscilloscope and memory scope.

The scopes provided test and post test monitoring of the resultant gage voltage outputs. Textronics model 502A oscilloscope provided visual display of the voltage output waveform while the Nicolet memory scope provided a voltage/time history of the signal over the particular time base of interest.

A Sangamo recorder simultaneously recorded the high frequency voltage response of all gages on individual channels.

To distinguish initiation of the impact event an external trigger was supplied to the recorder and scopes. The air cannon timing system photodiode start signal was utilized for triggering the dynamic strain measurement system. As the sabot gelatin projectile tripped the upstream photocell, a sweep signal was transmitted to both scopes and recorder.

FIG. 14

## STRAIN GAGE LOCATIONS ON BLADE–LIKE SPECIMENS

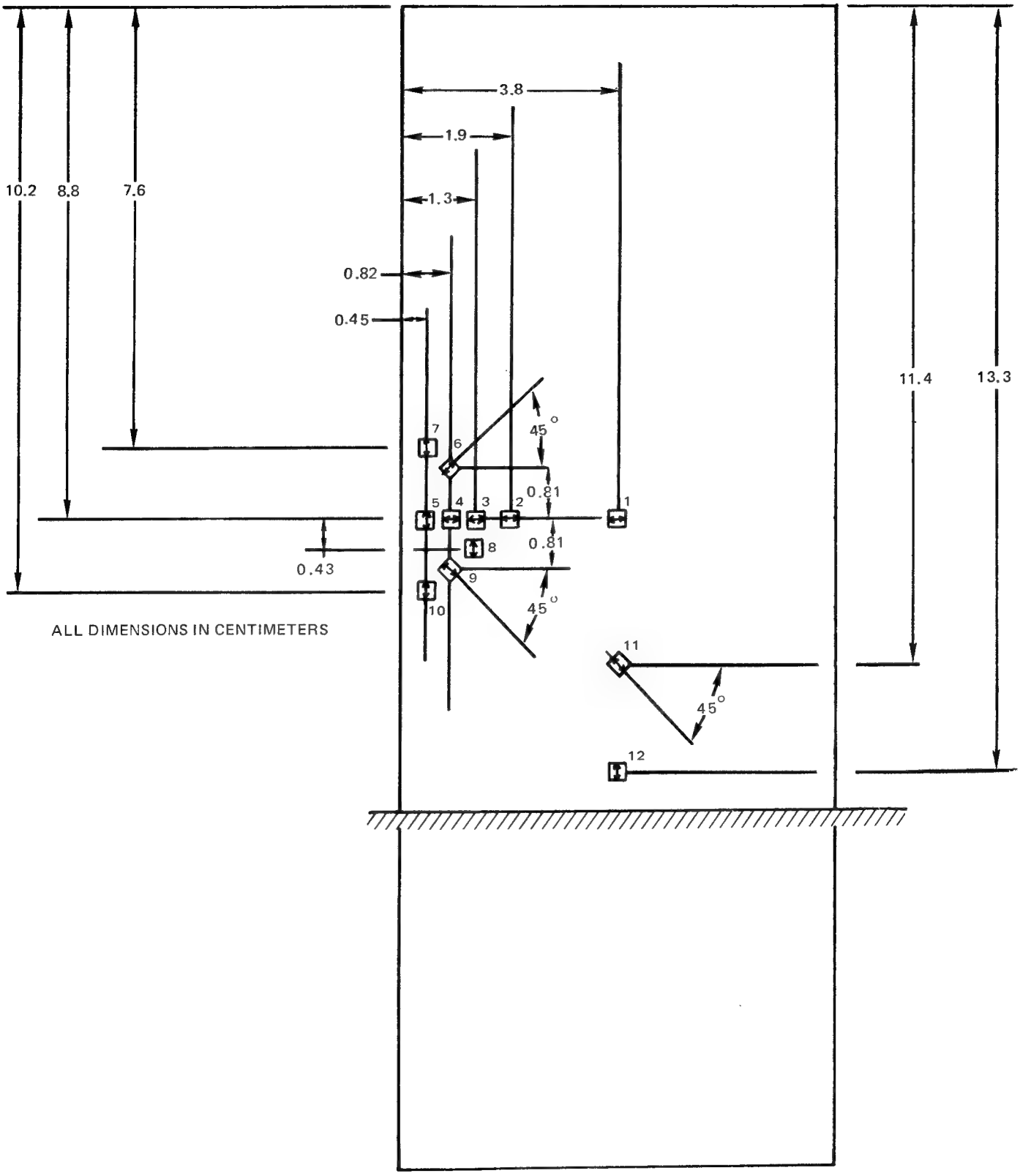


76–03–13–1

## IMPACT TESTING WIRING SCHEMATIC

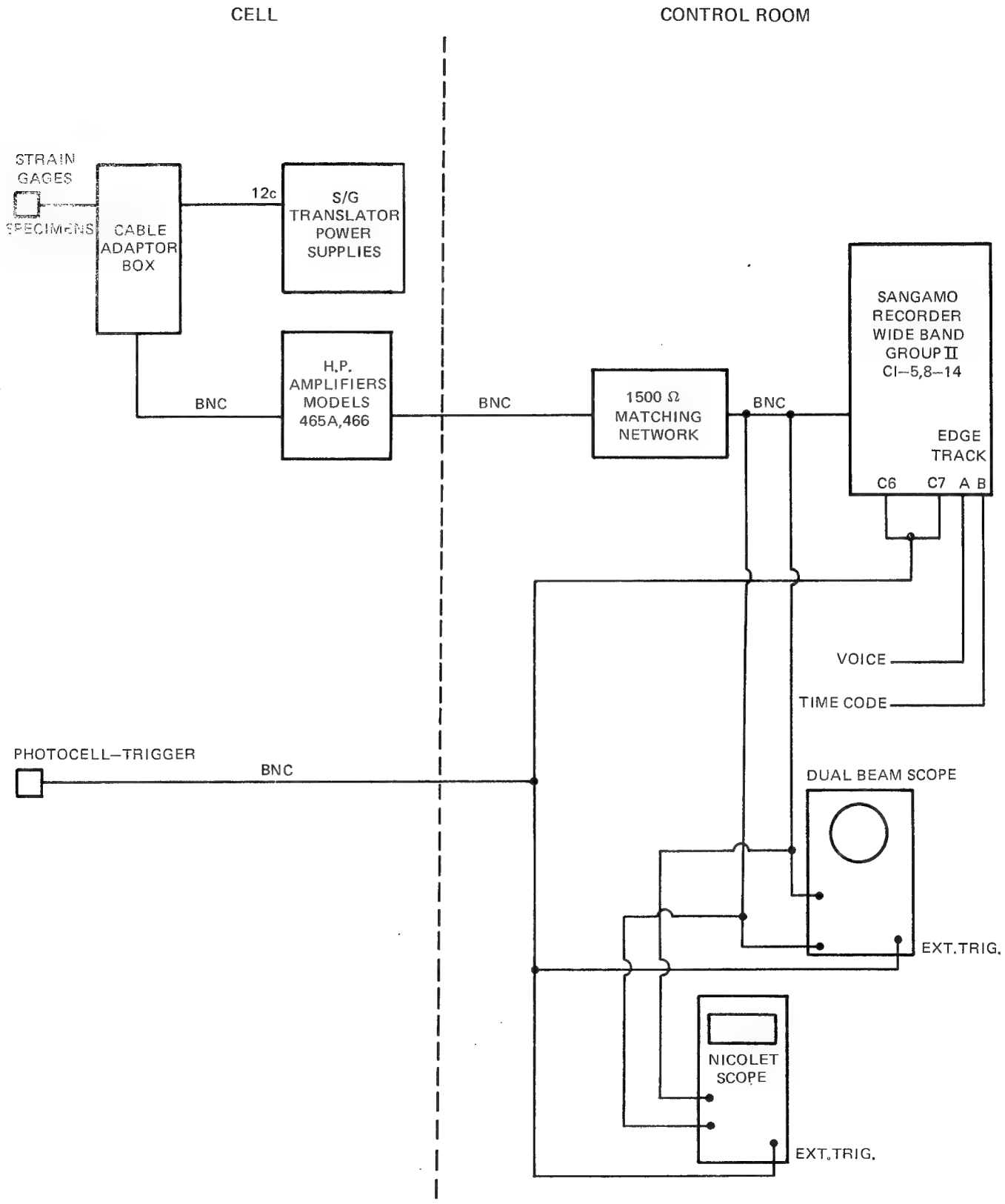


76–03–193–2

Calibration of the dynamic strain measurement system was conducted prior to testing by inputting a known oscillating voltage signal at the amplifier input for all channels. Voltage signals were input at various frequencies up to 120 KHZ using a Wavetex Analyzer. The calibration recordings were then played back for comparison with the input voltage signals.

Specimen data retrieval was accomplished by playing back the taped gage responses through the Nicolet memory scope and an X-Y plotter to obtain strain vs time plots for the initial 250 microsecond period after impact.

Gain settings of 40db and 20db were used during impact testing. The 40db gain setting was used for the 120-150 m/sec impacts to better resolve the output signal, at lower levels of strain. The 20db gain setting was used for the 270 m/sec impacts to prevent signal saturation in the event of high strains.

### 3.1.3 Analysis

The modal transient response capability of NASTRAN was used for the impact analysis of the blade-like specimens. The specimens were modeled with the QUADI anisotropic quadrilateral bending and membrane element. Anisotropic material properties were generated for each element from the specimen layup using classical lamination theory.

The specimen break up consisted of a rectangular mesh with 13 chordwise elements and 22 spanwise elements. The mesh was such that the break up was finest near the impact zone.

The Guyan reduction scheme was employed. As lumped masses were used, all rotations could be omitted from the problem set without any approximation. In addition, all in-plane displacement freedoms were omitted. Normal displacement freedoms were omitted in a logical manner until the model was reduced to 295 degrees of freedom. Retained freedom density was greater in the impact area to maintain local deformation capabilities at the impact site.

The transient analysis of the blade-like specimens used the first 60 modes of vibration of the reduced specimen model. A time step of 2.5 microseconds which has been shown to be acceptable, was used.

The transient load distribution was based on the gelatin projectile being treated as an incompressible fluid turning against an initially undeformed blade-like specimen. This loading model has also been shown to give satisfactory results.

## 3.2 Results and Discussion

### 3.2.1 Static and Pendulum Impact

The results which were obtained on angle-ply composites are presented in Tables VIII and VIIIa. All the materials exhibited substantially higher longitudinal tensile moduli than flexural moduli; more so than was observed with the unidirectional materials in Task I. This was attributed to the fact that the equation used to calculate the modulus in the three point bend test assumed no variation in modulus through the thickness of the beam. This assumption was violated in the $\pm 45°/0°$ angle-ply configuration of the specimens, and therefore the calculated modulus could be expected to be in error. The relatively low transverse tensile strength of the unidirectional boron/glass/epoxy was reflected in the transverse flexural and tensile strengths of the angle-ply composites. Similarly the low longitudinal tensile strength of the unidirectional AS graphite/glass/boron epoxy resulted in low longitudinal strength properties for angle ply composites of that material. The shear modulus data demonstrated the importance of high modulus relatively isotropic boron as a reinforcing agent in that both the hybrids containing boron had a substantially higher shear modulus than the T-300/glass/epoxy material. The same was true to a somewhat lesser degree with the other moduli. The pendulum impact data in the final two columns indicated a significant advantage for boron/glass/polysulfone over the other two materials in terms of both load carrying ability and energy absorption. The other two materials appeared to be equivalent although the AS graphite/glass/boron/epoxy specimens were slightly thicker, meaning the normalized data would be lower for that material.

Tables IX and IXa compare the averages of the angle-ply composite properties with those of the superhybrid material evaluated in Task II. Although the superhybrid consists of $0°$ plies in combination with titanium, it is intended to have a combination of properties suitable for blade applications. As the data in Table IX indicate, the tensile and flexural properties of the superhybrid generally exceeded those of the angle-ply hybrids, while the short beam shear strength of the superhybrid was somewhat lower than that of most of the others. The shear modulus was also lower than those of the two hybrids which contained boron reinforcement. Shear modulus is a very important parameter since it affects torsional frequency and flutter in blades; however, as discussed subsequently, the calculated torsional frequencies of the superhybrid blade-like specimen were as high as those of the other materials, indicating the importance of actual ply configuration and geometry in the structure of interest.

The pendulum impact results revealed that the superhybrids had poor energy absorbing characteristics relative to the other composites, although the maximum stresses developed in the beams during impact were quite high. It is important

Table VIII

Task II - Mechanical Test Results
$\pm 45°/0°$ Angle Ply Configuration
S.I. Units

| | Long. Flexure | | Trans. Flexure | | Long. Tension | | Trans. Tension | | Shear | | Thin Impact | |
|---|---|---|---|---|---|---|---|---|---|---|---|---|
| | $\sigma$ ($MN/m^2$) | E ($GN/m^2$) | $\sigma$ ($MN/m^2$) | E ($GN/m^2$) | $\sigma$ ($MN/m^2$) | E ($GN/m^2$) | $\sigma$ ($MN/m^2$) | E ($GN/m^2$) | $\tau$ ($MN/m^2$) | G ($GN/m^2$) | Load (N) | Energy (Joules) |
| B/Glass/P1700 | 925 | 56 | 139 | 24 | 794 | 91 | 72 | 17 | 76 | 19 | 1330 | 8.15 |
| | 952 | 61 | 164 | 20 | 752 | 94 | 78 | 20 | 65 | 20 | 1230 | 7.84 |
| | 910 | 59 | 135 | 21 | 765 | 90 | 80 | 20 | 75 | 20 | 1310 | 7.94 |
| T300/Glass/Epoxy | 938 | 60 | 293 | 18 | 794 | 76 | 178 | 19 | 92 | 12 | 875 | 3.87 |
| | 738 | 45 | 294 | 18 | 600 | 65 | 166 | 25 | 95 | 12 | 875 | 4.95 |
| | 814 | 54 | 271 | 18 | 690 | 76 | 156 | 21 | 88 | 12 | 854 | 4.18 |
| AS/Glass/Boron/Epoxy | 745 | 52 | 236 | 28 | 566 | 104 | 104 | 27 | 87 | 20 | 940 | 4.03 |
| | 642 | 58 | 244 | 27 | 566 | 109 | 94 | 28 | 83 | 20 | 815 | 3.85 |
| | 676 | 48 | 217 | 27 | 649 | 98 | 91 | 21 | 84 | 21 | 956 | 4.33 |

Table VIIIa

Task II - Mechanical Test Results
±45°/0° Angle Ply Configuration
English Units

| | Long. Flexure | | Trans. Flexure | | Long. Tension | | Trans. Tension | | Shear | | Thin Impact | |
|---|---|---|---|---|---|---|---|---|---|---|---|---|
| | σ (ksi) | E (msi) | σ (ksi) | E (msi) | σ (ksi) | E (msi) | σ (ksi) | E (msi) | τ (ksi) | G (msi) | Load (lbs) | Energy (ft-lbs) |
| B/Glass/P1700 | 134 | 8.1 | 20.1 | 3.4 | 115 | 13.2 | 10.5 | 2.5 | 11.1 | 2.8 | 298 | 6.00 |
| | 138 | 8.9 | 23.8 | 3.0 | 109 | 13.6 | 11.3 | 2.9 | 9.5 | 2.9 | 276 | 5.77 |
| | 132 | 8.5 | 19.5 | 3.1 | 111 | 13.0 | 11.6 | 2.9 | 10.9 | 2.9 | 293 | 5.85 |
| T300/Glass/Epoxy | 136 | 8.7 | 42.4 | 2.6 | 115 | 11.1 | 25.8 | 2.8 | 13.4 | 1.7 | 197 | 2.85 |
| | 107 | 6.5 | 42.6 | 2.6 | 87 | 9.4 | 24.1 | 3.6 | 13.8 | 1.8 | 197 | 3.65 |
| | 118 | 7.8 | 39.3 | 2.6 | 100 | 11.1 | 22.6 | 3.1 | 12.8 | 1.7 | 192 | 3.08 |
| AS/Glass/Boron/Epoxy | 108 | 7.6 | 34.2 | 4.0 | 82 | 15.1 | 16.5 | 3.9 | 12.6 | 2.9 | 211 | 2.97 |
| | 93 | 8.4 | 35.4 | 3.9 | 82 | 15.8 | 13.7 | 4.0 | 12.0 | 2.9 | 183 | 2.84 |
| | 98 | 6.9 | 31.5 | 3.9 | 94 | 14.2 | 13.2 | 3.1 | 12.2 | 3.1 | 215 | 3.19 |

Table IX

Angle-Ply Hybrid and Superhybrid Mechanical Properties
S.I. Units

| | Long. Flexure | | Long. Tension | | Transverse Tension | | Shear | | Thin Impact | | |
|---|---|---|---|---|---|---|---|---|---|---|---|
| | $\sigma$ ($MN/m^2$) | E ($GN/m^2$) | $\sigma$ ($MN/m^2$) | E ($GN/m^2$) | $\sigma$ ($MN/m^2$) | E ($GN/m^2$) | $\tau$ ($MN/m^2$) | G ($GN/m^2$) | Energy/Area ($10^3$ Joules/$m^2$) | Max Shear Stress ($MN/m^2$) | Max Flex Stress ($MN/m^2$) |
| B/Glass/P1700 | 932 | 59 | 773 | 92 | 77 | 19 | 72 | 20 | 311 | 38 | 1210 |
| T300/Glass/Epoxy | 828 | 53 | 696 | 72 | 167 | 22 | 92 | 12 | 160 | 23 | 718 |
| AS/Glass/Boron/Epoxy | 690 | 52 | 690 | 104 | 100 | 26 | 85 | 21 | 141 | 23 | 655 |
| S.H.#1$(Ti/BA1/AS/Ti)_s$ | 1210 | 97 | 808 | 117 | 152 | 39 | 71 | 12 | 74 | 50 | 1160 |

Table IXa

Angle-Ply Hybrid and Superhybrid Mechanical Properties
English Units

| | Long. Flexure | | Long. Tension | | Transverse Tension | | Shear | | Thin Impact | | |
|---|---|---|---|---|---|---|---|---|---|---|---|
| | σ (ksi) | E (msi) | σ (ksi) | E (msi) | σ (ksi) | E (msi) | τ (ksi) | G (msi) | Energy/Area (ft-lbs/in$^2$) | Max Shear Stress (ksi) | Max Flex Stress (ksi) |
| B/Glass/P1700 | 135 | 8.5 | 112 | 13.3 | 11.1 | 2.8 | 10.5 | 2.9 | 148 | 5.5 | 176 |
| T300/Glass/Epoxy | 120 | 7.7 | 101 | 10.5 | 24.2 | 3.2 | 13.3 | 1.7 | 76 | 3.4 | 104 |
| AS/Glass/Boron/Epoxy | 100 | 7.6 | 100 | 15.0 | 14.5 | 3.7 | 12.3 | 3.0 | 67 | 3.4 | 95 |
| S.H.#1$(Ti/BAl/AS/Ti)_s$ | 176 | 14.1 | 117 | 17.0 | 22.1 | 5.7 | 10.3 | 1.8 | 35 | 7.2 | 168 |

to recall, however, that the ply configuration of the blade-like ballistic specimen in the impact region near the leading edge consists primarily of titanium and boron/aluminum. The pendulum impact specimen configuration was more representative of the region near the blade specimen mid-chord in terms of the ratio of graphite/epoxy to titanium and boron/aluminum.

The ply configurations of the conventional hybrid pendulum specimens were representative of those utilized in the blade-like impact testing, and on the basis of both energy absorption and strength the ranking of materials would be boron/glass/polysulfone as best, followed by T-300/glass/epoxy, then AS/glass/boron/epoxy.

Examination of the stresses which were calculated from the loads recorded in the pendulum test and comparison of these with statically-measured failure stresses, reveals that all the materials failed due to flexural rather than shear stresses. The maximum shear stresses calculated from the pendulum test were generally half or less of those measured statically, while the flexural stresses were very close to the static values.

Typical load-time curves from the pendulum tests of the three angle-ply composites are shown in Figs. 16 and 17. In each case it can be observed that failure was not catastrophic, i.e. after initiation crack, propagation was interrupted and the specimen continued to carry additional load before the failure process reinitiated. This is believed to be the primary advantage of composites with a hybrid reinforcement in terms of impact improvement.

### 3.2.2 Ballistic Impact - Experimental

The test conditions and visual results of the Task II studies are given in Table X. Each tested specimen was photographed from the impact side as in Task I and these photographs are shown in Figs. 18-31. As indicated in Table X the three instrumented specimens were NAS-84A, 89B, and 91A, each of which was impacted at a 22° angle of incidence. In order to obtain reliable strain gage information the instrumented samples were first impacted at a velocity of approximately 150 meters per second which resulted in no visible damage.

The boron/glass/polysulfone specimens in Fig. 18 demonstrate the effect of angle of incidence. At 15° there was no visible damage while at 22° there was a slight delamination of the leading edge. This material in the same ply configuration when impacted at 30° (Fig. 10) sustained slightly more damage than the specimen struck at 22°. This indicates that there is a range of impact conditions over which damage will be initiated but will not be catastrophic. The $\pm 35°/0°$ and the $\pm 40°/\pm 10°/0°$ configurations in Figs. 19 and 20 were quite similar in behavior, both being somewhat more damaged than the $\pm 45°/0°$ specimens. The $\pm 80°/\pm 15°/0°$ specimens in Fig. 21 had the best visual appearance of any of

# THIN PENDULUM IMPACT LOAD–TIME CURVES FOR ANGLE–PLY HYBRIDS

BORON/GLASS/POLYSULFONE

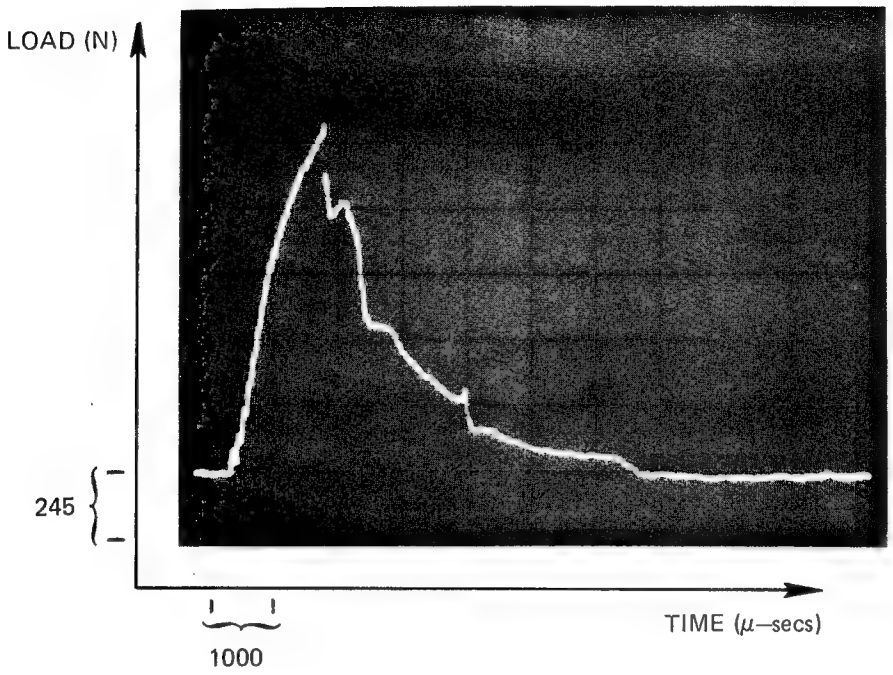


$P_{max}$ = 1230N (276 lbs)

ENERGY = $321 \times 10^3$ j/$m^2$

(153 ft–lbs/$in.^2$)

T300/GLASS/EPOXY

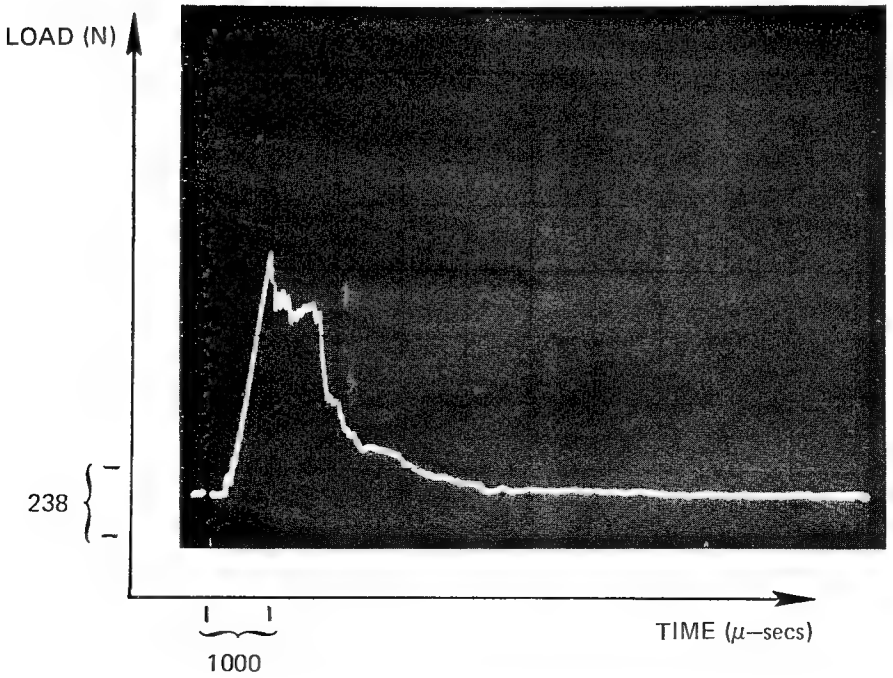


$P_{max}$ = 875N (197 lbs)

ENERGY = $144 \times 10^3$ j/$m^2$

(68 ft–lb/$in.^2$)

76–03–10–2

## THIN PENDULUM IMPACT LOAD–TIME CURVE FOR ANGLE–PLY HYBRID

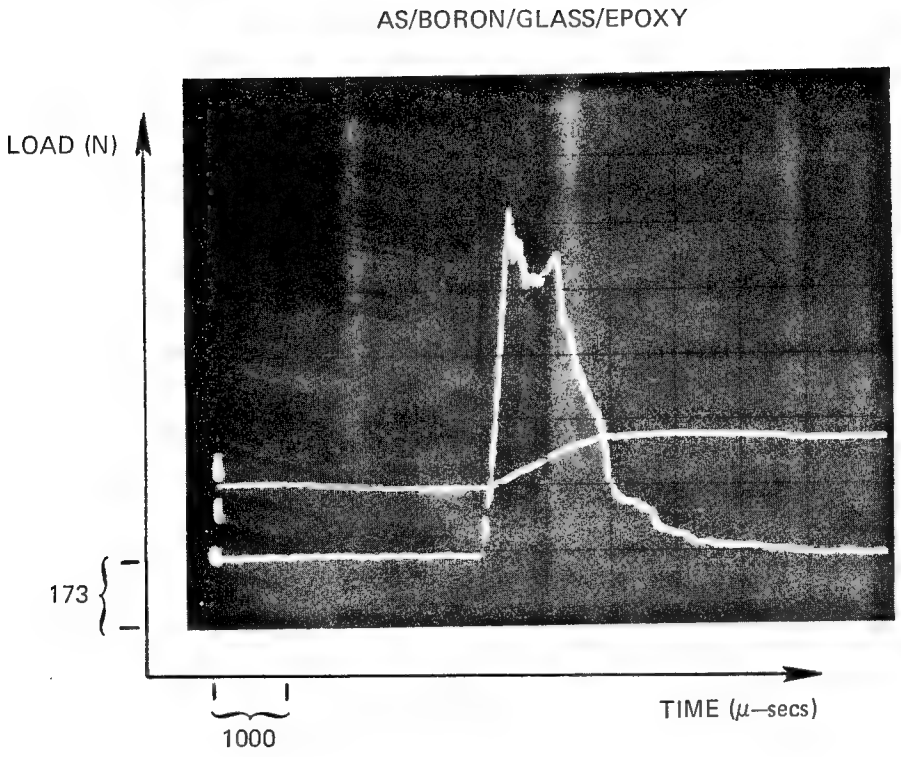

Table X

Task II - Ballistic Impact Results

| Specimen No. | Material | Ply Layup | L.E. Thickness cm | L.E. Thickness (in.) | Mid-Chord Thickness cm | Mid-Chord Thickness (in.) | Impact Angle (deg.) | Impact Velocity mps | Impact Velocity (fps) | Visual Observations |
|---|---|---|---|---|---|---|---|---|---|---|
| 78 | Boron/Glass/Polysulfone | ±45/0 | .086 | .034 | .416 | .164 | 15 | 286 | 939 | No damage |
| 78A | " | " | .094 | .037 | .419 | .165 | 22 | 261 | 855 | Very minor L.E. delamination |
| 79 | " | ±35/0 | .096 | .038 | .411 | .162 | 30 | 265 | 870 | Minor L.E. delamination |
| 79A | " | " | .102 | .040 | .419 | .165 | 22 | 272 | 893 | Minor L.E. delamination |
| 80 | " | ±40/±10/0 | .086 | .034 | .419 | .165 | 30 | 262 | 861 | Some L.E. delamination |
| 80A | " | " | .084 | .033 | .406 | .160 | 22 | 262 | 859 | Minor L.E. delamination |
| 81 | " | ±80/±15/0 | .094 | .037 | .416 | .164 | 30 | 271 | 890 | Very minor delamination @ impact |
| 81A | " | " | .089 | .035 | .419 | .165 | 22 | 272 | 892 | Minor resin flaking @ back face impact and tip |
| 84 [1] | T-300 Graphite/Glass/Epoxy | ±45/0 | .084 | .033 | .391 | .154 | 15 | 286 | 940 | No damage |
| 84A [1] | " | " | .089 | .035 | .394 | .155 | 22 | 254 | 834 | Severe delamination |
| 85 | " | ±35/0 | .079 | .031 | .381 | .150 | 30 | 278 | 911 | Severe delamination; some breakout |
| 85A | " | " | .079 | .031 | .389 | .153 | 22 | 263 | 862 | Delamination @ impact; trailing edge tip crack |
| 86 | " | ±40/±10/0 | .079 | .031 | .384 | .151 | 30 | 231 | 759 | Severe delamination |
| 86A | " | " | .079 | .031 | .381 | .150 | 22 | 266 | 873 | Some breakout; delamination @ impact and tip |
| 90 | " | ±80/±15/0 | .094 | .037 | .401 | .158 | 30 | - | - | Minor delamination @ impact |
| 90A | " | " | .107 | .042 | .419 | .165 | 22 | 263 | 863 | Minor L.E. and tip delamination |
| 89 | Ti/B-Al/Graphite/Epoxy | 0 | .102 | .040 | .414 | .163 | 15 | 274 | 899 | No damage |
| 89A | " | " | .107 | .042 | .424 | .167 | 30 | 276 | 906 | Span-wise and chord-wise fracture; delamination |
| 89B [1] | " | " | .091 | .036 | .406 | .160 | 22 | 267 | 876 | Small dent at impact |
| 89C | " | " | .102 | .040 | .427 | .168 | 30 | 268 | 879 | Small dent @ impact |
| 91 | AS Graphite/Boron/Glass/Epoxy | ±45/0 | .081 | .032 | .381 | .150 | 15 | 263 | 862 | Tip delamination; minor back face delamination |
| 91A [1] | " | " | .074 | .029 | .409 | .161 | 22 | 282 | 926 | Breakout; some delamination |
| 94 | " | ±35/0 | .076 | .030 | .406 | .160 | 30 | 275 | 904 | Breakout; delamination of back face |
| 94A | " | " | .067 | .026 | .399 | .157 | 22 | 245 | 805 | Breakout; some delamination of glass bundles |
| 95 | " | ±40/±10/0 | .061 | .024 | .406 | .160 | 30 | 264 | 867 | Breakout; some delamination of glass bundles |
| 95A | " | " | .067 | .026 | .396 | .156 | 22 | 260 | 854 | Breakout; some back face delamination |
| 96 | " | ±80/±15/0 | .076 | .030 | .406 | .160 | 30 | 253 | 829 | Breakout; delamination of back face |
| 96A | " | " | .063 | .025 | .404 | .159 | 22 | 242 | 794 | Breakout; delamination of glass bundles |

[1] Instrumented specimen; tested previously at approximately 150 mps

## BORON/GLASS/POLYSULFONE IMPACTED SPECIMENS

$\pm 45^{o}/0^{o}$

NAS–78 ($15^{o}$ IMPACT)

NAS–78A ($22^{o}$ IMPACT)

76–03–102 19

## BORON/GLASS/POLYSULFONE IMPACTED SPECIMENS

$\pm 35^{o}/0^{o}$

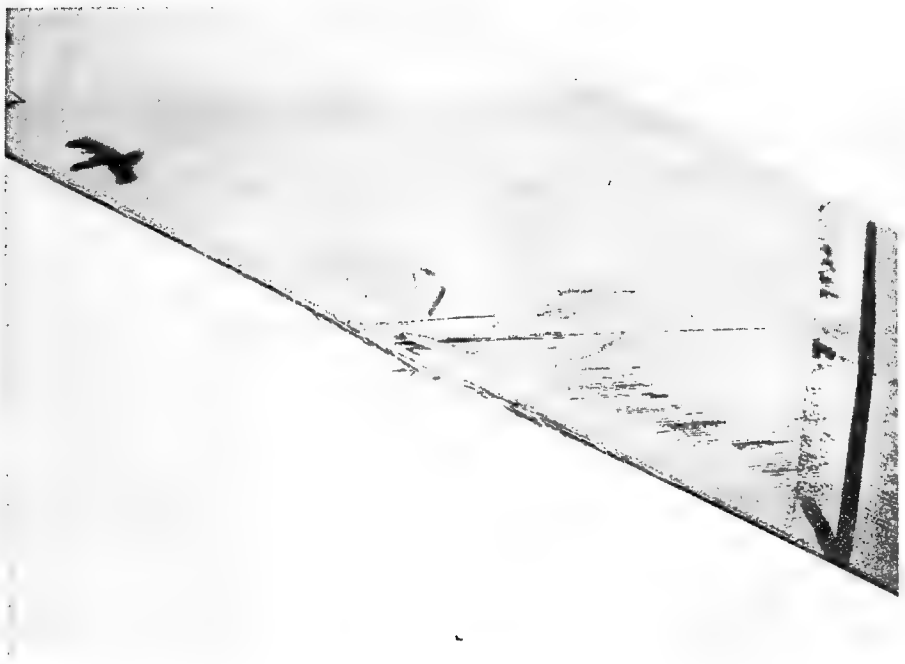

NAS–79 ($30^{o}$ IMPACT)

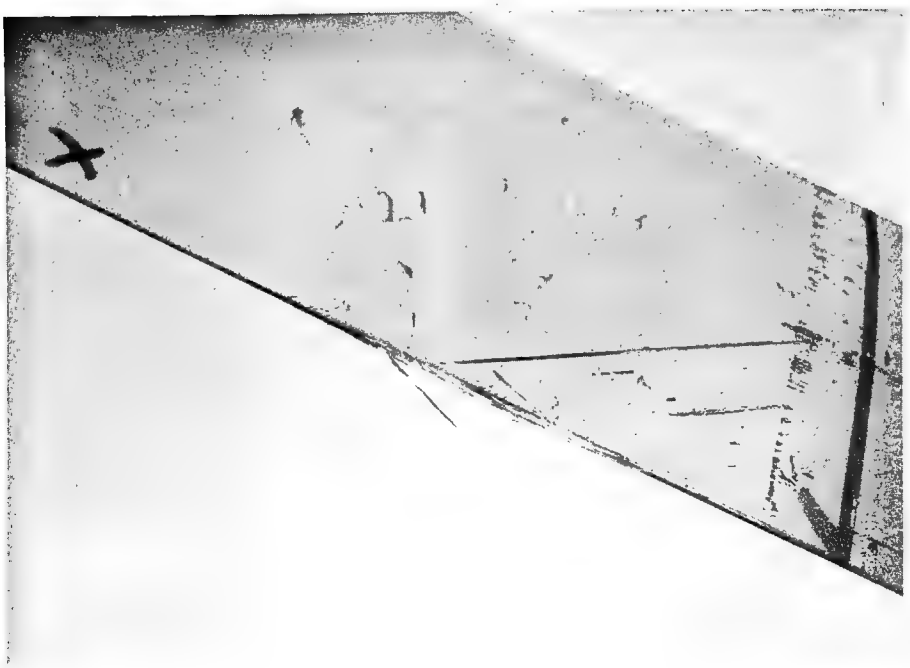

NAS–79A ($22^{o}$ IMPACT)

76–03–102–18

FIG. 20

## BORON/GLASS/POLYSULFONE IMPACTED SPECIMENS

$\pm 40^{o}/\pm 10^{o}/0^{o}$

NAS–80 ($30^{o}$ IMPACT)

NAS–80A ($22^{o}$ IMPACT)

76–03 102 -17

## BORON/GLASS/POLYSULFONE IMPACTED SPECIMENS

$\pm 80^{o}/\pm 15^{o}/0^{o}$

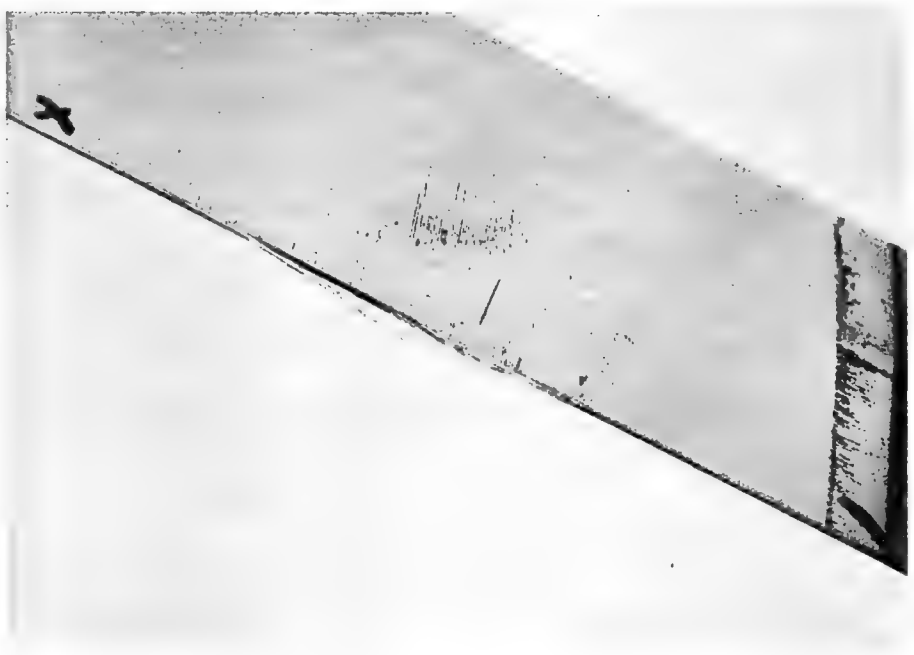

NAS–81 ($30^{o}$ IMPACT)

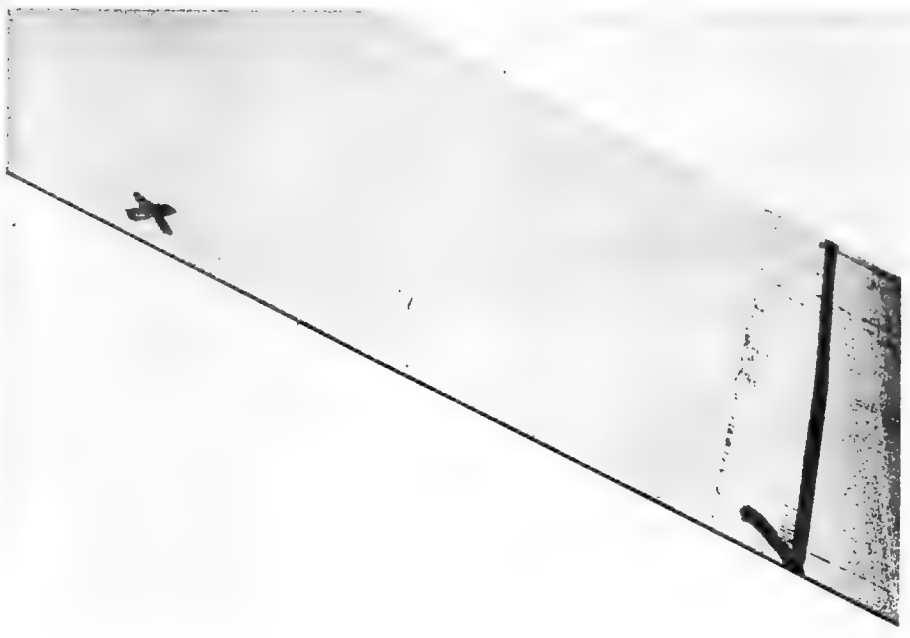

NAS–81A ($22^{o}$ IMPACT)

76–03–102–16

the specimens. Review of the movies of the impact of NAS-81 and 81A showed that both underwent a large torsional deflection upon impact yet did not undergo much visible damage. Low torsional stiffness may be a method for improving impact resistance by essentially allowing the specimen to move out of the way. However, it is not a viable approach for blade applications where frequency and flutter requirements must be met.

The $\pm 45°/0°$ specimen of T-300/glass/epoxy also survived the 15° impact with no visible damage, however the 22° impact caused a considerable amount of delamination which is evident in Fig. 22. The remaining specimens exhibited a response pattern very similar to that of the boron/glass/polysulfone. The $\pm 35°/0°$ and the $\pm 40°/\pm 10°/0°$ ply configurations were nearly identical while the $\pm 80°/\pm 15°/0°$ specimens suffered very little damage, apparently for the same reason as discussed previously.

Four superhybrid specimens were tested as shown in Figs. 26 and 27. The 15° impact resulted in no damage as might be expected. The 22° impact resulted in a small dent which can be observed in the lower portion of Fig. 26. The 30° impact on specimen NAS-89A resulted in severe damage. The failure consisted of spanwise and chordwise cracks accompanied by extensive delamination. Examination of the fracture surface showed that a large portion of the delamination occurred within the preconsolidated boron/aluminum plies, indicating that the tape was not fully densified during its preparation. A new boron/aluminum tape was prepared under a procedure which permitted better compaction of the plasma-sprayed aluminum powder, and another blade-like specimen was fabricated (no. 89C). The impact test of this specimen at 30° and a velocity of 268 mps confirmed the results of the testing in Task I; only a small dent was produced on the leading edge.

Figures 28-31 show the AS graphite/boron/glass/epoxy specimens. The damage was more extensive in general than was observed with the other materials. The 15° impact caused a small delamination in the area of the impact in the $\pm 45°/0°$ specimen. The dominant failure mode in most of the specimens was breakout rather than delamination, apparently reflecting the relatively low longitudinal strength properties of the material. The $\pm 80°/\pm 15°/0°$ specimens were significantly damaged in both tests in marked contrast to the performance of the other hybrids in that ply configuration.

As was done in Task I, the severity of each impact was determined by calculating the KE/t parameter. These results are given in Table XI along with the retention of torsional stiffness after the impact. The surprising fact about the boron/glass/polysulfone data was that two specimens which appeared to be undamaged or damaged very little, NAS-78 and 81A, exhibited relatively large losses in torsional stiffness as a result of impacts which were not too severe, especially NAS-78. This may be related to the pendulum impact response

# T–300 GRAPHITE/GLASS/EPOXY IMPACTED SPECIMENS

$\pm 45^{o}/0^{o}$

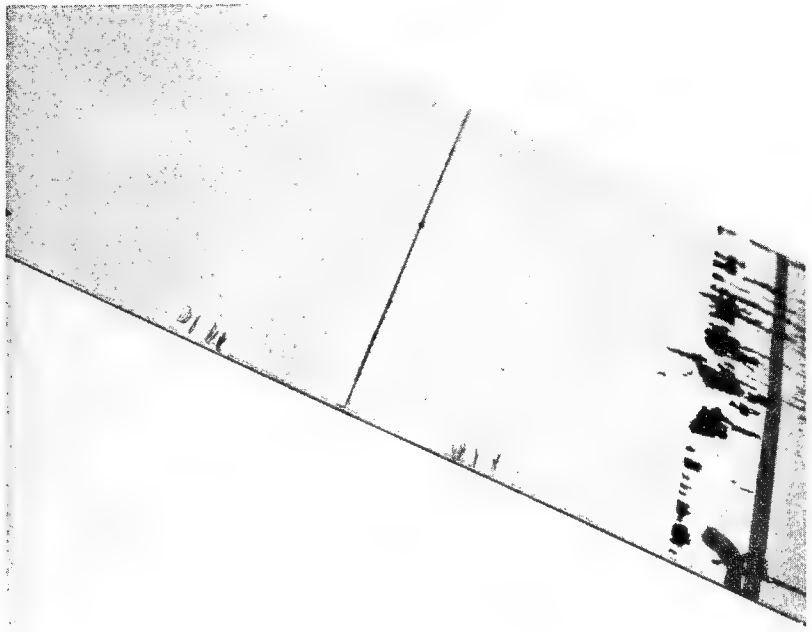

NAS–84 ($15^{o}$ IMPACT)

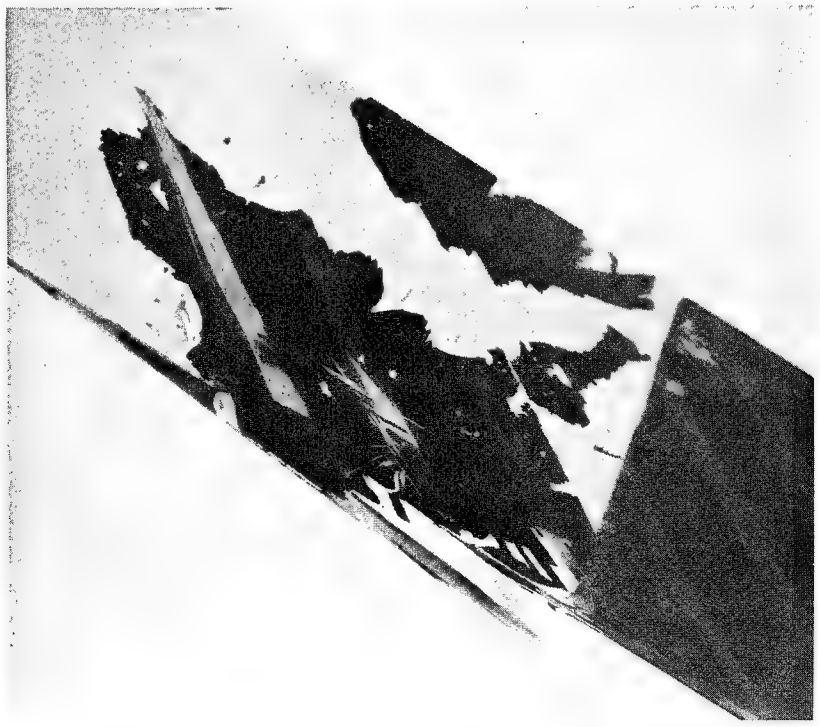

NAS–84A ($22^{o}$ IMPACT)

76–03–102–1

## T–300/GRAPHITE/GLASS/EPOXY IMPACTED SPECIMENS

$\pm 35^{o}/0^{o}$

NAS–85 (30° IMPACT)

NAS–85A (22° IMPACT)

76 -03–102–15

# T–300 GRAPHITE/GLASS/EPOXY IMPACTED SPECIMENS

$\pm 40^{o}/\pm 10^{o}/0^{o}$

NAS–86 ($30^{o}$ IMPACT)

NAS–86A ($22^{o}$ IMPACT)

76–03–102–14

## T–300 GRAPHITE/GLASS/EPOXY IMPACTED SPECIMENS

$\pm 80^{o}/\pm 15^{o}/0^{o}$

NAS–90 ($30^{o}$ IMPACT)

NAS–90A ($22^{o}$ IMPACT)

76–03–102–13

## Ti–6–4/B–Al/AS GRAPHITE/EPOXY IMPACTED SPECIMENS

NAS–89 (15° IMPACT)

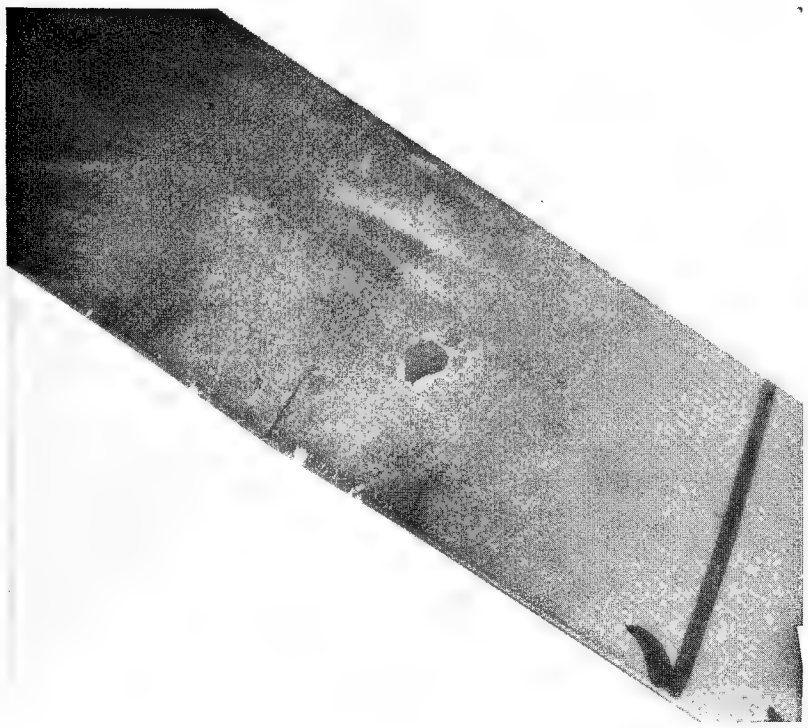

NAS–89 B (22° IMPACT)

76–03–102–2

## Ti–6–4 / B–Al / AS GRAPHITE / EPOXY IMPACTED SPECIMEN

NAS–89C (30° IMPACT)

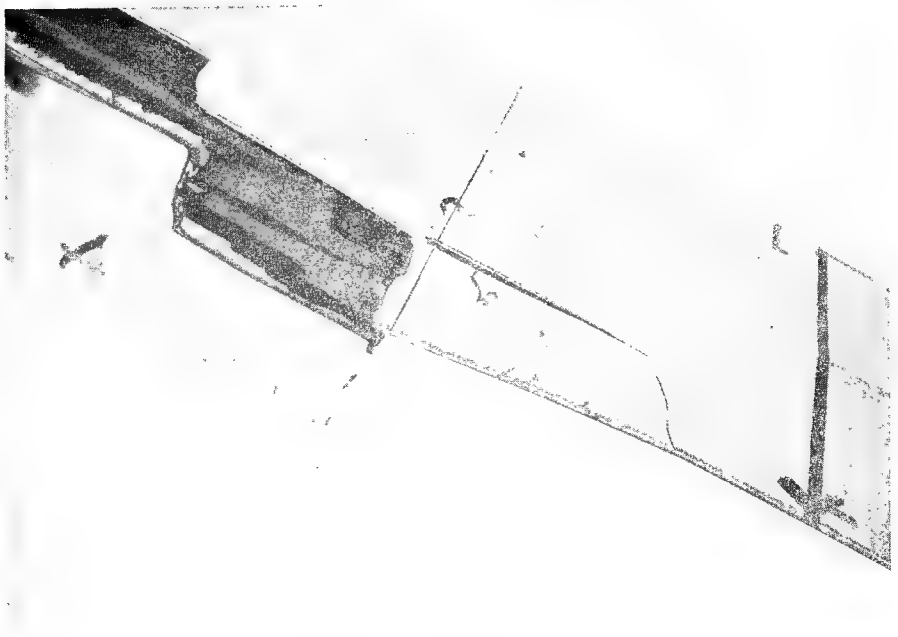

NAS–89A (30° IMPACT)

76-03-257-1

FIG. 28

## AS GRAPHITE/BORON/GLASS/EPOXY IMPACTED SPECIMENS

NAS–91 (15° IMPACT)

NAS–91A (22° IMPACT)

76–03–102–3

## AS GRAPHITE/BORON/GLASS/EPOXY IMPACTED SPECIMENS

$\pm 35^{o}/0^{o}$

NAS–94 ($30^{o}$ IMPACT)

NAS–94A ($22^{o}$ IMPACT)

76-03-102 12

FIG. 30

## AS GRAPHITE/BORON/GLASS/EPOXY IMPACTED SPECIMENS

$\pm 40^{o}/\pm 10^{o}/0^{o}$

NAS–95 ($30^{o}$ IMPACT)

NAS–95A ($22^{o}$ IMPACT)

76–03–102–11

# AS GRAPHITE/BORON/GLASS/EPOXY IMPACTED SPECIMENS

$\pm 80^{o}/\pm 15^{o}/0^{o}$

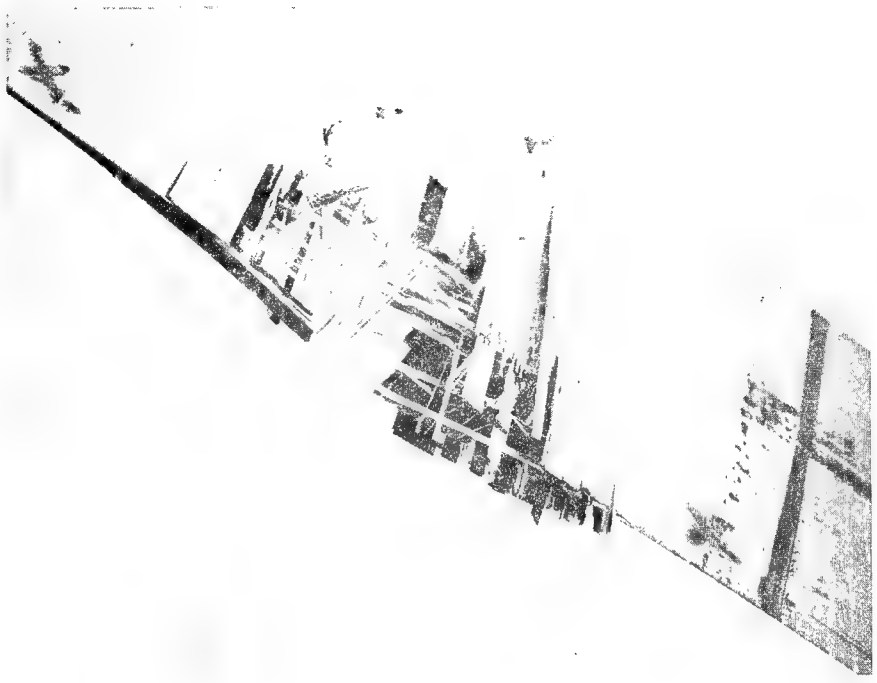

NAS–96 ($30^{o}$ IMPACT)

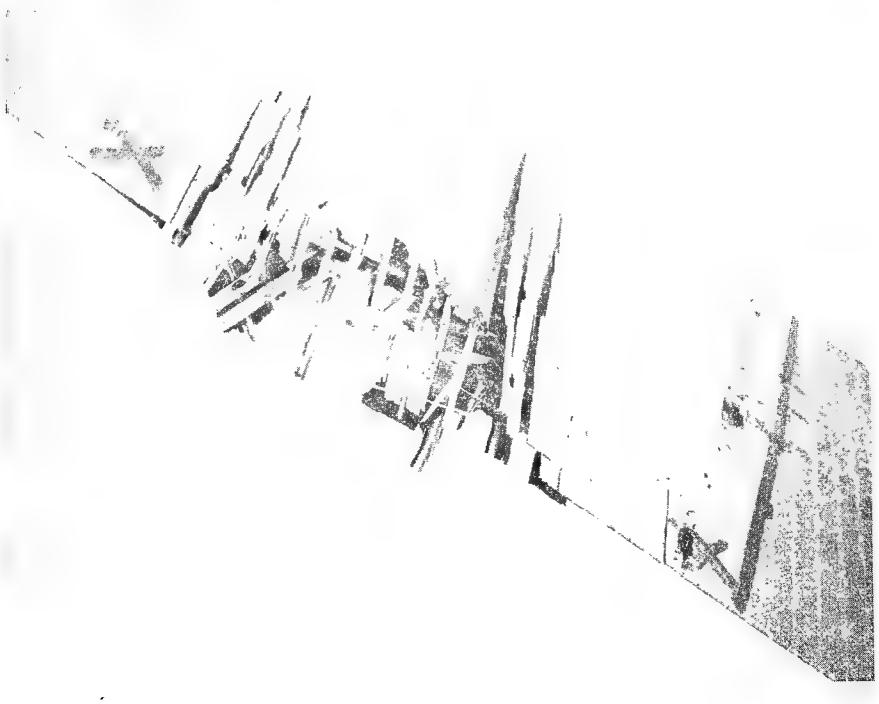

NAS–96A ($22^{o}$ IMPACT)

76-03-102-10

Table XI

Task II - Ballistic Test Data

| Specimen No. | Material | KE/t joules/cm | KE/t (ft-lbs/in) | Torsion Rigidity Retention (%) |
|---|---|---|---|---|
| 78 | Boron/Glass/Polysulfone | 106 | 198 | 89 |
| 78A | " | 267 | 500 | 95 |
| 79 | " | 415 | 776 | 90 |
| 79A | " | 222 | 415 | 97 |
| 80 | " | 454 | 850 | 90 |
| 80A | " | 275 | 515 | 98 |
| 81 | " | 447 | 835 | 75 |
| 81A | " | 255 | 477 | 80 |
| 84 | T-300 Graphite/Glass/Epoxy | 96 | 180 | 100 |
| 84A | " | 280 | 523 | 70 |
| 85 | " | 557 | 1042 | 90 |
| 85A | " | 267 | 500 | 85 |
| 86 | " | 311 | 582 | 82 |
| 86A | " | 273 | 510 | 83 |
| 90 | " | 267 | 500 | 96 |
| 90A | " | 203 | 379 | 98 |
| 89 | Ti/B-Al/Graphite/Epoxy | 83 | 155 | 100 |
| 89A | " | 436 | 815 | - |
| 89B | " | 297 | 556 | 100 |
| 89C | " | 335 | 626 | 100 |
| 91 | AS Graphite/Boron/Glass/Epoxy | 127 | 238 | 91 |
| 91A | " | 362 | 658 | 78 |
| 94 | " | 498 | 933 | 75 |
| 94A | " | 278 | 519 | 91 |
| 95 | " | 577 | 1079 | 90 |
| 95A | " | 368 | 688 | 98 |
| 96 | " | 433 | 810 | 70 |
| 96A | " | 291 | 544 | 67 |

discussed previously in which the specimens failed at lower stresses than anticipated, based on static results. Ballistic testing of this material in the $\pm 45°/0°$ ply configuration during Task I at an impact of KE/t = 517 joules/cm resulted in a 100% retention of the specimen's original stiffness, even though there was some damage visible at the leading edge. However, both Task II specimens of the $\pm 80°/\pm 15°/0°$ configuration suffered substantial drops in rigidity without showing visual evidence of appreciable damage. Other than those specimens the boron/glass/polysulfone demonstrated excellent impact resistance over a wide range of conditions and ply configurations.

The T-300 graphite/glass/epoxy specimens generally suffered greater reduction in stiffness than the boron/glass/polysulfone with the exception of the specimens of the $\pm 80°/\pm 15°/0°$ configuration which reflected the nearly undamaged appearance of the specimens in this instance (Fig. 25). Specimen NAS-85 was subjected to a quite severe impact yet retained a high fraction of its original stiffness. However, as indicated in Fig. 23 the damage consisted largely of break out and this mode of failure has been found to cause little or no change in torsional stiffness.

The superhybrid specimens which exhibited denting as a result of impact were subjected to relatively mild tests; the maximum KE/t was 335 joules/cm. All the specimens retained 100% of their original stiffness which was indicative of the lack of damage. None of the other materials performed in such a manner.

Many of the specimens of the AS graphite/boron/glass/epoxy specimens were subjected to severe impact tests which may explain, in part, their rather poor performance. However, the slight delamination in NAS-91 and the severe break out and delamination in NAS-91A, 94A, and 96A clearly indicated a greater susceptibility to damage in this material than was found with the other materials.

In summarizing the experimental results of the Task II ballistic tests the following conclusions were reached:

1. The boron/glass/polysulfone was much less damaged than the other two conventional hybrid materials under almost all test conditions. This was not necessarily reflected in the modulus retention measurements, however, the visual results were very striking. The T-300/glass/epoxy ranked second, while the AS/boron/glass/epoxy ranked third, confirming the prediction of impact resistance based on the thin pendulum impact tests of the angle-ply composites.

2. The boron/glass/polysulfone generally suffered very minor localized delamination, if any damage occurred. The T-300/glass/epoxy underwent more extensive delamination, sometimes accompanied by local break out, while the AS/boron/glass/epoxy failed primarily by local break out.

3. The ±80/±15/0 configuration produced better visual results than any of the other ply configurations for the boron/glass/polysulfone and the T-300/glass/epoxy materials. Such a ply configuration may not be suitable for blade applications due to a low torsional stiffness. The other ply configurations for those two materials were essentially equivalent. All ply configurations for the AS/glass/boron/epoxy material showed rather extensive damage as a result of impact.

4. The 15° angle of incidence impacts were below the visible damage threshold for all materials except AS/boron/glass/epoxy. Increasing the angle of incidence generally increased the amount of damage as would be expected.

5. Using the parameter KE/t to measure the severity of impact, the superhybrid was able to withstand the most severe impact without exhibiting any fracture.

### 3.2.3 Ballistic Impact - Analytical

As part of the NASTRAN procedure the natural frequencies of the blade-like specimens were calculated as shown in Table XII. The superhybrid specimen had generally higher bending and torsion frequencies than the two hybrid specimens. The torsion frequency results reflect the importance of the specific ply configuration of the structure being analyzed. As discussed previously, the torsion modulus of the superhybrid was lower than the AS/boron/glass/epoxy and not much higher than the T-300/glass/epoxy when measured on coupon specimens.

The results of the experimental and predicted strain responses for the three specimens, NAS-84A, 89B, and 91A, are given in Appendix A. Some gages malfunctioned for each specimen and no results were available. In general the agreement between experimental and analytical results was satisfactory. The highest absolute peak strains for each specimen are listed in Table XIII. In most instances the predicted maximum strains were higher than the measured values at a given location. This was expected since the analysis assumed perfectly elastic material behavior and the system was treated as being undamaged. Both these assumptions would tend to result in higher calculated peak strains than would be measured. One important exception to this trend was gage #2 on the superhybrid specimen, NAS-89B. The peak measured strain was the second highest of any location, and was higher than the predicted value by a factor of three.

Predicted and measured strains in the superhybrid were substantially lower than those of the other two materials, but this was at least partially due to the fact that the superhybrid specimen was thicker. The lower strains in NAS-91A compared with NAS-84A were a reflection of the higher moduli of the former material.

Table XII

NASTRAN Composite Specimen
Natural Frequencies

| | T-300/Glass/Epoxy 84A | S.H. #1 89B | AS/Boron/Glass/Epoxy 91A |
|---|---|---|---|
| $f_1$ (1B) | 141.0 cps | 177.9 | 147.3 |
| $f_2$ (1T) | 510.7 | 644.1 | 645.9 |
| $f_3$ (2B) | 826.9 | 1086.0 | 886.8 |
| $f_4$ (2T) | 1665.4 | 1998.3 | 1930.4 |
| $f_5$ (3B) | 2191.6 | 2839.9 | 2316.8 |

Table XIII

Maximum Strains in Task II Ballistic Specimens

| Specimen | Experimental | | Analysis | |
|---|---|---|---|---|
| | Gage No. | Strain - μin./in. | Gage No. | Strain - μin./in. |
| NAS-84A | 4 | -5700 | 3 | -14,700 |
| | 3 | -5600 | 4 | -12,000 |
| | 5 | 4700 | 5 | 10,700 |
| NAS-89B | 5 | 2600 | 3 | - 4,000 |
| | 2 | -2500 | 5 | 3,900 |
| | 4 | -2050 | 4 | - 3,400 |
| | 3 | -2000 | | |
| NAS-91A | 3 | -4400 | 3 | -11,100 |
| | 6 | -4250 | 4 | - 9,200 |
| | 4 | -3900 | 6 | - 7,250 |

The most important aspect of this phase of the program was the demonstrated ability of the analysis to predict the locations of highest strain with reasonable accuracy. In NAS-84A and 91A there was excellent agreement, with the three highest strain locations being correctly predicted. In each instance there was a misordering of two locations which had strains very close in magnitude. The predicted results in the superhybrid specimen were in somewhat poorer agreement due to the previously-mentioned discrepancy with gage #2. Other than that the correct locations were predicted although they were misordered. Having the ability to correctly determine the location of high strain around the impact location it should be possible to quickly examine a number of materials variables to determine their effect on the strains in the critical regions. Furthermore, it may be possible to modify the analysis, perhaps even on an empirical basis, to obtain better agreement between predicted and measured results. Then with the establishment of a suitable failure criterion it should be possible to analytically predict the impact conditions at which failure will initiate.

## IV. TASK III - LEADING EDGE PROTECTION

The objective of this task was to evaluate methods of enhancing composite impact resistance by protecting the specimens in the area of the impact. Based on the results of the first two tasks the superhybrid approach was followed as a means of protection since it accomplishes that objective by surrounding a resin composite with metallic layers of boron/aluminum and titanium. Testing in this task consisted of four ballistic impacts, two of which were instrumented for correlation with analytical prediction of response.

### 4.1 Experimental

All fabrication, test, and analytical procedures used in this task were the same as those described previously. The ply configurations of the four blade-like specimens are given in Tables XIV-XVII. The notation "wrap" indicates a ply which was wrapped around the leading edge of the specimen. Specimens NAS-109B and 110A had resin composite cores of boron/glass/polysulfone which was found to be the most impact resistant hybrid in the earlier portion of the program. The two specimens differed in the thickness of the Ti-6-4 foil. Specimens NAS-111 and 112 were variations of the superhybrid configuration evaluated during Task II. In NAS-111 the total thickness of Ti-6-4 was the same as the S.H. #1 configuration, but there were three layers in the shell rather than two. Specimen NAS-112 had a greater total thickness of Ti-6-4 and was intended to be similar to NAS-110A. Both NAS-111 and NAS-112 had leading edges which were substantially thicker than the specimens with the boron/glass/polysulfone cores. This resulted from a lateral displacement of the graphite/epoxy into the leading edge during the pressing operation. Specimens NAS-110A and 112 were instrumented in the same manner as the three samples in Task II.

### 4.2 Results and Discussion

The conditions and results of the ballistic impact tests are summarized in Table XVIII. One instrumented specimen, NAS-110A, was impacted only once at the condition indicated in the table. The other instrumented specimen, NAS-112, was struck first at a lower velocity of approximately 150 mps, then impacted twice at higher velocity. After the first high velocity hit the specimen was observed to have rotated approximately $4^{\circ}$ in the clamp, indicating that the clamp had not been properly tightened prior to the test. The specimen appeared undamaged after this test and consequently was retested.

Photographs of each specimen after impact are shown in Figs. 32 and 33. All the specimens failed in essentially the same manner; there was local break out at the point of impact generally accompanied by peeling of the backface plies of Ti-6-4. The boron/glass/polysulfone core materials in Fig. 32 received particularly severe impacts as a result of their thin leading edge and the high

Table XIV

NAS-109B

L.E. = .069 cm (.027 in.)
mid-chord = .396 cm (.156 in.)

| Layer | Material | Width cm | Width (in.) | Notes |
|---|---|---|---|---|
| 1 | Ti-6-4 (3 mil) | 7.62 | 3.00 | Wrap |
| 2 | FM-1000 | 7.62 | 3.00 | Wrap |
| 3 | Ti-6-4 (3 mil) | 7.62 | 3.00 | Wrap |
| 4 | FM-1000 | 7.37 | 2.9 | |
| 5 | B/Al | 6.98 | 2.75 | |
| 6 | FM-1000 | 6.98 | 2.75 | |
| 7 | B/Al | 6.35 | 2.50 | |
| 8 | FM-1000 | 6.35 | 2.50 | |
| 9 | B/G/polysulfone | 5.08 | 2.00 | |
| 10 | ↓ | 3.81 | 1.50 | |
| 11 | | 2.54 | 1.00 | |
| 12 | | 1.27 | 0.50 | |
| 13 | | 0.63 | 0.25 | |
| 14 | FM-1000 | 7.24 | 2.85 | |
| ~~15~~ | ~~Ti-6-4 (3 mil)~~ | ~~7.24~~ | ~~2.85~~ | ~~GE~~ |

Table XV

NAS-110A

L.E. = .069 cm (.027 in.)
mid-chord = .409 cm (.161 in.)

| Layer | Material | Width cm | Width (in.) | Notes |
|---|---|---|---|---|
| 1 | Ti-6-4 (3 mil) | 7.62 | 3.00 | Wrap |
| 2 | FM-1000 | 7.62 | 3.00 | Wrap |
| 3 | Ti-6-4 (5 mil) | 7.62 | 3.00 | |
| 4 | FM-1000 | 7.62 | 3.00 | |
| 5 | B/Al | 6.98 | 2.75 | |
| 6 | FM-1000 | 6.98 | 2.75 | |
| 7 | B/Al | 6.35 | 2.50 | |
| 8 | FM-1000 | 6.35 | 2.50 | |
| 9 | B/G/polysulfone | 5.08 | 2.00 | |
| 10 | ↓ | 3.81 | 1.50 | |
| 11 | | 2.54 | 1.00 | |
| 12 | | 1.27 | 0.50 | |
| 13 | | 0.63 | 0.25 | |
| 14 | FM-1000 | 7.24 | 2.85 | |
| ~~15~~ | ~~Ti-6-4 (3 mil)~~ | ~~7.24~~ | ~~2.85~~ | ~~℄~~ |

Table XVI

NAS-111

L.E. = .109 cm (.043 in.)
mid-chord = .419 cm (.165 in.)

| Layer | Material | Width cm | Width (in.) | Notes |
|---|---|---|---|---|
| 1 | Ti-6-4 (2 mil) | 7.62 | 3.00 | Wrap |
| 2 | FM-1000 | 7.62 | 3.00 | Wrap |
| 3 | Ti-6-4 (2 mil) | 7.62 | 3.00 | Wrap |
| 4 | FM-1000 | 7.62 | 3.00 | Wrap |
| 5 | Ti-6-4 (2 mil) | 7.62 | 3.00 | Wrap |
| 6 | FM-1000 | 7.62 | 3.00 | |
| 7 | B/Al | 6.98 | 2.75 | |
| 8 | FM-1000 | 6.98 | 2.75 | |
| 9 | B/Al | 6.35 | 2.50 | |
| 10 | FM-1000 | 6.35 | 2.50 | |
| 11 | AS/Epoxy | 5.72 | 2.25 | |
| 12 | ↓ | 5.08 | 2.00 | |
| 13 | ↓ | 4.04 | 1.75 | |
| 14 | ↓ | 3.81 | 1.50 | |
| 15 | ↓ | 3.18 | 1.25 | |
| 16 | ↓ | 2.54 | 1.00 | |
| 17 | ↓ | 1.91 | 0.75 | |
| 18 | ↓ | 1.27 | 0.50 | |
| 19 | ↓ | 0.63 | 0.25 | |
| 20 | FM-1000 | 7.24 | 2.85 | |
| ~~21~~ | ~~Ti-6-4 (3 mil)~~ | ~~7.24~~ | ~~2.85~~ | ℄ |

Table XVII

NAS-112

L.E. = .112 cm (.044 in.)
mid-chord = .407 cm (.160 in.)

| Layer | Material | Width cm | Width (in.) | Notes |
|---|---|---|---|---|
| 1 | Ti-6-4 (3 mil) | 7.62 | 3.00 | Wrap |
| 2 | FM-1000 | 7.62 | 3.00 | Wrap |
| 3 | Ti-6-4 (5 mil) | 7.62 | 3.00 | |
| 4 | FM-1000 | 7.62 | 3.00 | |
| 5 | B/Al | 6.98 | 2.75 | |
| 6 | FM-1000 | 6.98 | 2.75 | |
| 7 | B/Al | 6.35 | 2.50 | |
| 8 | FM-1000 | 6.35 | 2.50 | |
| 9 | AS/Epoxy | 5.72 | 2.25 | |
| 10 | ↓ | 5.08 | 2.00 | |
| 11 | ↓ | 4.04 | 1.75 | |
| 12 | ↓ | 3.81 | 1.50 | |
| 13 | ↓ | 3.18 | 1.25 | |
| 14 | ↓ | 2.54 | 1.00 | |
| 15 | ↓ | 1.91 | 0.75 | |
| 16 | ↓ | 1.27 | 0.50 | |
| 17 | ↓ | 0.63 | 0.25 | |
| 18 | FM-1000 | 7.24 | 2.85 | |
| 19 | Ti-6-4 (3 mil) | 7.24 | 2.85 | ℄ |

Table XVIII

Task III - Ballistic Test Results

| Specimen No. | L.E. Thickness (cm) | Mid-chord Thickness (cm) | Impact Angle (deg) | Velocity (mps) | KE/t (joules/cm) | KE/t (ft-lbs/in) | Torsion Rigidity Retention (%) | Visual Observations |
|---|---|---|---|---|---|---|---|---|
| 109B | .069 | .396 | 30 | 278 | 585 | 1280 | 73 | Large breakout; backface delamination |
| 110A[1] | .069 | .409 | 30 | 302 | 850 | 1590 | 86 | Local breakout; spanwise crack |
| 111 | .109 | .419 | 30 | 251 | 508 | 950 | - | Fracture into two pieces; trailing edge split |
| 112[1,2] | .112 | .407 | 30 | 279 | 476 | 890 | | Specimen loose in clamp; no damage |
| | | | 30 | 279 | 556 | 1040 | 20 | Very large breakout; backface delamination |

[1] instrumented specimen

[2] tested previously at approximately 150 mps

## BORON/GLASS/POLYSULFONE SUPERHYBRID IMPACTED SPECIMENS

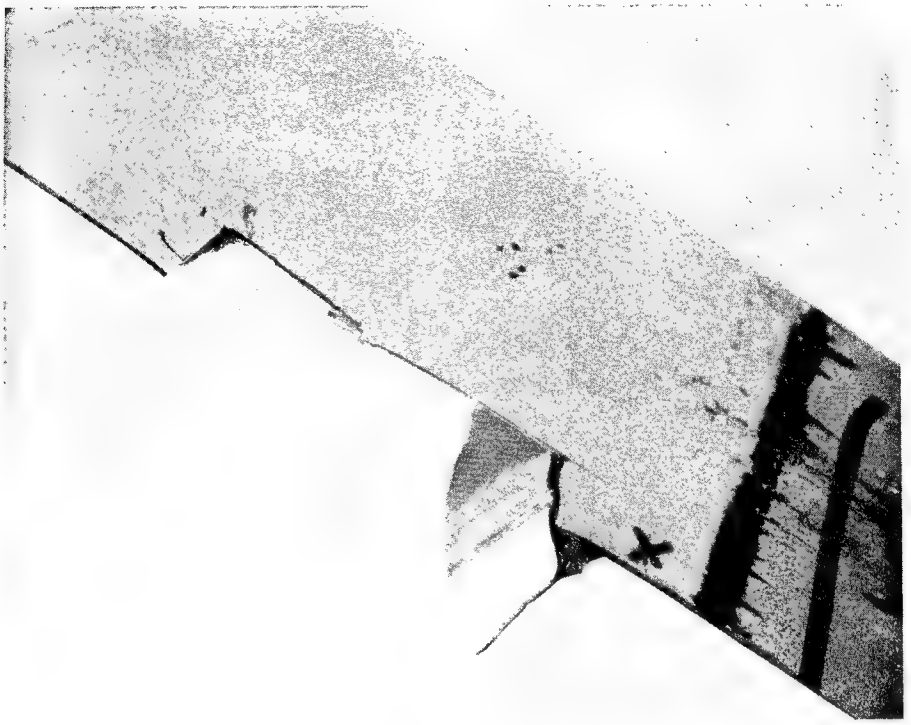

NAS–109B

NAS–110A

76–03–168–1

FIG. 33

## AS GRAPHITE/EPOXY SUPERHYBRID IMPACTED SPECIMENS

NAS–111

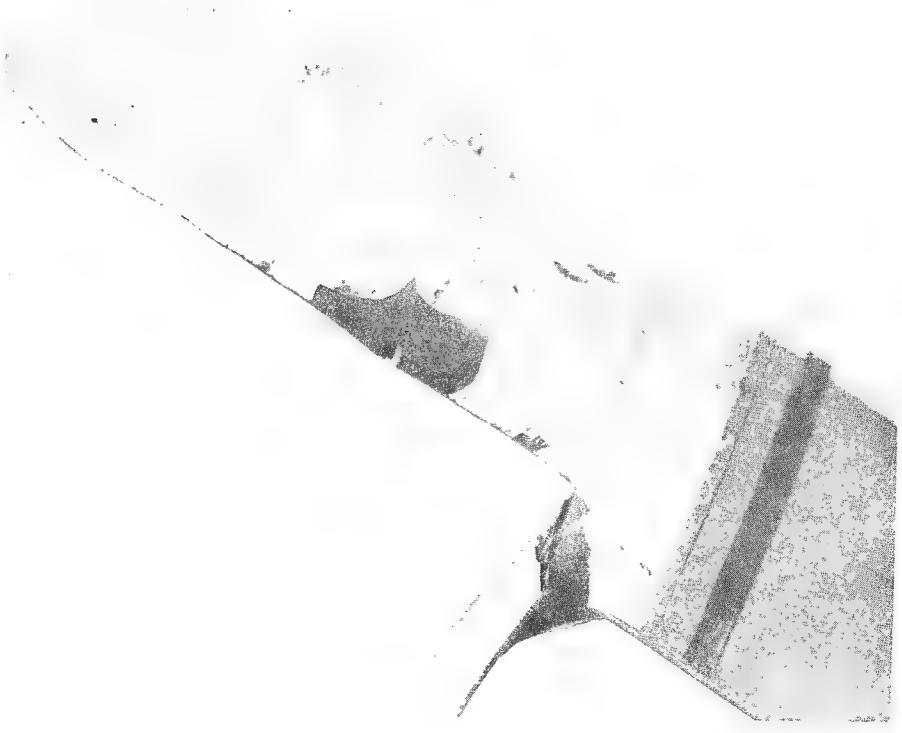

NAS–112

76–03 -168 -2

projectile velocities. The KE/t for NAS-110A was the highest of the entire program. Considering that, the damage to the specimen was not too severe, consisting of a localized breakout and a span-wise crack. The breakout in NAS-109B was somewhat larger and there was a large area of Ti-6-4 peeled from the backface. As a result of the more extensive damage in NAS-109B, particularly the peeled outer ply, the torsional stiffness retention of that specimen was substantially less than NAS-110A. This evidence could be construed to mean that the slightly thicker Ti-6-4 foil used in NAS-110A was very effective in improving the damage resistance of the material, but additional testing would be required to confirm this conclusion.

The AS graphite/epoxy core superhybrids shown in Fig. 33 were tested under conditions somewhat less severe than the boron/glass/polysulfone superhybrids, but still quite severe relative to the other tests conducted during the program. Specimen NAS-111 was badly damaged but this may have been partially due to the fact that the 2 mil Ti-6-4 foil was not wide enough to wrap around the leading edge and extend across the full chord of the specimen. As a result a butt joint was made in each ply approximately 2.5 cm from the trailing edge. As can be seen in Fig. 33, fracture occurred along that joint. However, review of the movie of the test indicated that the breakout at the point of impact occurred first and was essentially unrelated to the trailing edge failure. The subsequent break of the specimen at mid span probably was related to both earlier failures. As a result of the trailing edge failure, it was difficult to relate the intended variable, Ti-6-4 layer thickness, to the performance of the specimen. The KE/t was higher than that of any of the superhybrids of standard configuration tested during Task II, but the damage was much more extensive than in any of those or the boron/glass/polysulfone superhybrids which were tested under more severe conditions.

The final specimen, NAS-112, was tested twice at high velocity as discussed previously. After the first test it is possible that the specimen suffered some internal damage which was not discerned from the visual inspection. This may have accounted for the extensive damage which occurred after the second impact at 279 mps. If no internal damage had been initiated after the first high velocity test, or in the previous test at low velocity for strain measurement, then this specimen was clearly inferior to NAS-110A which had the same metallic portection but a boron/glass/polysulfone core and withstood a more severe impact with less extensive damage. In order to fully assess the merits of the resin composite portion of the superhybrid, much more impact testing would be required. Furthermore, other factors must be taken into account including cost, ease of fabrication, density, and all the mechanical properties which enter into the design of a gas turbine engine fan blade. Such an assessement is beyond the scope of this program, however.

Unfortunately no useful strain data were obtained from NAS-110A as a result of its being tested and severely damaged at a high impact velocity. The results for specimen NAS-112 were plotted for each strain gage location and are contained in Appendix B. The data were similar to those obtained from the superhybrid specimen in Task II. In this instance the incident angle was 30° rather than 22° so the strains would be expected to be somewhat higher which was found to be the case with most of the experimental measurements. The highest measured and predicted strains for NAS-112 are listed below:

| Measured | | Predicted | |
|---|---|---|---|
| Gage No. | Strain - μin./in. | Gage No. | Strain - μin./in. |
| 5 | 2900 | 5 | 4300 |
| 2 | -2600 | 3 | -3700 |
| 8 | 2400 | 4 | 3100 |
| 10 | 2300 | 8 | 2700 |
| 3 | 2300 | | |

As with the previous superhybrid, gage #2 produced a much higher measured strain than the NASTRAN prediction, but the other high strain gage locations were in reasonable agreement. Since NAS-112 was impacted at a different angle than NAS-89B it was difficult to discern the effect of the additional thickness of Ti-6-4 in NAS-112. The predicted peak strains were generally somewhat lower in NAS-112 indicating a beneficial effect. However the experimental values were slightly higher as mentioned above.

## V. CONCLUSIONS

1. The leading edge thickness of the blade-like specimen is extremely important in determining specimen load carrying ability under impact conditions.

2. Superhybrid resin matrix composites incorporating metallic layers for impact protection and property enhancement are capable of withstanding relatively severe gelatin impact with no evidence of fracture.

3. Based on visual appearance, boron/glass/polysulfone intraply hybrid is the most impact resistant unprotected composite of those tested.

4. Of the four ply configurations investigated, only the $\pm 80/\pm 15/0$ resulted in enhanced impact resistance. That configuration may have unsuitable torsional stiffness for blade applications.

5. Increasing the angle of incidence of the impacting projectile generally increased the degree of damage to the blade-like specimens.

6. NASTRAN predictions of surface strains during impact were in satisfactory agreement with experimental measurements.

## REFERENCES


1. R. C. Novak and M. A. DeCrescente: "Impact Behavior of Unidirectional Resin Matrix Composites Tested in the Fiber Direction", Composite Materials: Testing and Design, ASTM STP 497, 1972.

2. C. C. Chamis, M. P. Hanson, and T. T. Serafini: "Impact Resistance of Unidirectional Fiber Composites", Composite Materials: Testing and Design, ASTM STP 497, 1972.

3. L. A. Friedrich: "Impact Resistance of Hybrid Composite Fan Blade Materials", NASA CR-134712, May 1974.

4. R. C. Novak: "Materials Variables Affecting the Impact Resistance of Graphite and Boron Composites", AFML-TR-74-196, Parts I and II, Sept. 1974 and June 1975, respectively.

5. G. C. Murphy and C. T. Salemme: "Low-Cost FOD-Resistant Organic Matrix Fan Blades", Fifth Interim Technical Report, Contract F33615-74-C-5072, June 1975.

6. R. A. Pike and R. C. Novak: "Design, Fabrication and Test of Multi-Fiber Laminates", NASA CR-134763, Jan. 1975.

7. C. C. Chamis, R. F. Lark, and T. L. Sullivan: "Boron/Aluminum-Graphite/Resin Advanced Fiber Composite Hybrids", NASA TMX-71580, Oct. 1974.

8. R. A. Pike and R. C. Novak: "The Pendulum Impact Test: A Method for Assessing the Impact Response of Composite Materials", Proceedings of the 31st Annual Technical Conference SPI Reinforced Plastics/Composites Institute, Feb. 1976.

# APPENDIX A

FIG. A1

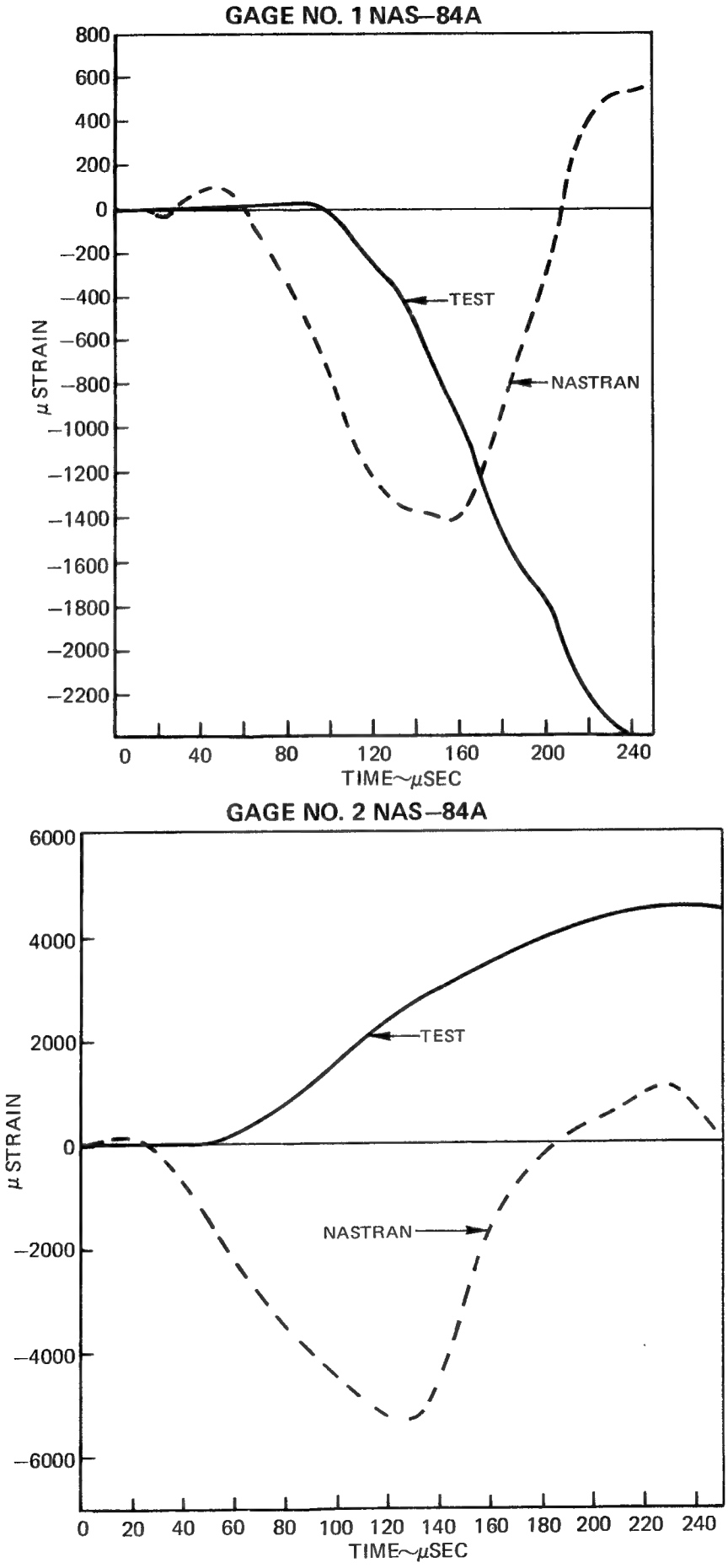


76–06–69–1

FIG. A2

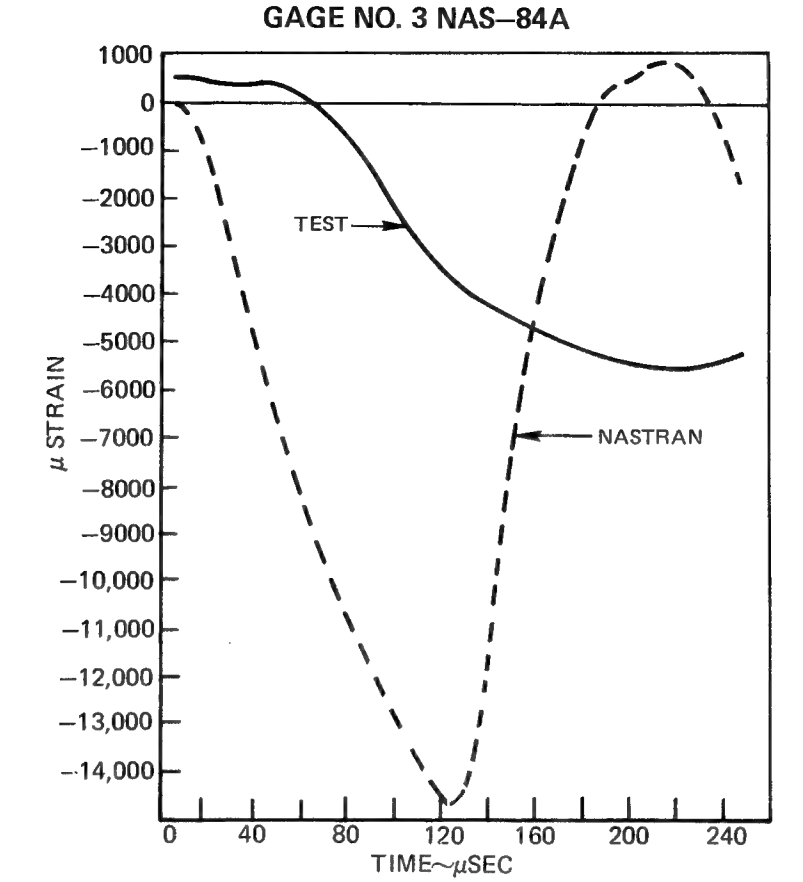


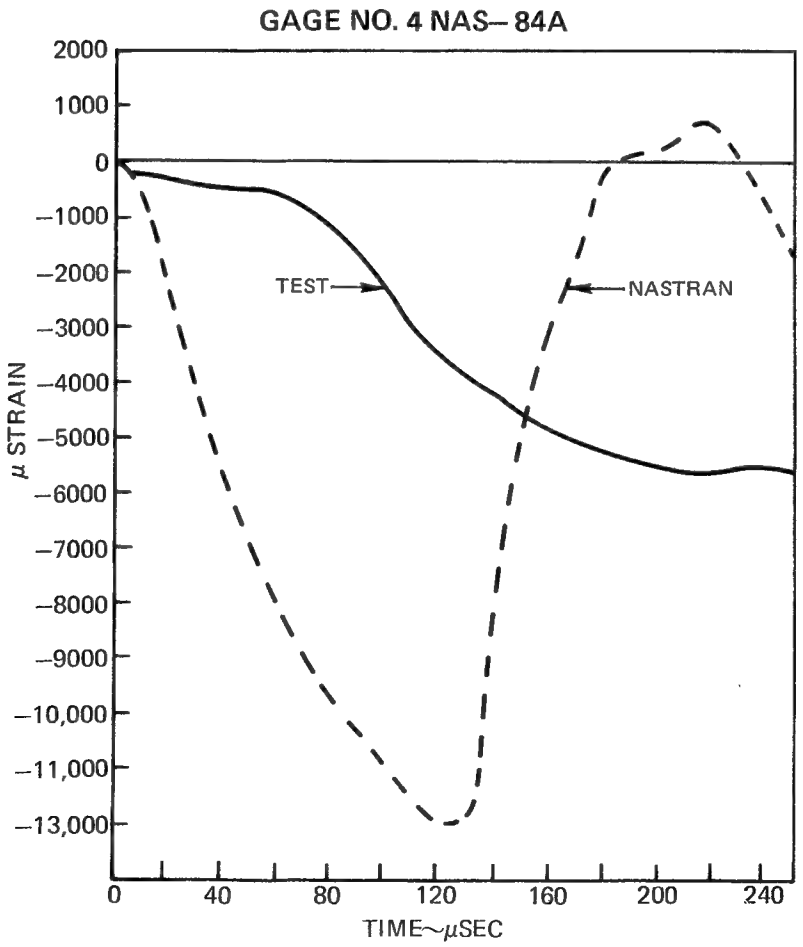


76–06–69–2

FIG. A3

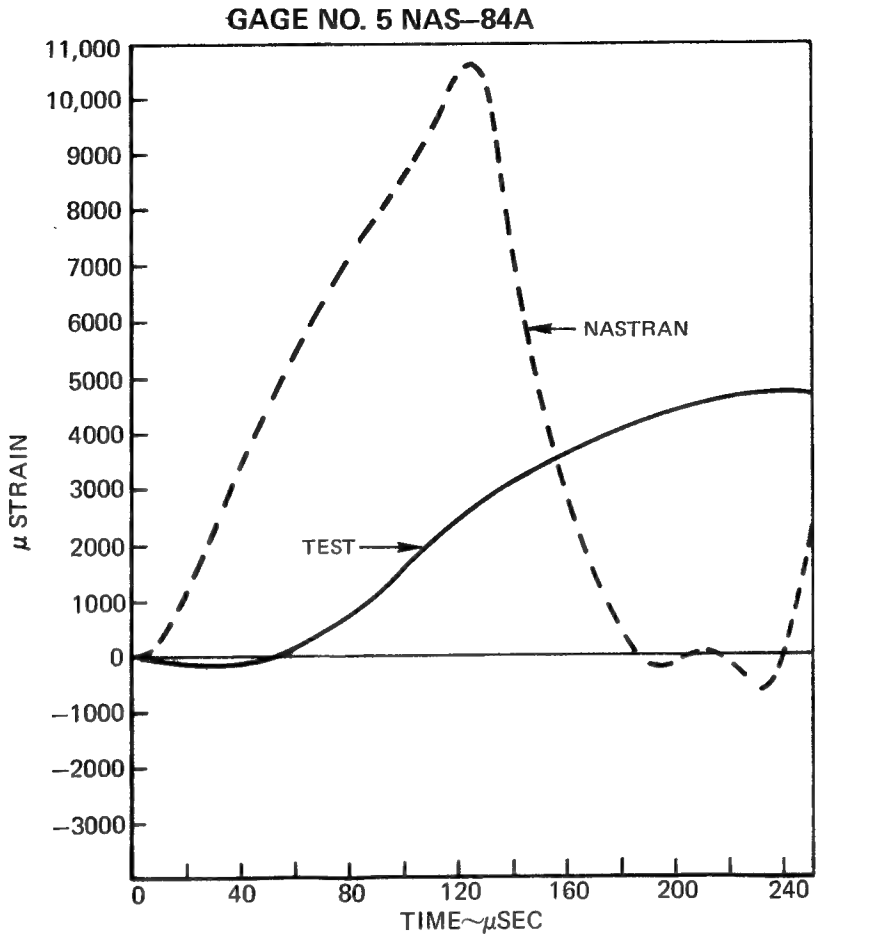


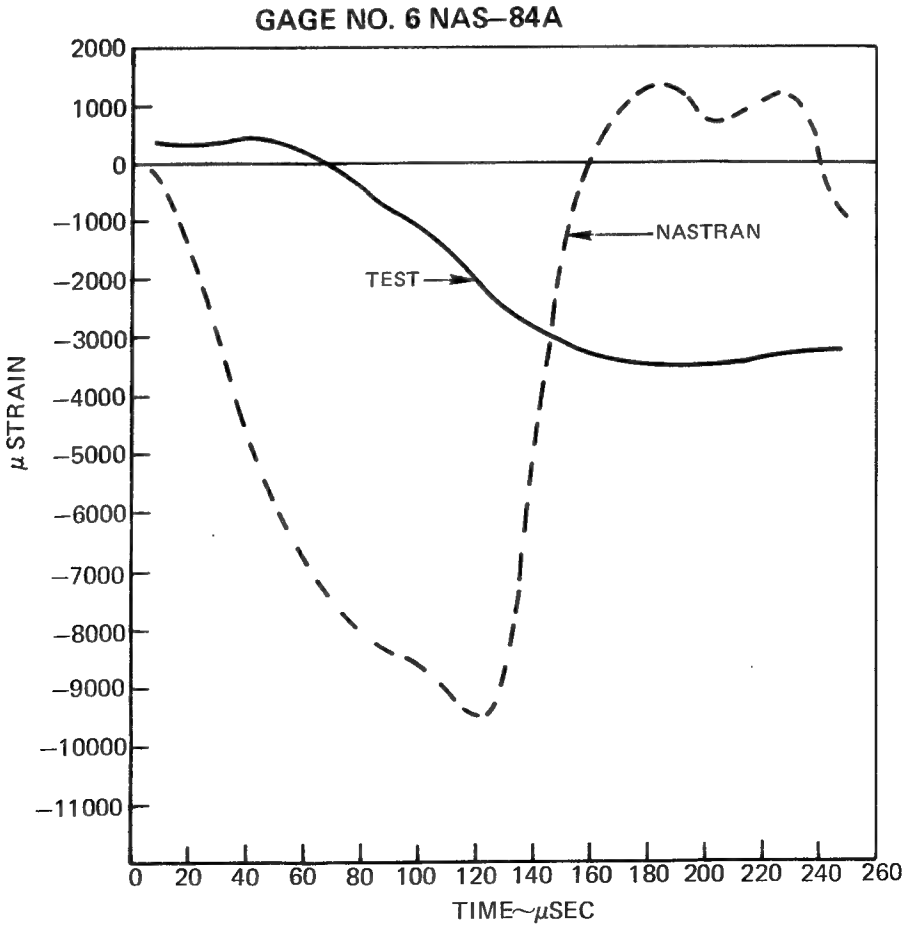


76–06–69–3

FIG. A4

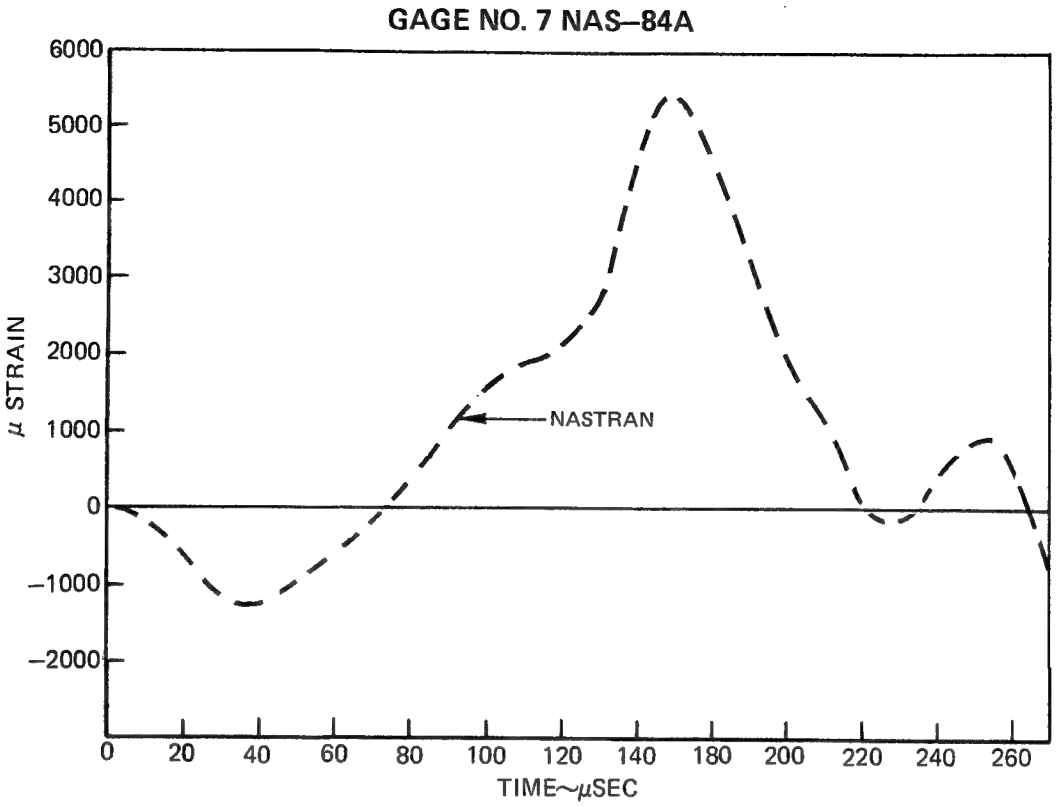


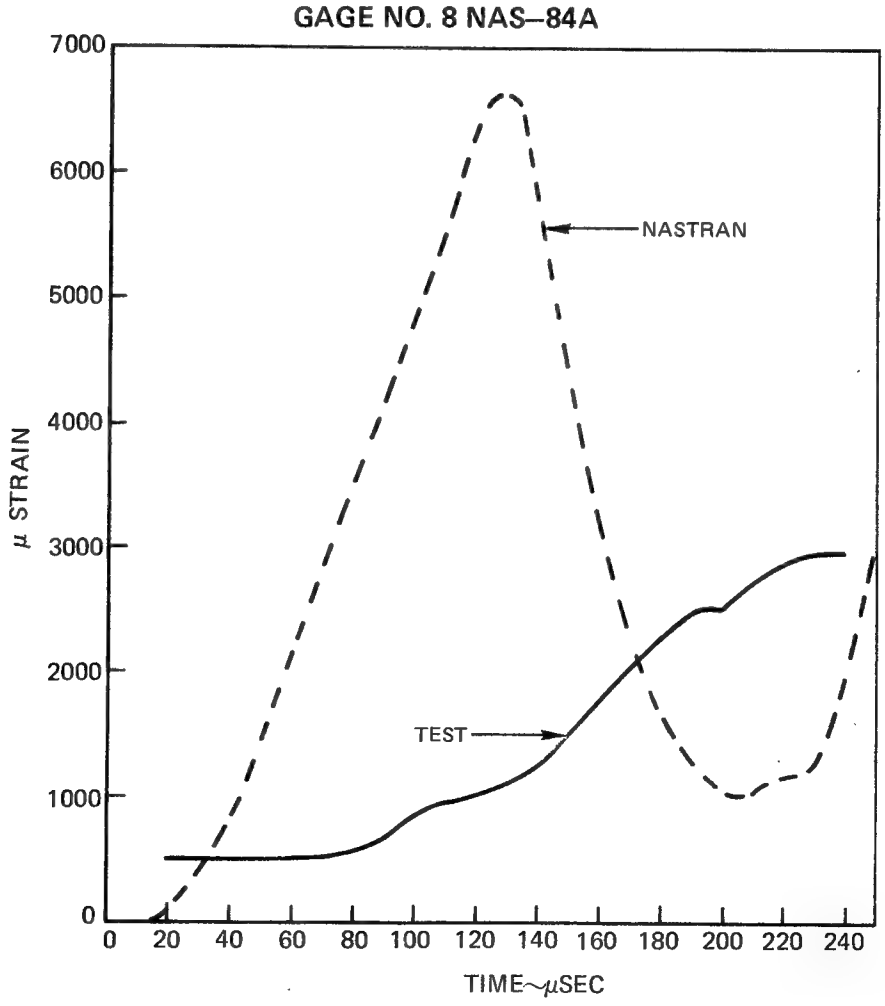


76–06–69–4

FIG. A5

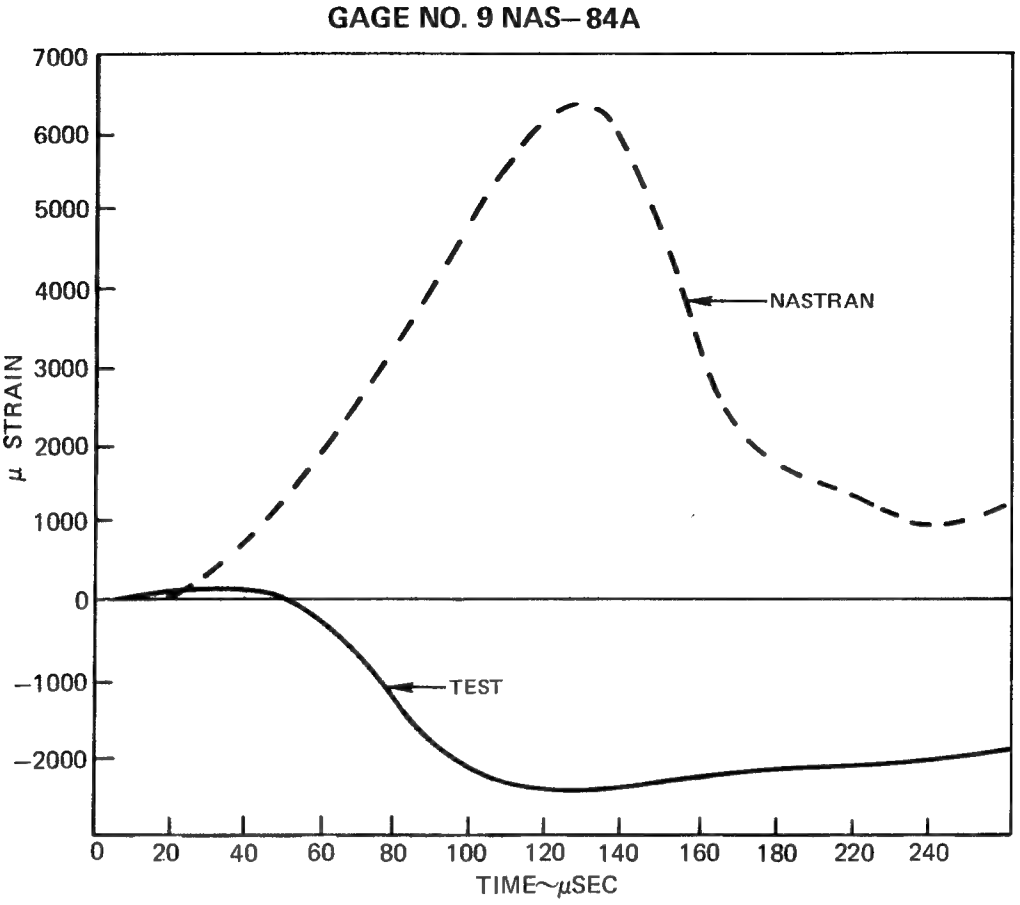


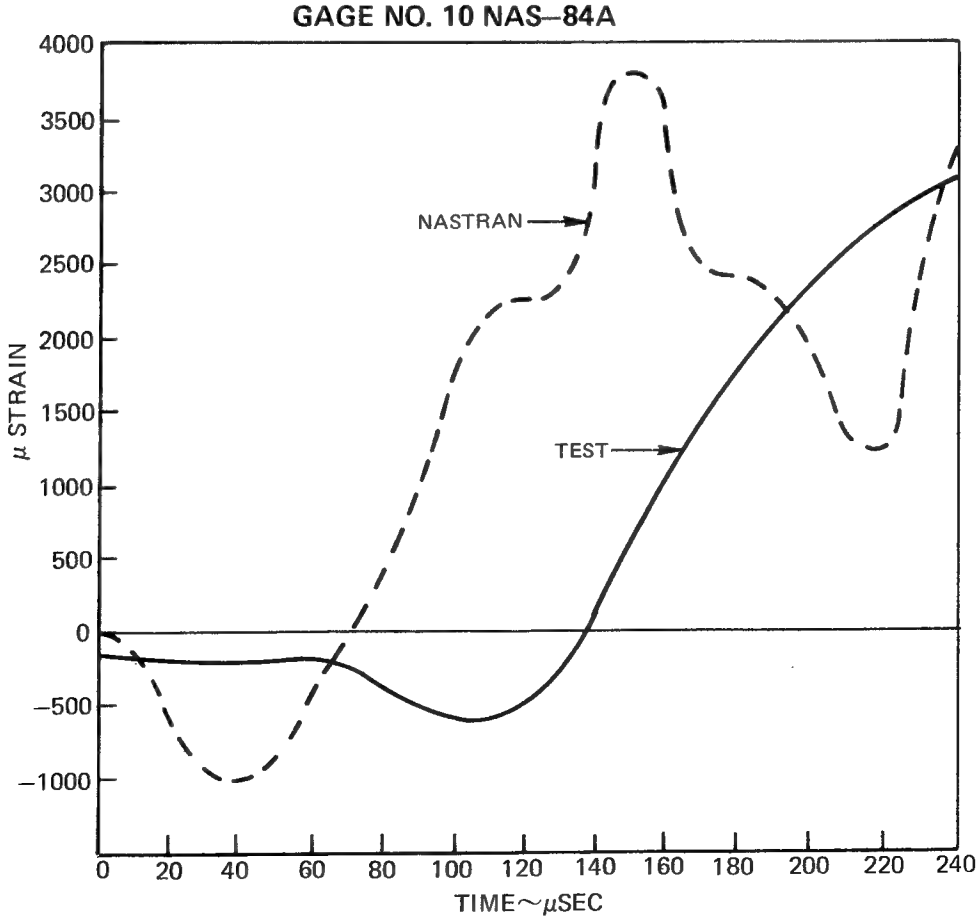


76–06–69–5

GAGE NO. 11 NAS–84A

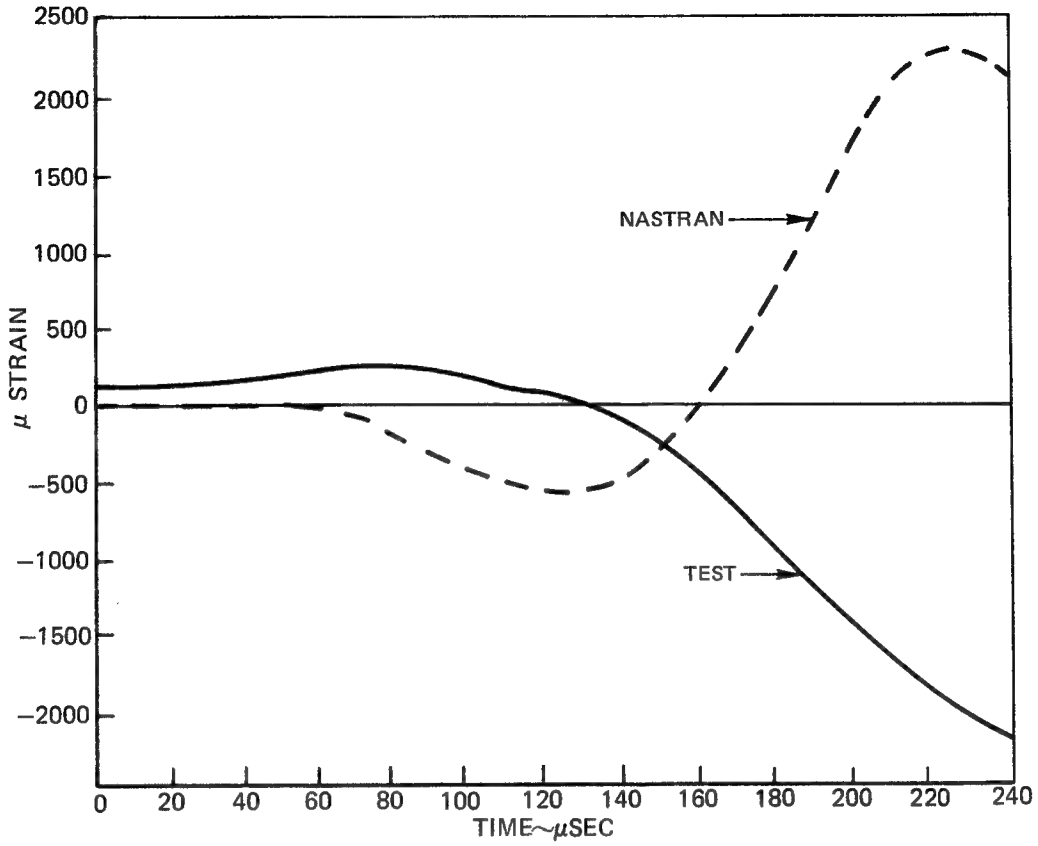


GAGE NO. 12 NAS–84A

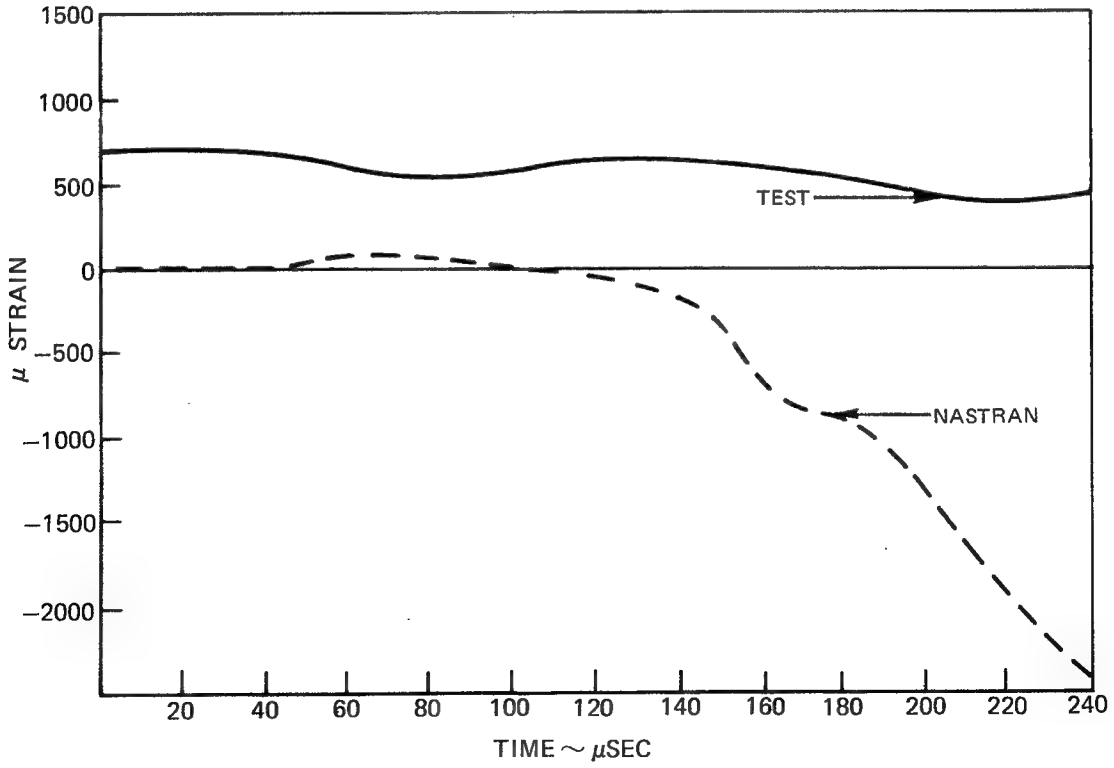


76–06–69–6

FIG. A7

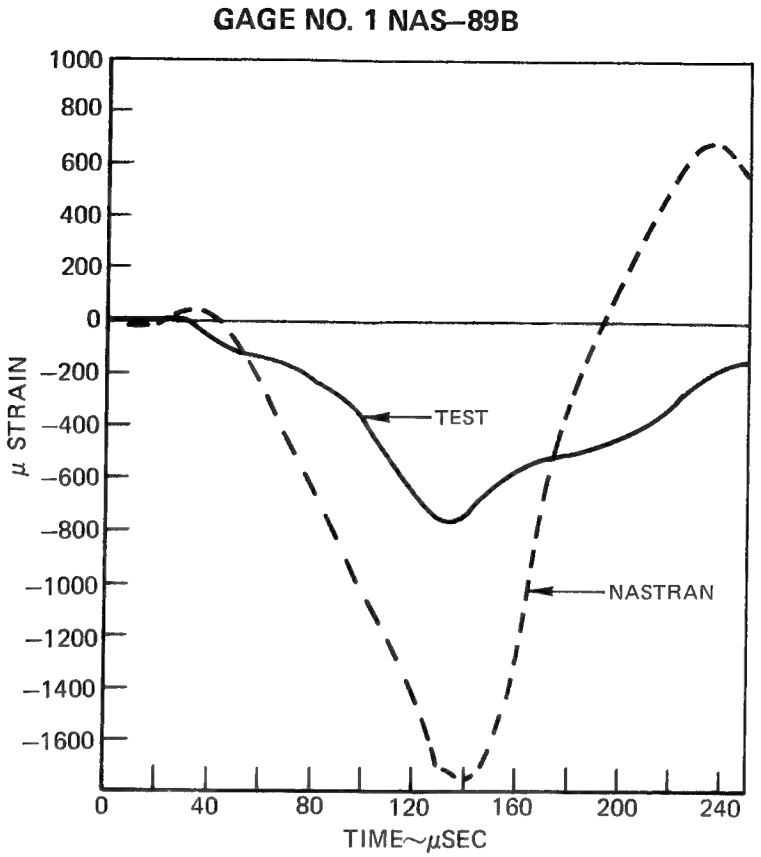


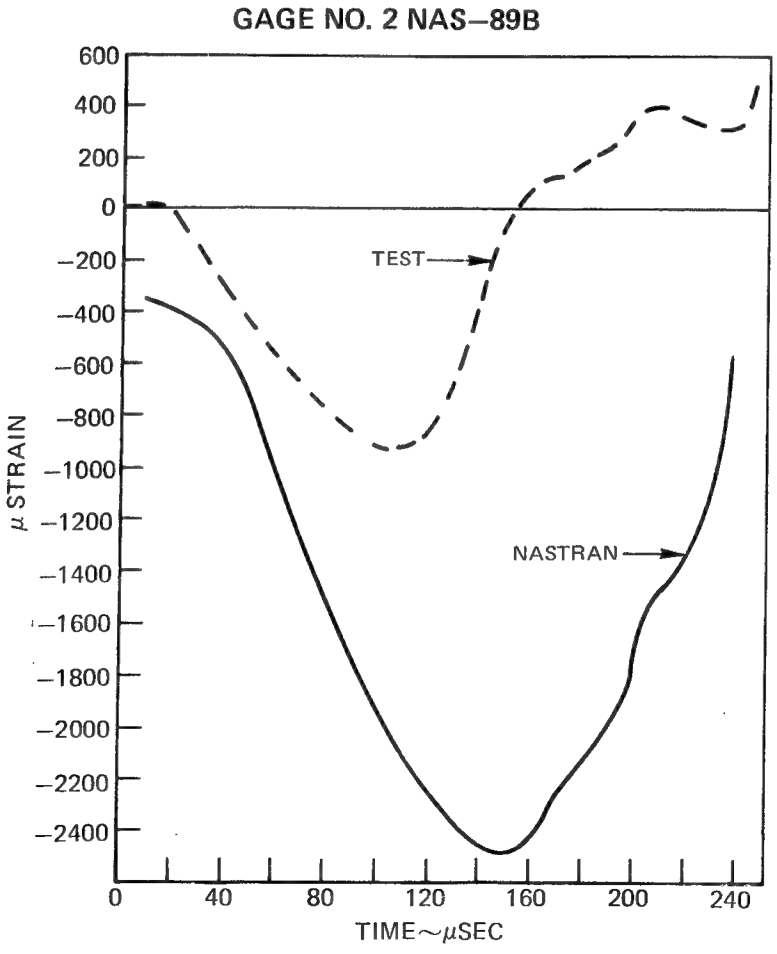


76–06–69–7

FIG. A8

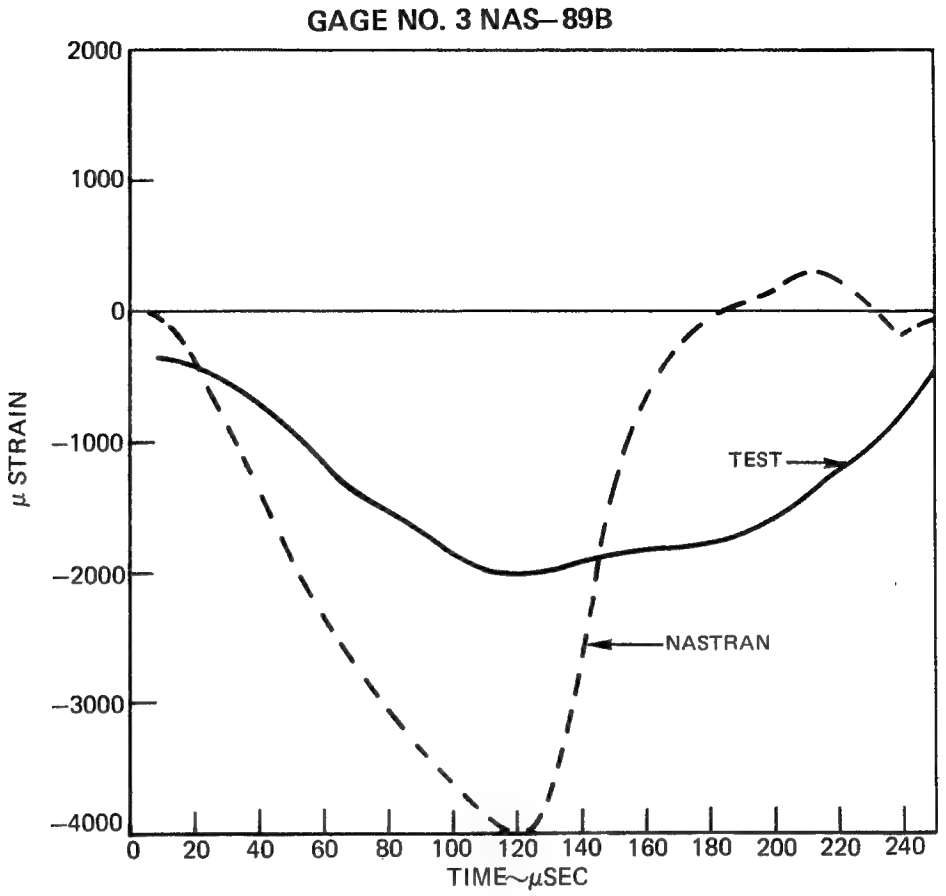


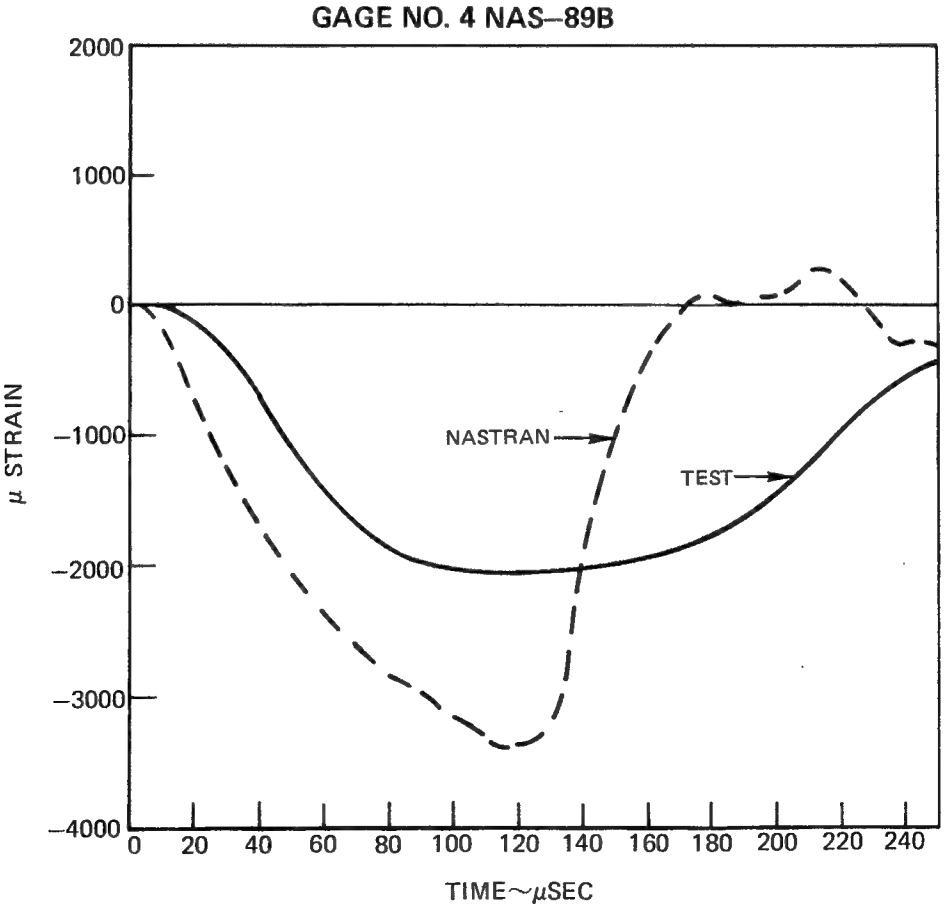


76–06–69–8

FIG. A9

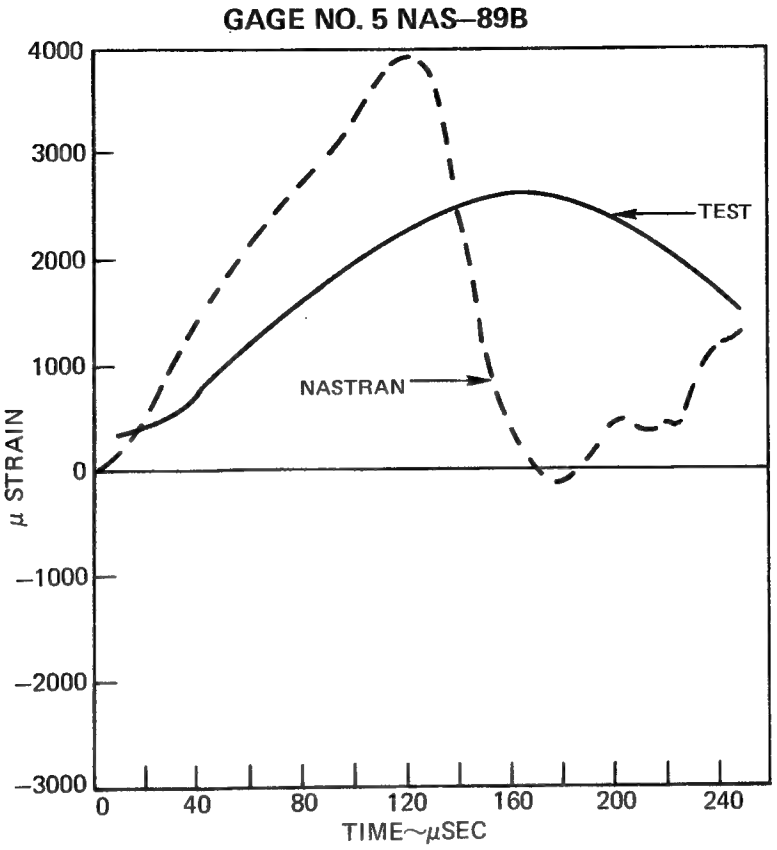


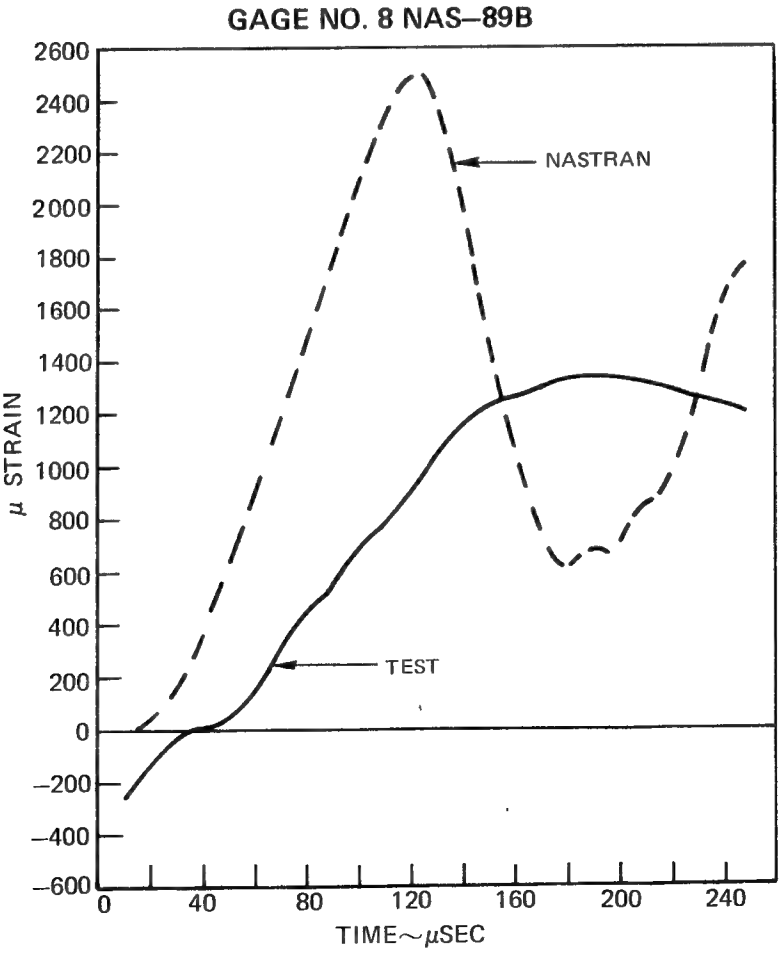


76-06-69-9

GAGE NO. 10 NAS–89B

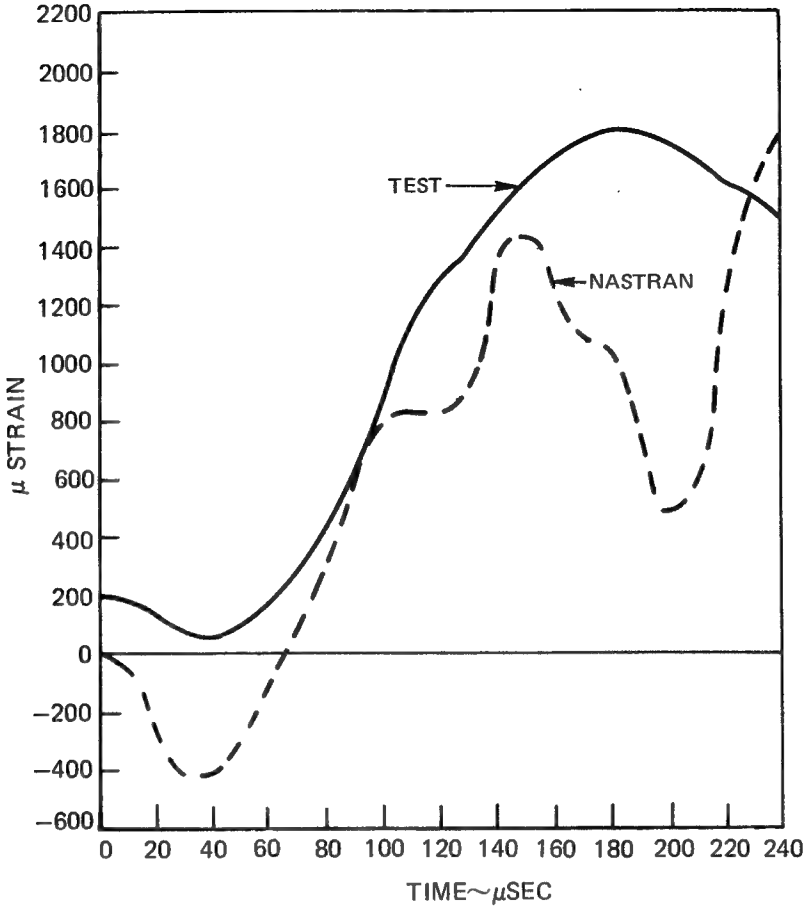


GAGE NO. 12 NAS–89B

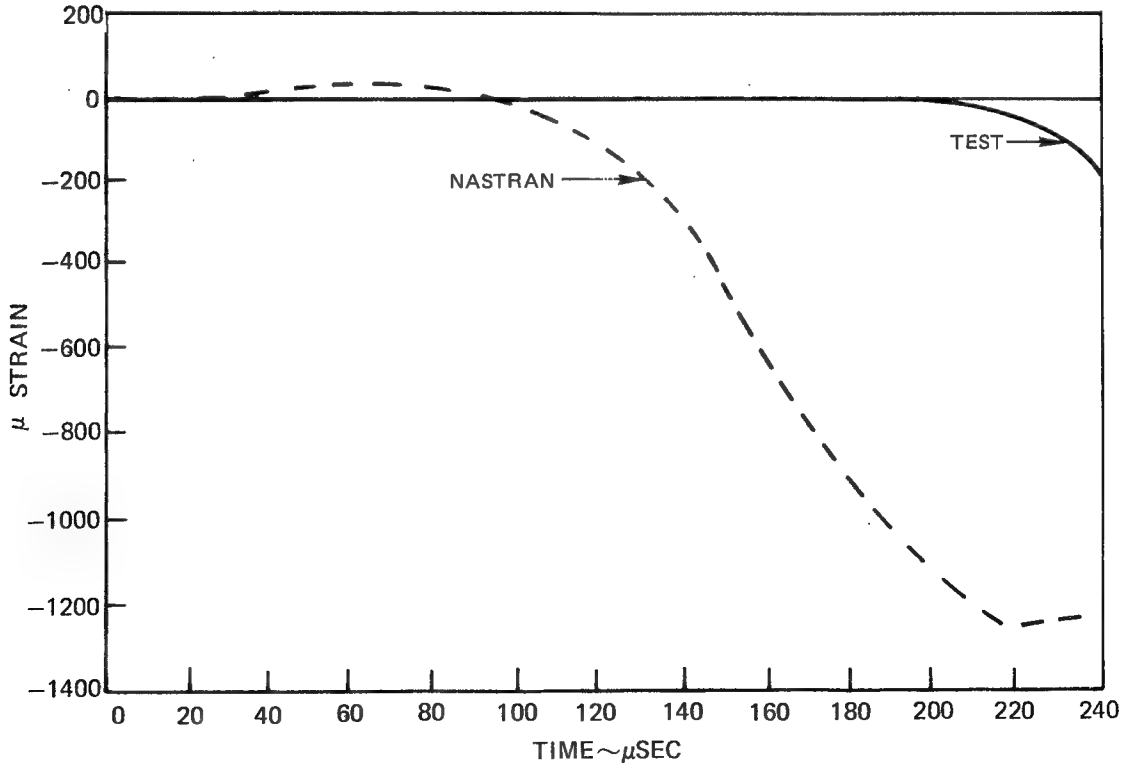


76–06–69–10

FIG. A11

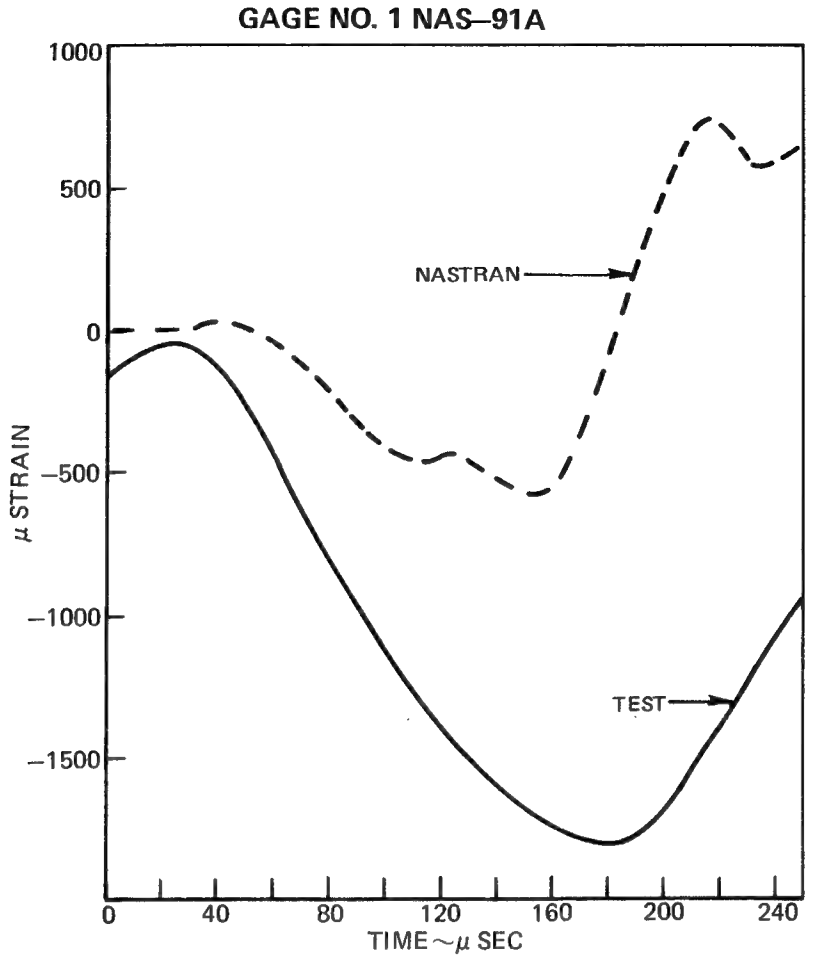


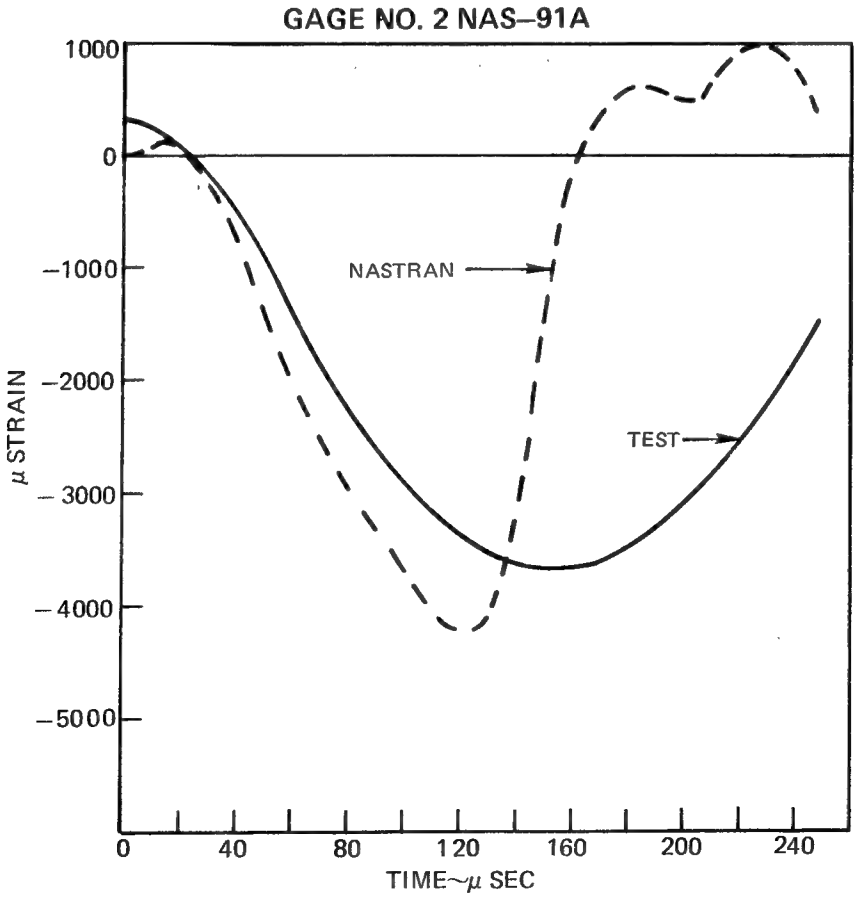


76–06–69–11

FIG. A12

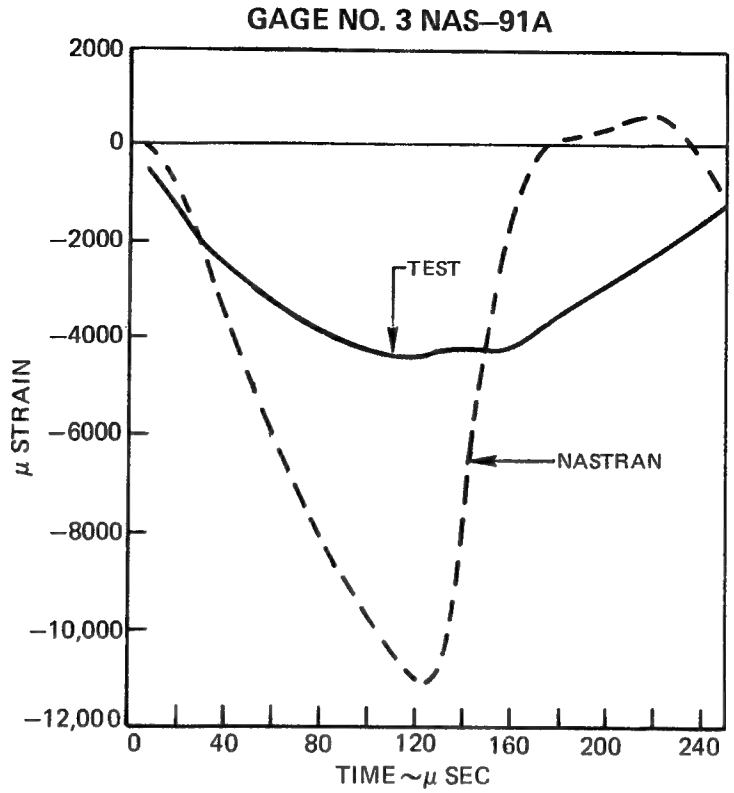


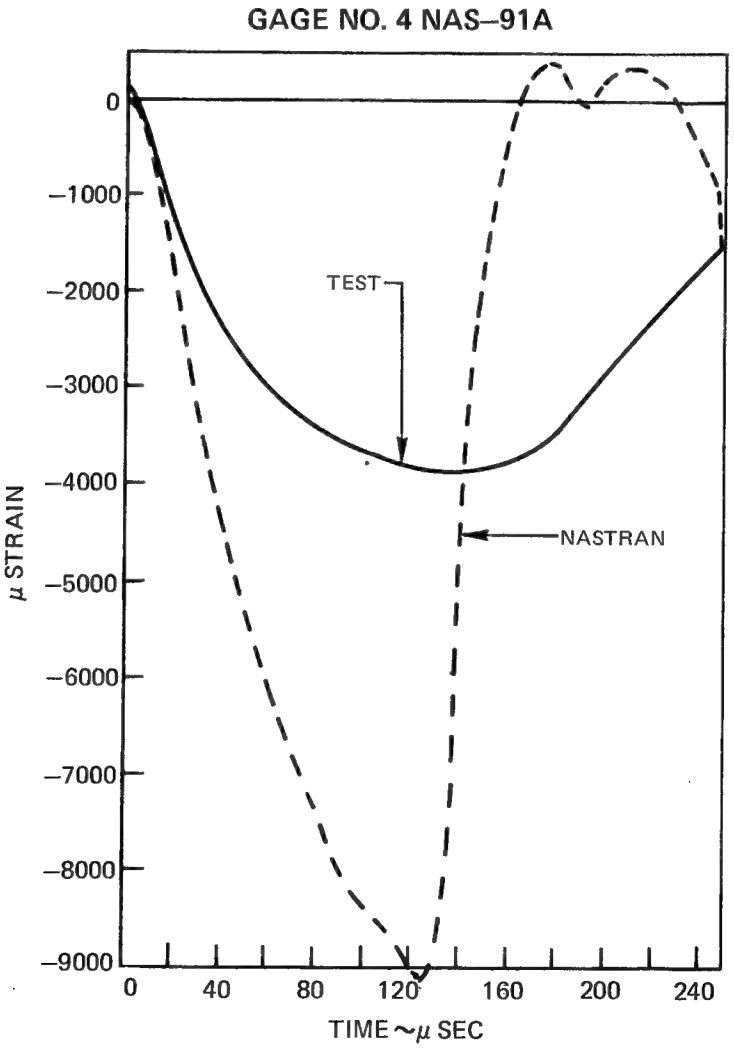


76–06–69–12

FIG. A13

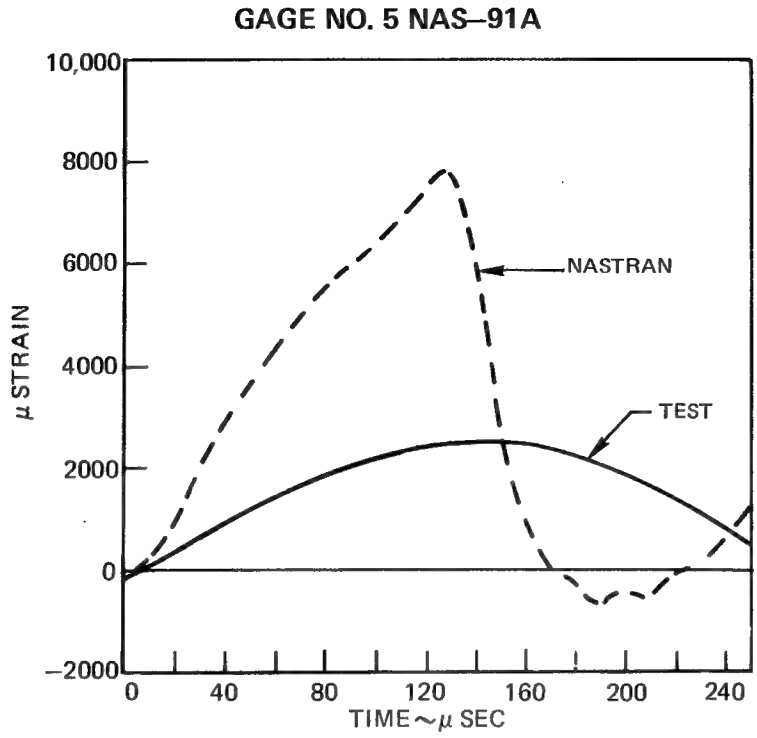


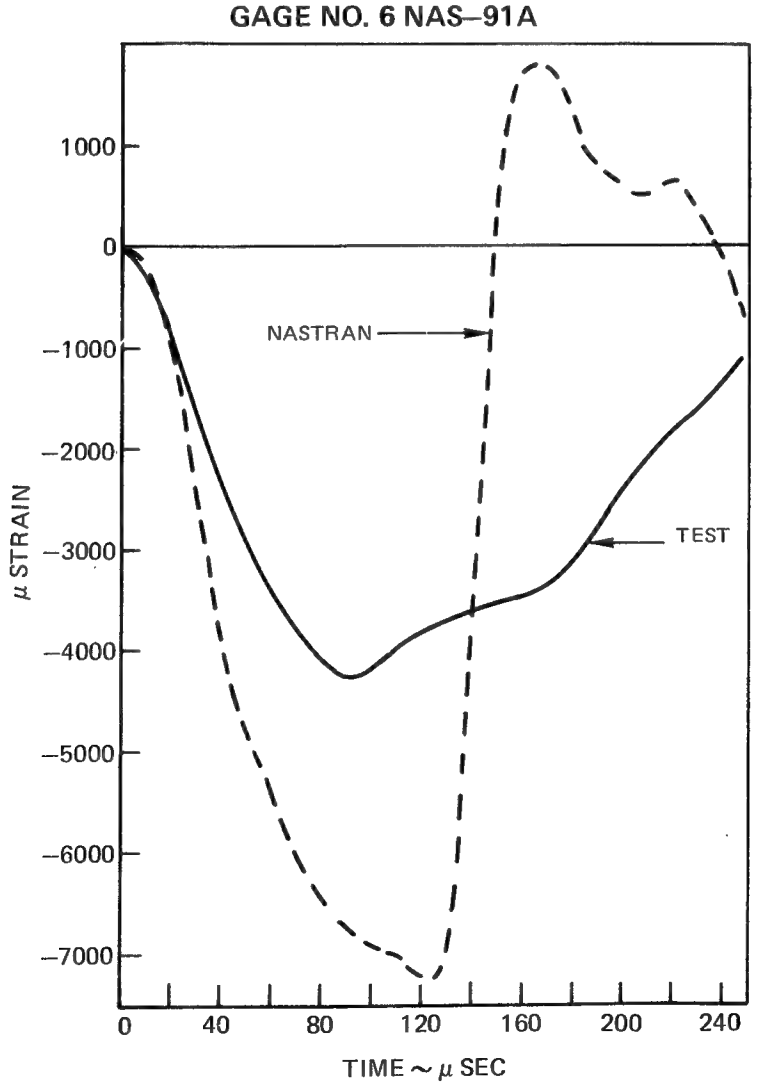


76–06–69 -13

FIG. A14

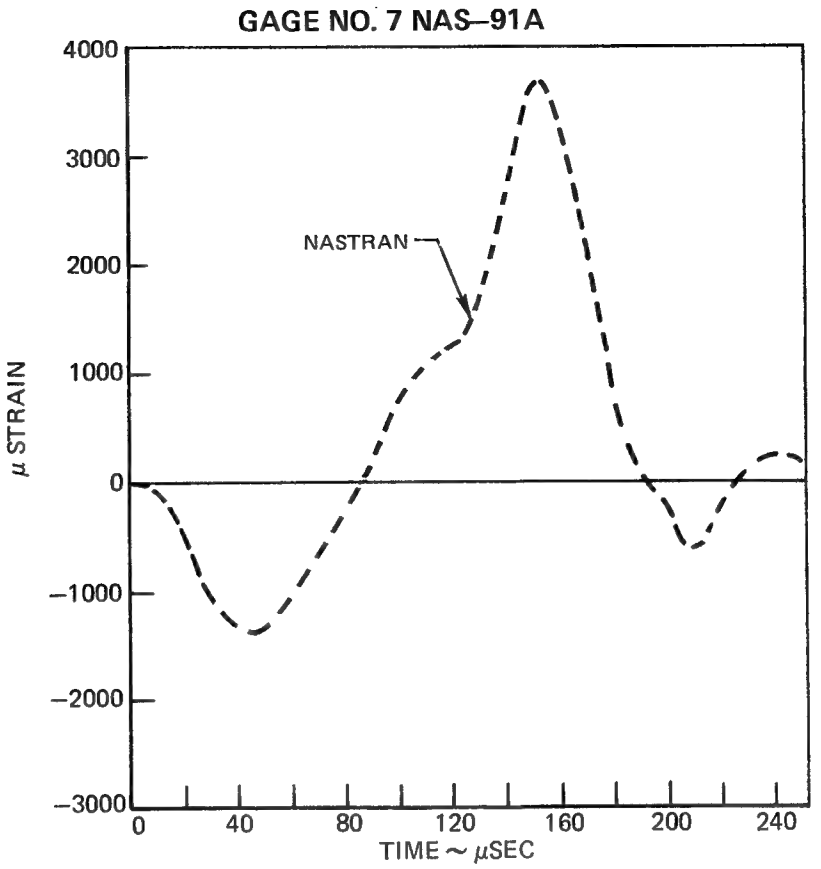


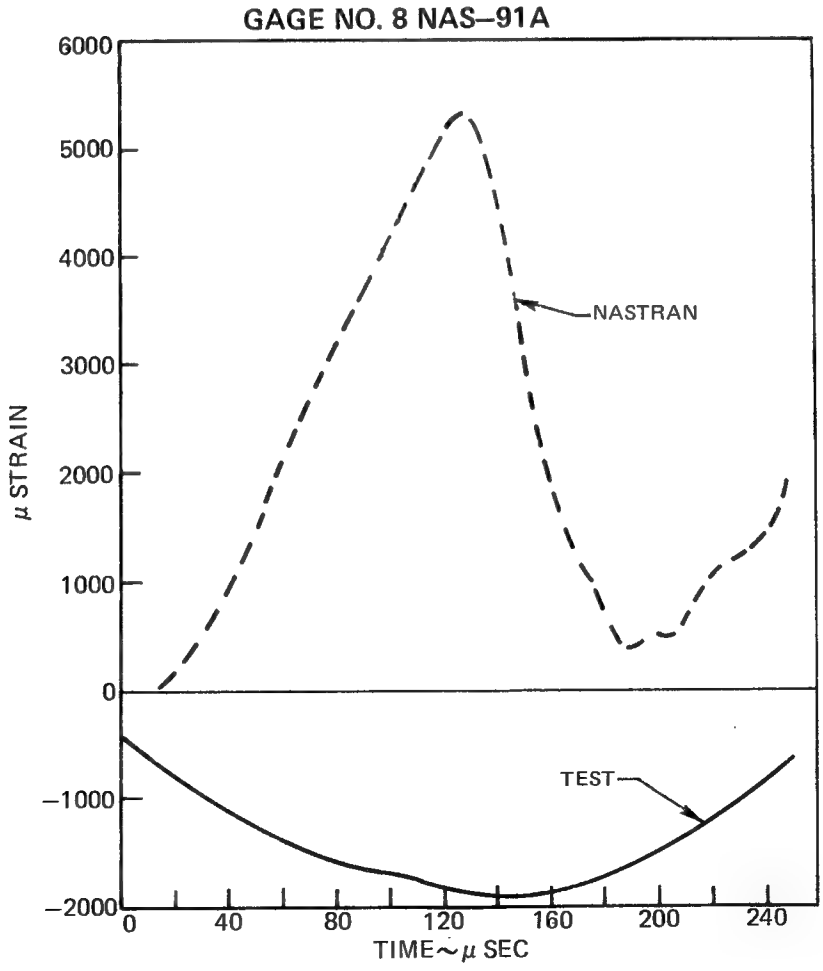


76–06–69–14

## GAGE NO. 10 NAS–91A

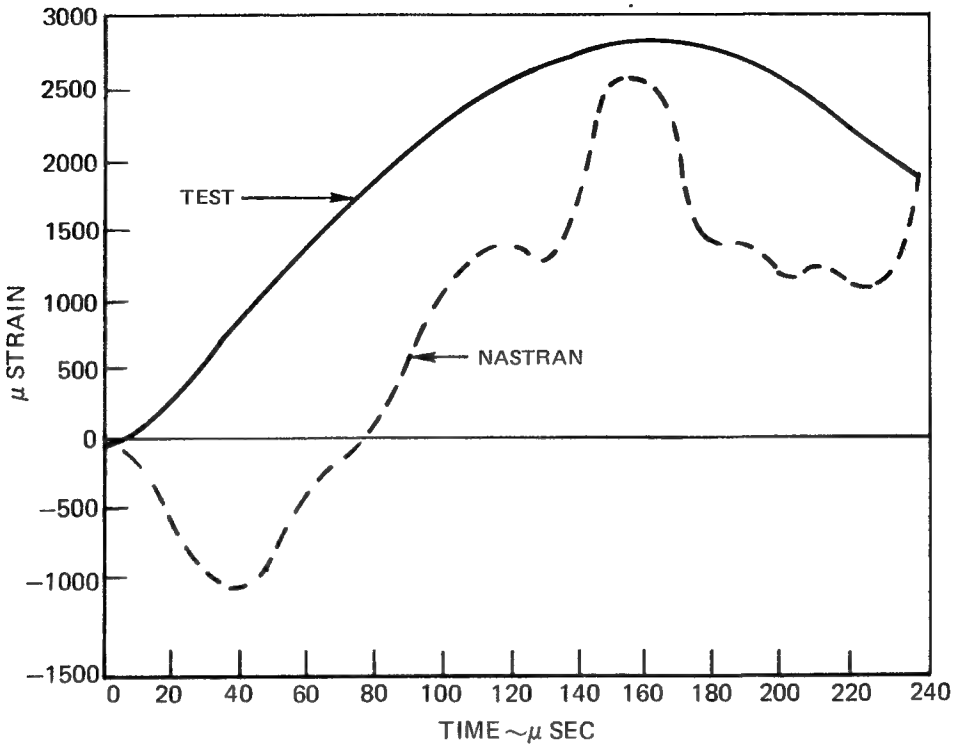


## GAGE NO. 12 NAS–91A

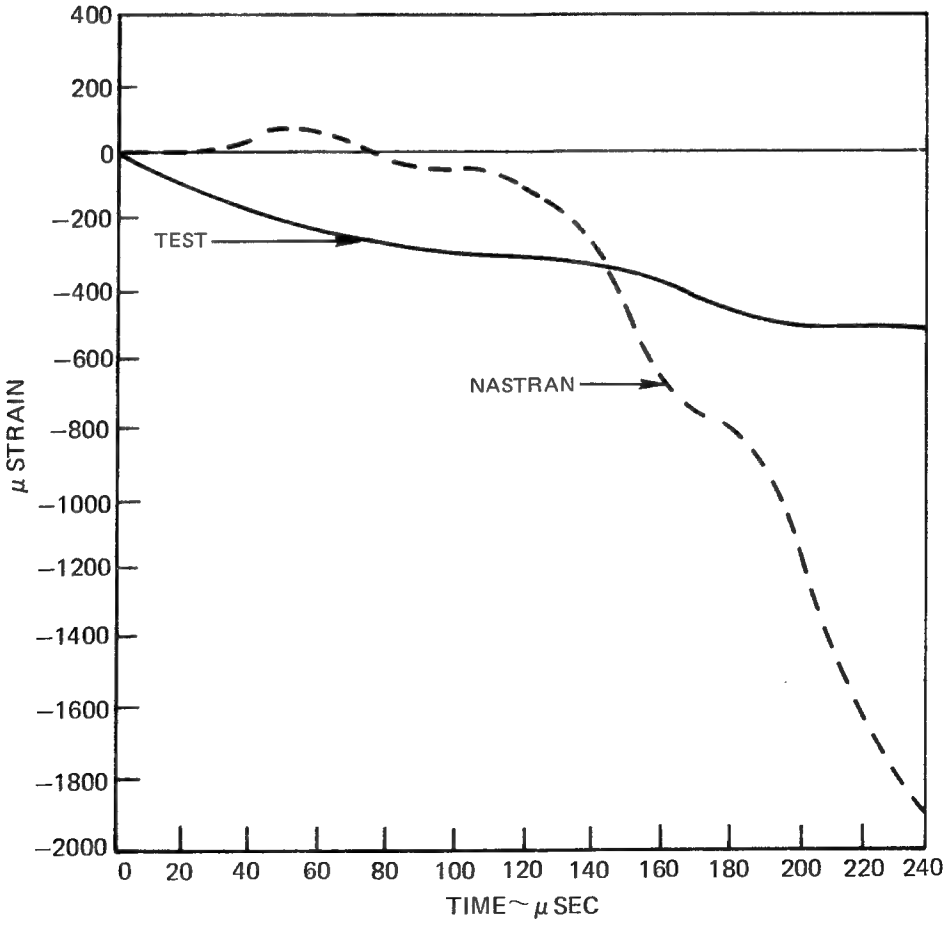


76–06–69- 15

APPENDIX B

FIG. B1

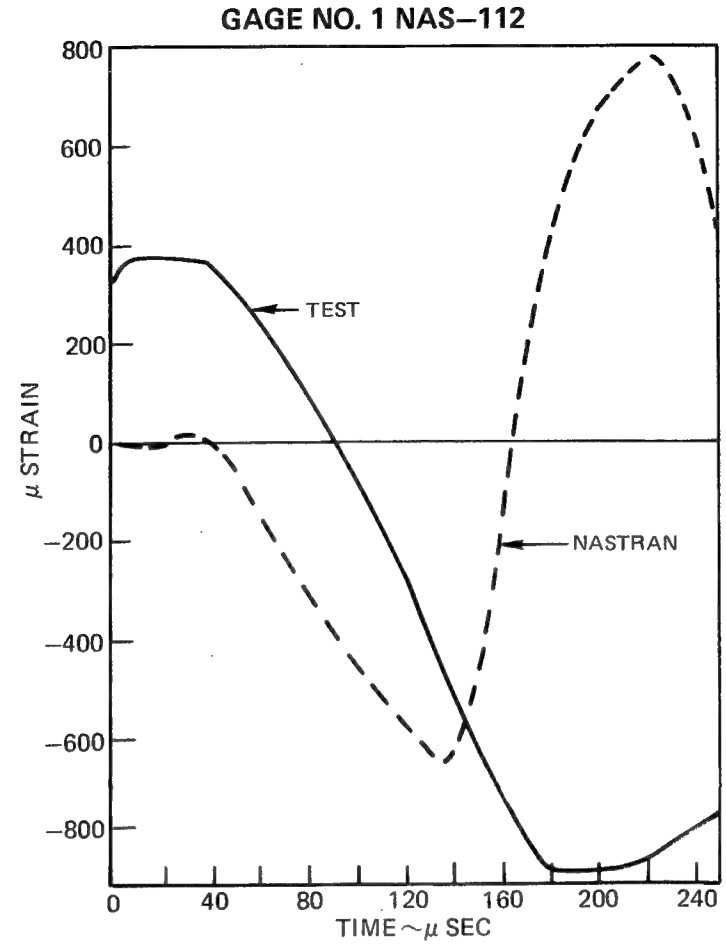


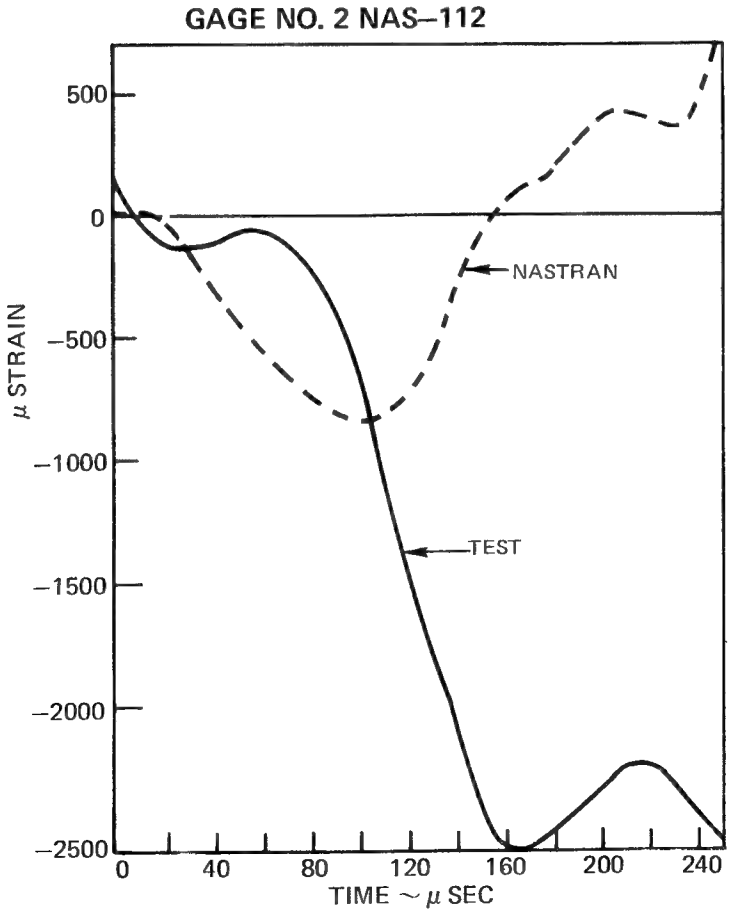


76–06–69–16

FIG. B2

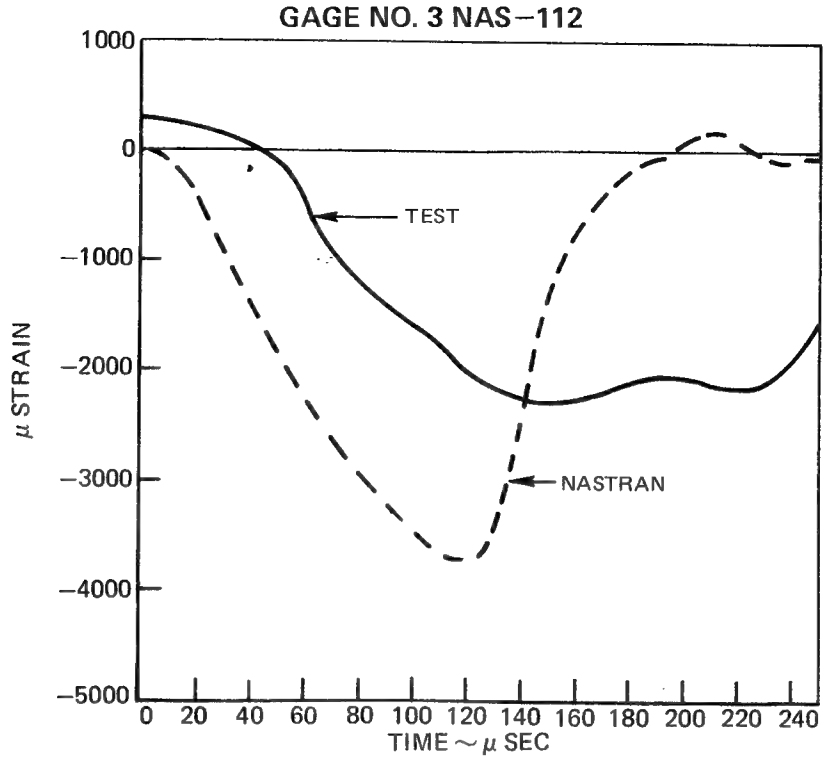


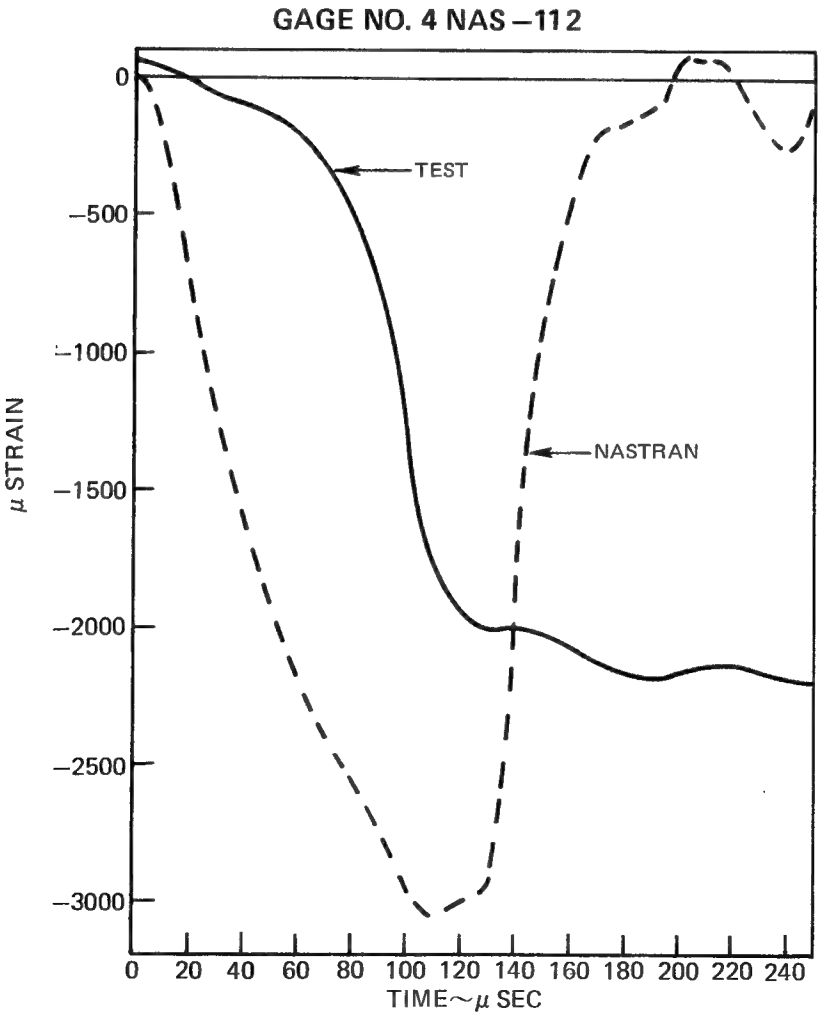


76–6–69–18

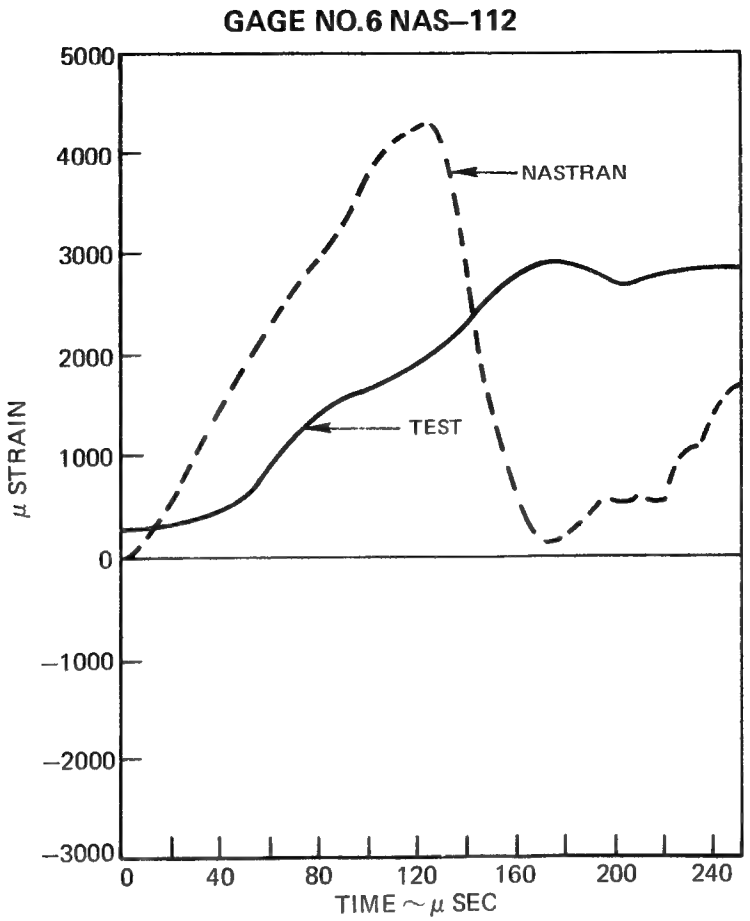
GAGE NO.6 NAS–112
5000
4000
3000
2000
1000
0
–1000
–2000
–3000
μ STRAIN
NASTRAN
TEST
0
40
80
120
160
200
240
TIME ~ μ SEC

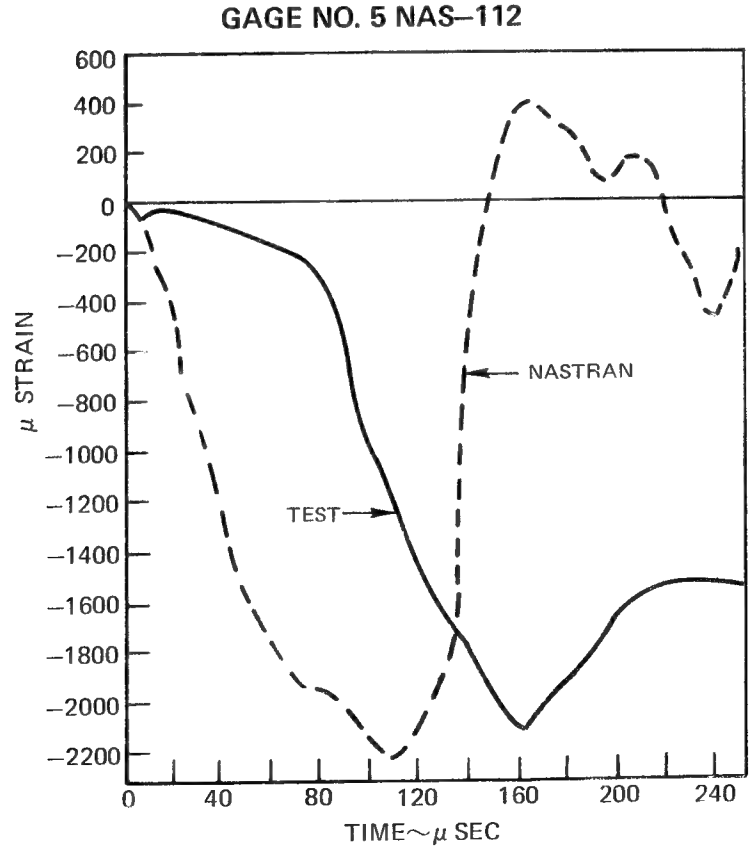
GAGE NO. 5 NAS–112
600
400
200
0
–200
–400
–600
–800
–1000
–1200
–1400
–1600
–1800
–2000
–2200
μ STRAIN
NASTRAN
TEST
0
40
80
120
160
200
240
TIME~μ SEC

76-06-69-1

FIG. B4

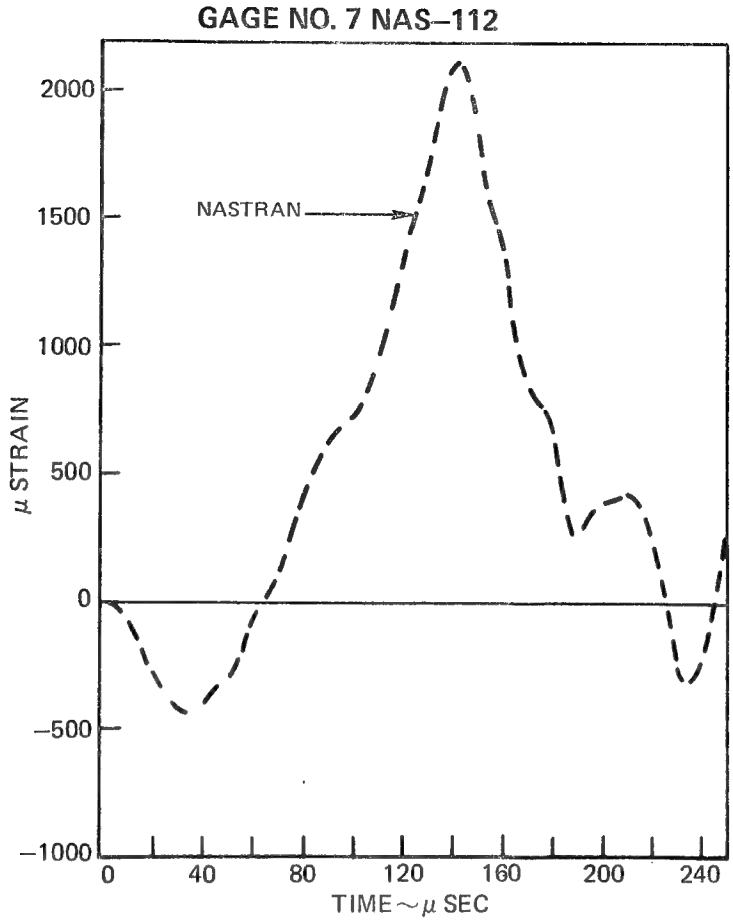


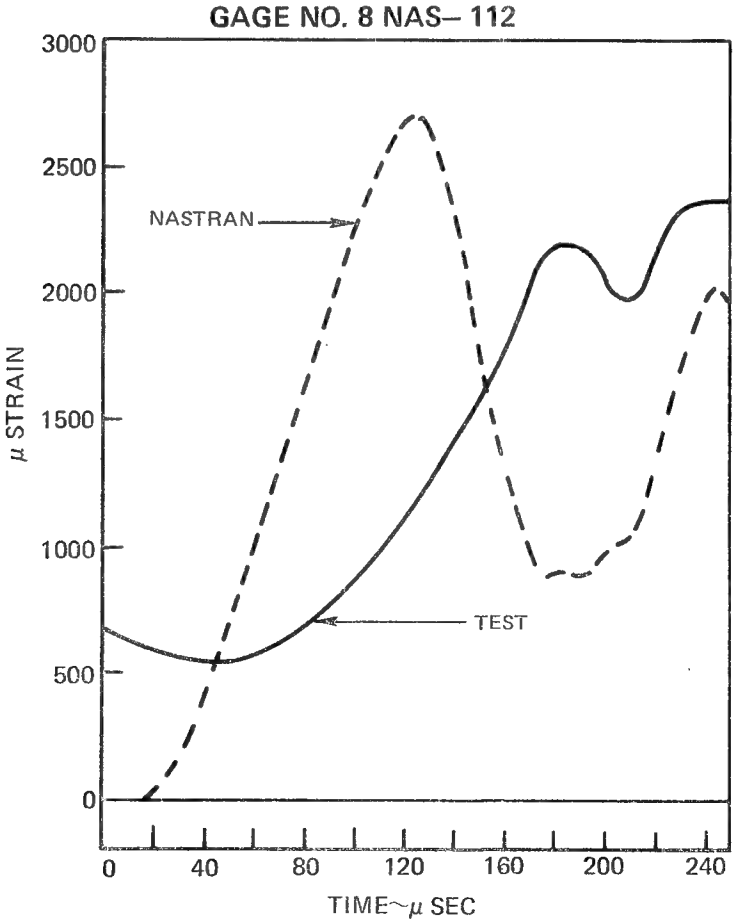


76–06–69–19

FIG. B5

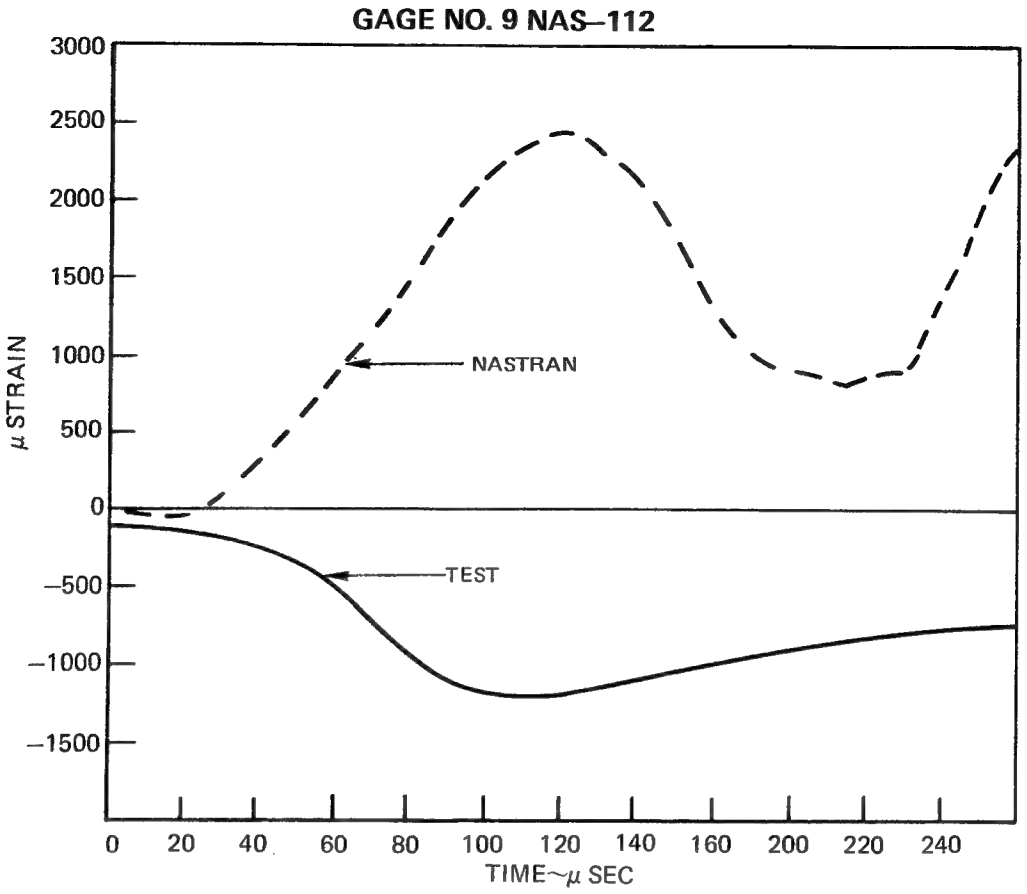


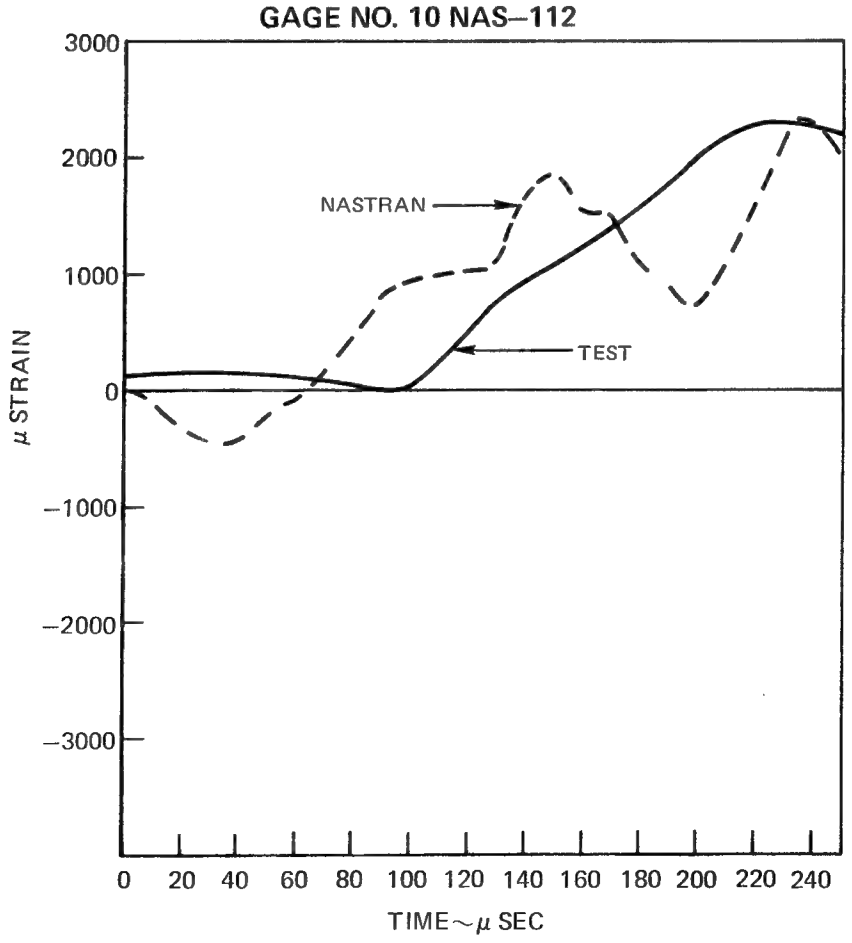


76–06–69–20

## GAGE NO. 11 NAS–112

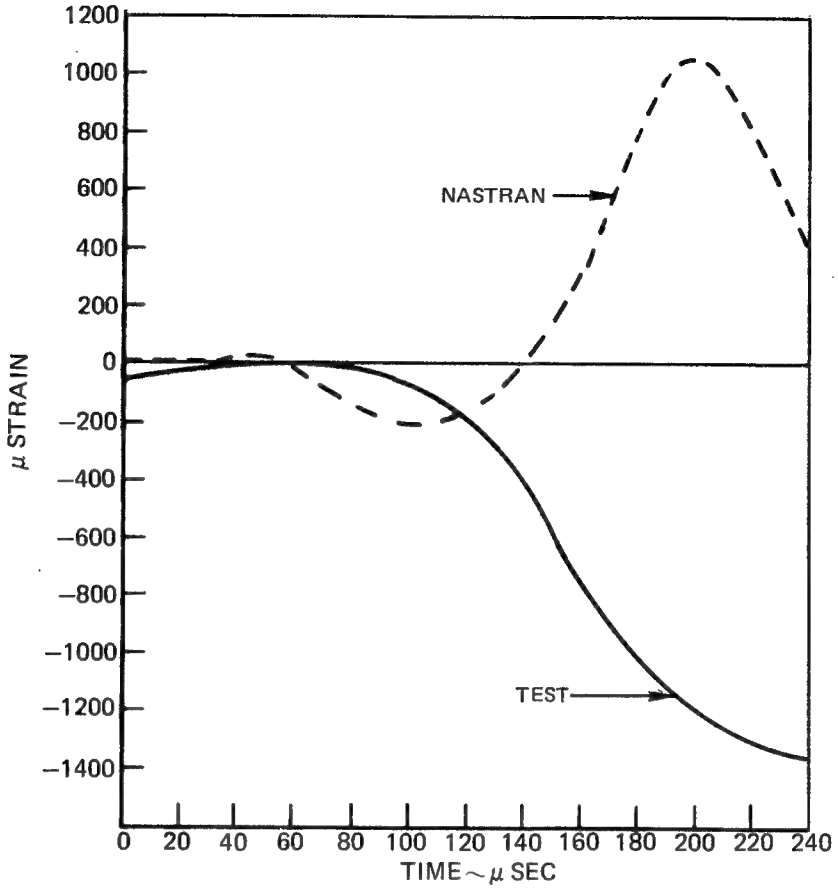


## GAGE NO. 12 NAS–112

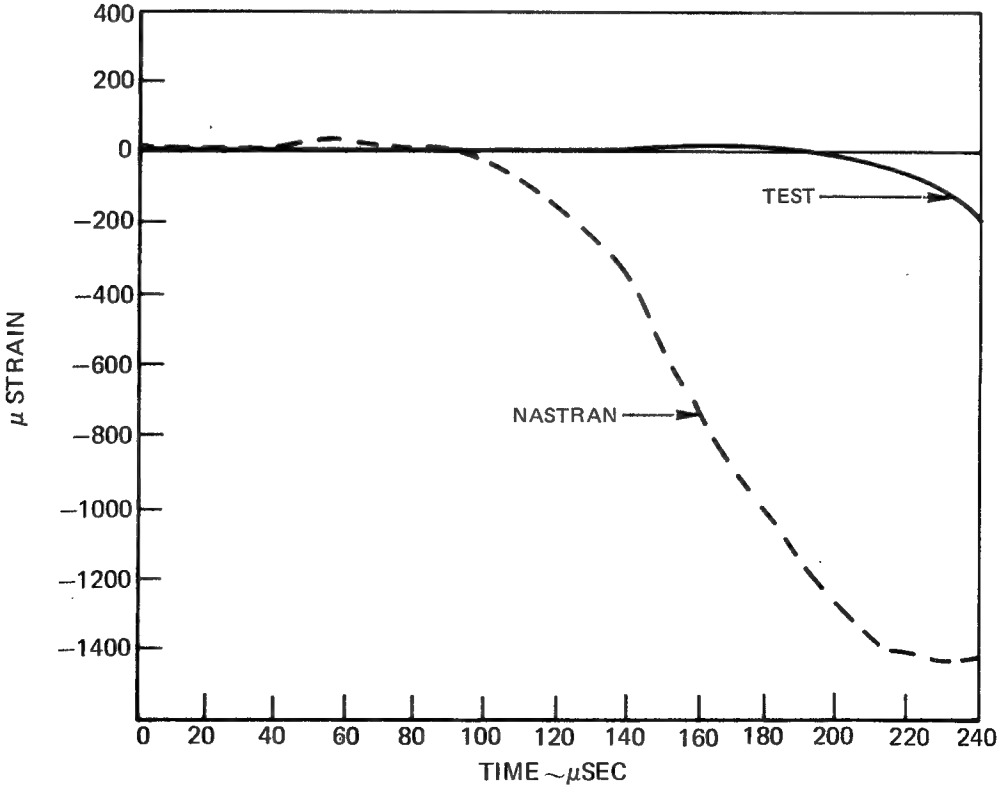


76–06–69–21

FINAL REPORT DISTRIBUTION LIST
NASA CR-135062

"MULTI-FIBER COMPOSITES"
CONTRACT NAS3-18941

UNITED TECHNOLOGIES RESEARCH CENTER
EAST HARTFORD, CT. 06108

| ADDRESSEE | NO. OF COPIES |
|---|---|
| Advanced Research Projects Agency<br>Washington, DC 20525<br>Attn: Library | 1 |
| Advanced Technology Center, Inc.<br>LTV Aerospace Corp.<br>P.O. Box 6144<br>Dallas, TX 75222<br>Attn: D. H. Petersen | 1 |
| Air Force Flight Dynamics Laboratory<br>Wright-Patterson Air Force Base, Ohio 45433<br>Attn: C. D. Wallace<br>P. A. Parmley<br>G. P. Sendeckyj (FBC) | <br>1<br>1<br>1 |
| Air Force Materials Laboratory<br>Wright-Patterson Air Force Base, Ohio 45433<br>Attn: H. S. Schwartz (LN)<br>T. J. Reinhart (MBC)<br>G. P. Peterson (LC)<br>E. J. Morrisey (LAE)<br>A. Hopkins (LLN)<br>S. Litvak (LTF)<br>J. Rodehamel (MXE)<br>S. Tsai (MBM) | <br>1<br>1<br>1<br>1<br>1<br>1<br>1<br>1<br>1 |
| Air Force Office of Scientific Research<br>Washington, DC 20333<br>Attn: J. F. Masi, SREP | 1 |
| Air Force Aeronautical Propulsion Laboratory<br>Wright-Patterson Air Force Base, Ohio 45433<br>Attn: T. Norbut (TBP)<br>L. J. Obery (TBP) | <br>1<br>1 |

| ADDRESSEE | NO. OF COPIES |
|---|---|
| Air Force Office of Scientific Research<br>1400 Wilson Blvd.<br>Arlington, VA 22209<br>Attn: SIGL | 1 |
| Babcock and Wilcox Co.<br>Advanced Composites Department<br>P.O. Box 419<br>Alliance, OH 44601<br>Attn: R. C. Young | 1 |
| Bell Helicopter Co.<br>P.O. Box 482<br>Ft. Worth, TX 76101<br>Attn: H. Zinberg | 1 |
| Boeing Aerospace Co.<br>P.O. Box 3999<br>Seattle, WA 98124<br>Attn: J. T. Hoggatt | 1 |
| The Boeing Co.<br>Vertol Division<br>Morton, PA 19070<br>Attn: R. Pickney | 1 |
| Chemical Propulsion Information Agency<br>Applied Physics Laboratory<br>8621 Georgia Avenue<br>Silver Spring, MD 20910<br>Attn: Library | 1 |
| Commander<br>Natick Laboratories<br>U.S. Army<br>Natick, MA 01762<br>Attn: Library | 1 |
| Commander<br>Naval Air Systems Command<br>U.S. Navy Department<br>Washington, DC 20360<br>Attn: P. Goodwin, AIR-5203<br>C. Bersch, AIR-5203A<br>M. Stander, AIR-42032D | 1<br>1<br>1 |

| ADDRESSEE | NO. OF COPIES |
|---|---|
| Commander<br>Naval Ordnance Systems Command<br>U.S. Navy Department<br>Washington, DC 20360 | |
| Attn: B. Drimmer, ORD-033 | 1 |
| M. Kinna, ORD-033A | 1 |
| Composite Materials Corp.<br>P.O. Box 385<br>Broad Brook, CT 06016 | |
| Attn: M. H. Mildwurf | 1 |
| Composites Horizons<br>6342 N. Irwindale Ave.<br>Azusa, CA 91702 | |
| Attn: I. Petker | 1 |
| Cornell University<br>Theoretical & Applied Mechanics, Thurston Hall<br>Ithaca, NY 14853 | |
| Attn: F. C. Moon | 1 |
| Defense Metals Information Center<br>Battelle Memorial Institute<br>Columbus Laboratories<br>505 King Avenue<br>Columbus, OH 43201 | 1 |
| Department of the Army<br>U.S. Army Material Command<br>Washington, DC 20315 | |
| Attn: AMCRD-RC | 1 |
| Department of the Army<br>U.S. Army Aviation Materials Laboratory<br>Ft. Eustis, VA 23604 | |
| Attn: I. E. Figge, Sr. | 1 |
| R. Berrisford | 1 |
| Library | 1 |
| Department of the Army<br>U.S. Army Aviation Systems Command<br>P.O. Box 209<br>St. Louis, MO 63166 | |
| Attn: R. Vollmer, AMSAV-A-UE | 1 |
| Library | 1 |

| ADDRESSEE | NO. OF COPIES |
|---|---|
| Department of the Army<br>Plastics Technical Evaluation Center<br>Picatinny Arsenal<br>Dover, NJ 07801 | |
| Attn: H. E. Pebly, Jr. | 1 |
| Department of the Army<br>Watervliet Arsenal<br>Watervliet, NY 12189 | |
| Attn: F. W. Schmiedershoff | 1 |
| Library | 1 |
| Department of the Army<br>Mechanics Research Center<br>Watertown Arsenal<br>Watertown, MA 02172 | |
| Attn: A. Thomas | 1 |
| B. M. Halpin, Jr. | 1 |
| Library | 1 |
| S. Arnold | 1 |
| Department of the Navy<br>Office of Naval Research<br>Washington, DC 20360 | |
| Attn: Library | 1 |
| Department of the Navy<br>Naval Surface Weapons Center<br>White Oak, Silver Spring, MD 20910 | |
| Attn: R. Simon | 1 |
| Library | 1 |
| Department of the Navy<br>U.S. Naval Ship R&D Laboratory, Annapolis<br>Annapolis, MD 21402 | |
| Attn: C. Hershner, Code 2724 | 1 |
| Library | 1 |
| Director<br>Deep Submergence Systems Project<br>6900 Wisconsin Avenue<br>Washington, DC 20015 | |
| Attn: H. Bernstein, DSSP-221 | 1 |
| Library | 1 |

| ADDRESSEE | NO. OF COPIES |
|---|---|
| Director<br>Naval Research Laboratory<br>Washington, DC 20390 | |
| Attn: Code 8430 | 1 |
| I. Wolock, Code 8433 | 1 |
| Library | 1 |
| Drexel University<br>Philadelphia, PA | |
| Attn: P. C. Chou | 1 |
| E. I. DuPont DeNemours and Co.<br>DuPont Experimental Station<br>Wilmington, DE 19898 | |
| Attn: C. Zweben | 1 |
| E. I. DuPont DeNemours and Co.<br>Experiment Station<br>Wilmington, DE 19898 | |
| Attn: E. A. Merriman | 1 |
| Fiber Science, Inc.<br>245 East 157th Street<br>Gardena, CA 90248 | |
| Attn: L. J. Ashton | 1 |
| General Dynamics<br>P.O. Box 748<br>Ft. Worth, TX 76101 | |
| Attn: C. W. Rogers | 1 |
| General Dynamics/Convair<br>P.O. Box 1128<br>San Diego, CA 92112 | |
| Attn: J. E. Ashton | 1 |
| General Electric Co.<br>Aircraft Engine Group<br>Evendale, OH 45215 | |
| Attn: C. Stotler | 1 |
| M. Grandy | 1 |
| C. Salemme | 1 |

| ADDRESSEE | NO. OF COPIES |
|---|---|
| General Electric Co.<br>Space Sciences Laboratory<br>Philadelphia, PA 19101<br>Attn: Library | 1 |
| General Motors Corporation<br>Detroit Diesel Allison Division<br>Indianapolis, IN<br>Attn: M. Herman | 1 |
| Grumman Aerospace Corporation<br>Bethpage, Long Island, NY 11714<br>Attn: B. Aleck | 1 |
| Hercules, Inc.<br>Wilmington, DE 19898<br>Attn: G. Kuebeler | 1 |
| IIT Research Institute<br>Technology Center<br>Chicago, IL 60616<br>Attn: L. M. Daniel | 1 |
| Jet Propulsion Laboratory<br>4800 Oak Grove Dr.<br>Pasadena, CA 91103<br>Attn: Library | 1 |
| Lawrence Livermore Laboratory<br>P.O. Box 808<br>Livermore, CA 94550<br>Attn: T. T. Chiao | 1 |
| Lockheed-Georgia Co.<br>Advanced Composites Information Center<br>Dept. 72-14, Zone 402<br>Marietta, GA 30060 | 1 |
| Lockheed Missiles and Space Co.<br>P.O. Box 504<br>Sunnyvale, CA 94087<br>Attn: R. W. Fenn | 1 |

| ADDRESSEE | NO. OF COPIES |
|---|---|
| McDonnell-Douglas Astronautics Co.<br>5301 Bolsa Ave.<br>Huntington Beach, CA 92647 | |
| Attn: L. B. Greszczuk | 1 |
| R. W. Siebold | 1 |
| McDonnell-Douglas Aircraft Corp.<br>P.O. Box 516<br>Lambert Field, MS 63166 | |
| Attn: J. C. Watson | 1 |
| McDonnell-Douglas Aircraft Corp.<br>3855 Lakewood Blvd.<br>Long Beach, CA 90810 | |
| Attn: H. C. Schjelderup | |
| Massachusetts Institute of Technology<br>Cambridge, MA 02139 | |
| Attn: Prof. F. J. McGarry | 1 |
| Materials Sciences Corp.<br>1777 Walton Rd.<br>Blue Bell, PA 19422 | |
| Attn: B. W. Rosen | 1 |
| NASA-Flight Research Center<br>P.O. Box 273<br>Edwards, CA 93523 | |
| Attn: Library | 1 |
| NASA-Ames Research Center<br>Moffett Field, CA 94035 | |
| Attn: Library | 1 |
| NASA-George C. Marshall Space Flight Center<br>Huntsville, AL 35812 | |
| Attn: J. M. Stuckey, S&E-ASTN-MNM | 1 |
| Library | 1 |
| NASA-Goddard Space Flight Center<br>Greenblet, MD 20771 | |
| Attn: Library | 1 |

| ADDRESSEE | NO. OF COPIES |
|---|---|
| NASA-Langley Research Center<br>Hampton, VA 23365 | |
| Attn: M. Card, Mail Code 190, Bldg. 1148 | 1 |
| Library | 1 |
| NASA-Lewis Research Center<br>21000 Brookpark Road<br>Cleveland, OH 44135 | |
| Attn: Contracting Officer, MS 500-313 | 1 |
| Tech. Report Control, MS 5-5 | 1 |
| Technical Utilization, MS 3-19 | 1 |
| AFSC Liaison, MS 501-3 | 1 |
| Rel. and Quality Assur., MS 500-211 | 1 |
| R. A. Signorelli, MS 106-1 | 1 |
| C. C. Ciepluch, MS 501-7 | 1 |
| M. P. Hanson, MS 501-7 | 1 |
| R. H. Kemp, MS 49-3 | 1 |
| R. F. Lark, MS 49-3 | 11 |
| J. R. Faddoul, MS 49-3 | 1 |
| R. J. Denington, MS 501-7 | 1 |
| J. C. Freche, MS 49-1 | 1 |
| R. H. Johns, MS 49-3 | 1 |
| N. T. Saunders, MS 105-1 | 1 |
| T. L. Sullivan, MS 49-3 | 1 |
| C. C. Chamis, MS 49-3 | 1 |
| T. T. Serafini, MS 49-1 | 1 |
| Library, MS 60-3 | 2 |
| NASA-Lyndon B. Johnson Space Center<br>Houston, TX 77001 | |
| Attn: Library | 1 |
| NASA Scientific & Technical Info. Facility<br>P.O. Box 8757<br>Balt/Wash International Airport<br>MD 21240 | |
| Attn: Accessioning Department | 10 |
| National Aeronautics & Space Administration<br>Office of Advanced Research and Technology<br>Washington, DC 20546 | |
| Attn: RWM/J. J. Gangler | 1 |
| National Aeronautics & Space Administration<br>Office of Technology Utilization<br>Washington, DC 20546 | 1 |

| ADDRESSEE | NO. OF COPIES |
|---|---|
| National Technical Information Service<br>Springfield, VA 22151 | 6 |
| North American Rockwell Corp.<br>Space Division<br>12214 Lakewood Blvd.<br>Downey, CA 90241 | |
| Attn: Max Nabler | 1 |
| L. Korb | 1 |
| Northrop Space Laboratories<br>3401 West Broadway<br>Hawthorne, CA 90250 | |
| Attn: D. Stanbarger | 1 |
| Purdue University<br>West Lafayette, IN | |
| Attn: C. T. Sun | 1 |
| Sikorsky Aircraft Division<br>United Aircraft Corp.<br>Stratford, CT 06602 | |
| Attn: J. D. Ray | 1 |
| Southwest Research Institute<br>8500 Culebra Road<br>San Antonio, TX 78284 | |
| Attn: G. C. Grimes | 1 |
| Space and Missile Systems Organization<br>Air Force Unit Post Office<br>Los Angeles, CA 90045 | |
| Attn: Technical Data Center | 1 |
| Structural Composites Industries, Inc.<br>6344 N. Irwindale Avenue<br>Azusa, CA 91702 | |
| Attn: E. E. Morris | 1 |
| TRW, Inc.<br>23555 Euclid Avenue<br>Cleveland, OH | |
| Attn: W. E. Winters | 1 |
| Union Carbide Corp.<br>P.O. Box 6116<br>Cleveland, OH 44101 | |
| Attn: J. C. Bowman | 1 |